

**USING THE FLOWING AFTERGLOW AS A CHEMICAL REACTION MASS
SPECTROMETER**

by

Mark W Morris

B.S. Chemistry, California University of Pennsylvania, 2000

Submitted to the Graduate Faculty of
Arts and Sciences in partial fulfillment
of the requirements for the degree of
Doctor of Philosophy

University of Pittsburgh

2007

UNIVERSITY OF PITTSBURGH

Arts and Sciences

This dissertation was presented

by

Mark Morris

It was defended on

May 1, 2007

and approved by

Adrian C. Michael

Stephen Weber

Christopher M. Hadad

Dissertation Advisor: Joseph J. Grabowski

This dissertation is dedicated to:

My Wife, Jessica

My Children, Xavier and Nathaniel

And my late father, Willard

Using the Flowing Afterglow as a Chemical Reaction Mass Spectrometer

Mark W Morris, PhD

University of Pittsburgh, 2007

The flowing afterglow was used to study the formation and reaction of protonated hexamethyldisiloxane, protonated trimethylsilanol, and the trimethylsilyl cation with a variety of neutrals. The neutrals were selected based on their importance in volatile organic compound (VOC) monitoring and/or their type (i.e. amines, ketones, etc.). The reagent ions contain the trimethylsilyl group, which has been referred as a “large proton”. The hydronium ion is used in VOC analysis; this ion clusters with water and only provides molecular weight information. Various products were identified such as proton transfer, trimethylsilyl transfer, hydride ion transfer, etc. Secondary products were also identified, which formed because of the presence of excess neutrals. These secondary products are unimportant if the reagent ions listed above are used for trace gas analysis.

The flowing afterglow was used as a chemical reaction mass spectrometer to measure Henry’s law constants. The Henry’s law constant for acetonitrile was measured to be 49 ± 7 , while the average value in the literature is 52 ± 3 mol/kg bar; the constant for acetone was measured to be 27 ± 3 and the literature value is 28 ± 3 mol/kg bar.

The chemical reaction mass spectrometer was also used to detect VOCs from thermal decomposition of phenolic resin coated on a graphitic board. A custom SS vessel was used to decompose the resin. Phenol, ammonia, methyl and dimethyl phenol, and other VOCs were detected and quantified. Concentrations ranged from 0.1 to 10 ppm for a 50.5 mg piece of graphitic board.

TABLE OF CONTENTS

PREFACE	XVII
1.0 INTRODUCTION	1
1.1 CONCLUSIONS	3
1.2 REFERENCES	4
2.0 EXPERIMENTAL METHODOLOGY	5
2.1 EXPERIMENTAL PROTOCOL	5
2.2 DERIVATION OF QUANTITATION OF THE CRMS	8
2.3 EVALUATING ASSUMPTIONS	10
2.4 PROPAGATION OF ERRORS	11
2.5 REFERENCES	14
3.0 FACILE TRIMETHYLSILYL TRANSFER INVOLVING ION/MOLECULE REACTIONS OF PROTONATED HEXAMETHYLDISILOXANE	15
3.1 INTRODUCTION	15
3.2 EXPERIMENTAL	17
3.3 RESULTS	20
3.3.1 Formation of protonated hexamethyldisiloxane	20
3.3.2 Reaction of protonated hexamethyldisiloxane with neutrals	23
3.3.3 Terpenoids	28

3.4	DISCUSSION.....	29
3.5	CONCLUSIONS.....	36
3.6	REFERENCES	39
4.0	PROTONATED TRIMETHYLSILANOL: ITS CAPACITY AS A TRIFUNCTIONAL REAGENT ION	41
4.1	INTRODUCTION	41
4.2	EXPERIMENTAL.....	42
4.3	RESULTS.....	44
4.3.1	Reaction of protonated trimethylsilanol with neutrals.....	44
4.3.2	Protonated trimethylsilanol with terpenes	51
4.4	DISCUSSION.....	52
4.4.1	Non terpenoid compounds	52
4.4.2	Terpenoids	59
4.5	CONCLUSIONS.....	59
4.6	REFERENCES	60
5.0	ION/MOLECULE REACTION STUDIES USING THE TRIMETHYLSILYL CATION.....	62
5.1	INTRODUCTION	62
5.2	EXPERIMENTAL.....	63
5.3	RESULTS	65
5.4	DISCUSSION.....	69
5.5	CONCLUSIONS.....	76
5.6	REFERENCES	78

6.0	USING HENRY’S LAW AND THE EXPONENTIAL FLASK TO VALIDATE	
	QUANTITATION OF THE CRMS	79
6.1	INTRODUCTION	79
6.2	EXPERIMENTAL.....	80
6.2.1	Henry’s Law	80
6.2.2	Exponential Dilution Flask	83
6.3	RESULTS	84
6.3.1	Henry’s Law	84
6.3.2	Exponential Dilution Flask	87
6.4	DISCUSSION.....	90
6.4.1	Henry’s Law	90
6.4.2	Exponential Dilution Flask	91
6.5	CONCLUSIONS.....	92
6.6	REFERENCES	93
7.0	USING THE CRMS TO DETERMINE VOLATILE ORGANIC COMPOUNDS	
	EMITTED FROM A GRAPHITIC BOARD COATED WITH PHENOLIC RESIN.....	94
7.1	INTRODUCTION	94
7.2	EXPERIMENTAL.....	94
7.3	RESULTS	97
7.4	DISCUSSION.....	104
7.5	CONCLUSIONS.....	109
7.6	REFERENCES	109
	APPENDIX A.....	110

APPENDIX B	111
APPENDIX C	115

LIST OF TABLES

Table 2-1 Common Experimental Conditions used for VOC analysis.....	11
Table 2-2 Errors in accuracy from various measurement sources.....	12
Table 3-1 Summary of the reactions of AH^+ with hexamethyldisiloxane.....	20
Table 3-2 Reactions of protonated hexamethyldisiloxane with neutrals.....	25
Table 3-3 Reaction of protonated hexamethyldisiloxane with selected terpenes.....	29
Table 4-1 Summary of the reactions of M^+ to form the trimethylsilyl cation.....	45
Table 4-2 Reactions of protonated trimethylsilanol with neutrals. Shaded areas indicate where no rate coefficients were measured due to their previous measurements in the literature.	50
Table 4-3 Observations when protonated trimethylsilanol is allowed to react with selected terpenes. Known literature data are shown for comparison.....	52
Table 5-1 Summary of the reactions of the trimethylsilyl cation with various neutrals. The dark shaded area is a rate coefficient not measured since it is present in the literature.....	68
Table 6-1 Errors associated with volume delivery involving the volumetric glassware.....	81
Table 6-2 Comparison of measured Henry's Law constants and constants listed in the literature. The percent difference reported is the difference between the average value measured using the flowing afterglow and the average value reported in the literature.	91
Table 7-1 Hypothesized Identities of VOCs detected.....	98

Table 7-2 Neutrals detected by Iwakami and coworkers..... 106

LIST OF FIGURES

- Figure 2.1 A schematic diagram of the University of Pittsburgh's FA apparatus illustrating its major sections. The pressures indicated are uncalibrated ion gauge readings for a typical experiment at a flow tube pressure of 0.3 Torr of helium (capacitance manometer measurement). The pumping speeds listed are for diffusion pumps and reflect values for air. 6
- Figure 3.1 A branching ratio plot of the reaction of protonated hexamethyldisiloxane with pyridine. Note the disappearance of protonated pyridine (m/z 80, x) and formation of the trimethylsilyl transfer product (m/z 152, ■) and the proton-bound dimer of pyridine (m/z 159, ◆).
..... 27
- Figure 3.2 A branching ratio plot of the reaction of protonated hexamethyldisiloxane with diethylamine. Note the disappearance of protonated diethylamine (m/z 74, x), and formation of the trimethylsilyl transfer product (m/z 146, ■) and the proton-bound dimer of diethylamine (m/z 147, ◆). 28
- Figure 4.1 A representative spectrum of protonated trimethylsilanol. The spectrum is normalized to the intensity of protonated trimethylsilanol 49
- Figure 4.2 Branching Ratio plots indicating the appearance of a secondary trimethylsilyl transfer product. The reaction of protonated trimethylsilanol with either dimethylformamide (left) or

pyridine (right) demonstrates the reaction of protonated base (x) to form the trimethylsilyl transfer product (■) and the proton-bound dimer (□).	51
Figure 5.1 Typical spectrum of the trimethylsilyl cation formed from the reaction of Ar ⁺ with Me ₄ Si.....	66
Figure 5.2 Plots of <i>k_{obs}</i> vs pressure. The data from 1 X 10 ⁻⁷ to 1 X 10 ⁻⁶ Torr was generated by Munson and coworkers. ²⁴	74
Figure 6.1 Setup of Headspace Collection using a 250 mL RB flask and sealed with a septum. Notice the modified hypodermic syringe.....	82
Figure 6.2 Overview of the exponential dilution flask. A known flow of helium gas is passed through the flask. A known volume of vapor is injected into the flask via the septum.....	83
Figure 6.3 Plot of intensities of the hydronium ion (<i>m/z</i> 19) and protonated acetonitrile (<i>m/z</i> 42) vs. time as the septum is pierced and the flask removed for 50, 500, and 500 ppm acetonitrile solutions.	84
Figure 6.4 Plot of headspace concentration (ppm) vs. concentration of the liquid (M) for acetonitrile. The inset is an expansion showing data from the 5, 50, and 500 ppm standards. ..	85
Figure 6.5 Graph of the intensity of protonated acetone (<i>m/z</i> 59) and the hydronium ion (<i>m/z</i> 19) vs. time for 50, 500, and 5000 ppm MeCN solutions.	86
Figure 6.6 Plots of the headspace concentration (ppm) vs. the concentration of liquid (M) for acetone. See text for description of error bars.	87
Figure 6.7 Semi logarithmic (top) and linear (bottom) graphs of ethyl acetate vapor being injected into an exponential dilution flask. <i>m/z</i> 19 is the hydronium ion (reactant ion), 89 is protonated ethyl acetate, and 90 is an isotopomer of protonated ethyl acetate.....	88

Figure 6.8 A graph comparing the concentration detected using the CRMS vs. the concentration predicted using the exponential dilution flask theory. The inset includes the full range of CRMS data. See the introduction for an explanation of exponential flask theory..... 89

Figure 7.1 An overview drawing of the SS heated cell. Note that the drawing is not to scale. For other drawings, see appendix C..... 95

Figure 7.2 Picture of the custom made SS flange at ~900°C (left) and the programmed temperature ramp of the apparatus from RT-900°C 96

Figure 7.3 Selected ion chromatograms for the sampling of the headspace of a graphitic board from RT-900°C. The blank (right) and 1.2360 g sample (left) are normalized to the sum of the ions extracted. 99

Figure 7.4 Selected ion chromatograms for the sampling of the headspace of a graphitic board from RT-900°C. The blank (left) and 71.5 mg sample (right) are normalized to the total ion current. The spikes observed on the blank are from the isobaric H₂O⁺ ion (*m/z* 18)..... 100

Figure 7.5 Real-time quantification of the 71.5 mg piece of graphitic board as shown in Figure 7.4 and discussed in the text. The blank (left) and 71.5 mg sample (right) are normalized to the total ion current. 101

Figure 7.6 Selected Ion Chromatograms for the sampling of the headspace of a 8.0 mg sample of pure phenolic resin heated from room temperature to 900°C. The blank (left) and 8.0 mg sample (right) are normalized to the total ion current. 102

Figure 7.7 Selected ion chromatograms for the sampling of the headspace of a graphitic board from room temperature to 750 °C using protonated hexamethyldisiloxane (Me₃Si)₂OH⁺ as the reagent ion. The blank (left) and 80.6 mg sample (right) are normalized to the total ion current. 103

Figure 7.8 The study of VOCs that are released when 5 mg of phenolic resin is heated (right) and its blank (left). The VOCs detected correlate with the findings of Iwakami and coworkers: trimethylamine (m/z 60) and ethylenimine (m/z 44). 107

Figure 7.9 The detection of VOCs from a 5 mg sample of phenolic resin (right) and a blank (left). The VOCs detected from our analysis which correlates with Bouajula and coworkers are phenol (m/z 95), methylated phenol (m/z 109), dimethylated phenol (m/z 123), xylenes (m/z 107), and toluene (m/z 93). 108

LIST OF SCHEMES

- Scheme 3-1 Formation and reaction of protonated hexamethyldisiloxane via proton transfer with acetone. Note the isomeric m/z 117 formed due to the excess exothermicity of the reaction. 22
- Scheme 3-2 Reaction of protonated hexamethyldisiloxane with a base B. The primary products formed are proton transfer, trimethylsilyl transfer, and/or cluster ion formation. A secondary product of a proton-bound dimer can be formed from either the protonated neutral or the cluster ion. 33
- Scheme 3-3 The reaction of protonated hexamethyldisiloxane with pyridine forming the primary products of protonated pyridine and the trimethylsilyl transfer product. An unconventional secondary product of protonated pyridine reacting with an equivalent of hexamethyldisiloxane is formed in addition to the proton-bound dimer of pyridine. 34
- Scheme 4-1 Preferred Formation of protonated trimethylsilanol and subsequent reaction with excess water present in the flow tube. Enthalpies of reaction are in units of kcal/mol. 48
- Scheme 4-2 Reaction of protonated trimethylsilanol with a base B 55
- Scheme 5-1 Formation of the trimethylsilyl cation and subsequent reaction with excess tetramethylsilane. All thermochemical data are in units of kcal/mol. 70
- Scheme 5-2 Generalized scheme for the reaction of a base B with the trimethylsilyl cation..... 71

Scheme 5-3 Hypothesized scheme of methane loss for the reaction of the trimethylsilyl cation
with acetic acid 75

PREFACE

I would first like to thank Prof. Joseph Grabowski for his guidance and support through my graduate student career. Joe has not only introduced me to the world of mass spectrometry, but has trained me on how to be a professional in the world of chemistry. I would also like to thank Drs. Adrian Michael, Stephen Weber, and Hadad for their additional assistance and guidance in my “career” here. Even though he is at another position, I would like to thank Dr. Kasi Somalujula for his training in the area of commercial mass spectrometry. Not only did he train me in that area, he also trained me in the area of problem solving and personal interaction, which I will find invaluable. I also would like to thank former and current Grabowski group members: Kevin Davies, Christopher Taormina, Kyle Tilger, Thomas Watson, Abdil Ozdemir, Daniel Owusu, and Slava Fishman for all of their assistance.

I also would like to thank everyone in the electronic shop: David Emala, Robert Muha, for their help. They have been helpful in fixing everything that needed to be fixed in addition to helping me design the SS heated cell. The machine shop and its staff: Jeff and Dennis Sicher have been helpful in getting the CRMS detection end upgraded in addition to manufacturing the SS heated cell. Bob Greer at the glass shop has been helpful in the repair and fabrication of many apparatus. I also would like to thank all of the secretaries of the main office and all of the acquaintances I have met during my “tenure” here at Pitt.

I would like to thank my wife, Jessica and my sons, Xavier and Nathaniel, for their patience during this time. I know it has been hard on all of us. I would like to thank my mother and late father, Bonnie and Willard, for their upbringing and believing in me.

1.0 INTRODUCTION

The flowing afterglow is a device that was originally used to study ion/molecule reactions occurring in space. Norton and coworkers published a paper using the flowing afterglow to investigate ion/molecule reactions originating in the Martian ionosphere.¹ Since that time, the uses of the flowing afterglow have been modified to study organic reactions in the absence of solvent in addition to trace gas detection.^{2,3}

The use of the flowing afterglow for trace detection of volatile organic compounds (VOCs) has occurred in the last 10 years. The technique utilizes known ion/molecule reaction products along with quantitative data (i.e. rate coefficients, branching ratios). Quantitation of VOCs in a sample can occur without any external or internal standards once the fundamental ion chemistry is known.

The first attempt of quantifying VOCs was published by Lindinger and coworkers.⁴ They used the radical cation of xenon to detect benzene. The fragmentation products from the ion/molecule reaction with benzene did not allow for any meaningful interpretation. Lindinger and coworkers published the use of the hydronium ion as the reactant ion placed in a uniform electric field (PTR-MS).⁵ The hydronium ion usually transfers a proton to a neutral whose proton affinity (PA) is larger than that of water, which allows for less fragmentation than by other methods. Lagg and coworkers have used the PTR-MS for a variety of applications, such as detecting the VOCs emitted from strawberries to detect spoilage.²

Smith and coworkers have used the selected ion flow tube (SIFT) to detect and quantify VOCs. One advantage in using the SIFT over the flowing afterglow is that one ion can be selected out of many, which simplifies the interpretation of the ion chemistry. The fundamental ion chemistry of the hydronium ion (H_3O^+), the radical cation of oxygen ($\text{O}_2^{+\bullet}$), and NO^+ have been investigated with a variety of compounds such as amines,⁶ ketones,⁷ aromatics,⁸ and alcohols.⁹ The products of the ion/molecule reaction are identified along with the determination of the branching ratio (if needed) and the rate coefficient. The SIFT has been used to determine the amount of isoprene in breath, which has been linked to the amount of cholesterol present in blood.¹⁰ Another experiment using the SIFT was to determine the concentration of ammonia and amines in urine headspace.¹¹ Amines found in urine have been linked to renal failure.

Other groups have utilized the ability of the SIFT to detect VOCs. Wilson and coworkers have used the SIFT to determine the concentration of ethanol present in blood using Henry's law by sampling the headspace.¹² Custer and coworkers have used the negative ion complement to the hydronium ion, the hydroxide anion (OH^-), to detect VOCs present from leaf wounding and specifically the formation of HCN.¹³

The elucidation of isobaric species present in VOC analysis is a challenge since the mass spectrometer only returns an m/z value. Smith and coworkers have suggested to use H_3O^+ , $\text{O}_2^{+\bullet}$, and NO^+ concurrently to detect VOCs.¹⁴ The ions react with the same neutral differently, which would then lend insight to the VOC's identification. Another means of identifying isobaric VOCs has been the use of gas chromatography to separate compounds and then to allow them to elute from the column into a PTR-MS.¹⁵ Lindinger alluded to the varying of the electric field strength in the drift tube to determine isobaric species.² Each technique has its drawbacks and benefits. For example, the gas chromatograph can be used to separate isobaric compounds if

their retention times are different. The drawback of this technique is that the real time analysis of VOCs is limited to the chromatographic run time. Varying the electric field of the drift tube or using various reagent ions allow positive identification of the VOCs present in the sample, but does not allow for “online and real-time” VOC analysis.

The hydronium is a commonly used reagent ion for VOC analysis. One problem with its use is that it transfers a proton to most VOCs, only allowing tentative identification of VOCs. Smith and coworkers have used O_2^{+*} and NO^+ in addition to H_3O^+ to facilitate identification.¹⁴ While NO^+ can be used in conjunction with the hydronium ion to facilitate identification, O_2^{+*} usually generates a myriad of product ions especially if more than one neutral is introduced.¹⁴

1.1 CONCLUSIONS

The experimental methodology of the flowing afterglow is discussed in chapter 2. The ion/molecule chemistry of protonated hexamethyldisiloxane (Ch 3), protonated trimethylsilanol (Ch 4), and the trimethylsilyl cation (Ch 5) are discussed in this manuscript as candidates to replace the hydronium ion for VOC analysis. Control experiments involving Henry’s law and the exponential flask technique in the quantitation of VOCs are discussed in chapter 6. The VOCs emitted from phenolic resin placed on a graphitic board are discussed in chapter 7.

1.2 REFERENCES

1. Norton, R. B.; Ferguson, E. E.; Fehsenfeld, F. C.; Schmeltekopf, A. L. *Planetary Space Sci.* **1966**, *14*, 969-978.
2. Lagg, A.; Taucher, J.; Hansel, A.; Lindinger, W. *Int J Mass Spectrom Ion Proc* **1994**, *134*, 55-66.
3. Spanel, P.; Pavlik, M.; Smith, D. *Int J Mass Spectrom Ion Proc* **1995**, *145*, 177-186.
4. Lindinger, W.; Hirber, J.; Paretzke, H. *Int J Mass Spectrom Ion Proc* **1993**, *129*, 79-88.
5. Lindinger, W.; Hansel, A.; Jordan, A. *Int J Mass Spectrom Ion Proc* **1998**, *173*, 191-241.
6. Spanel, P.; Smith, D. *Int. J. Mass Spectrom.* **1998**, *176*, 203-211.
7. Spanel, P.; Ji, Y. F.; Smith, D. *Int J Mass Spectrom Ion Proc* **1997**, *165/166*, 25-37.
8. Spanel, P.; Smith, D. *Int. J. Mass Spectrom.* **1998**, *181*, 1-10.
9. Spanel, P.; Smith, D. *Int J Mass Spectrom Ion Proc* **1997**, *167/168*, 375-388.
10. Spanel, P.; Smith, D. *Rap. Comm. Mass Spectrom.* **1999**, *13*, 1733-1738.
11. Smith, D.; Spanel, P.; Holland, T. A.; Singari, W. A.; Elder, J. B. *Rap. Comm. Mass Spectrom.* **1999**, *13*, 724-729.
12. Wilson, P. F.; Freeman, C. G.; McEwan, M. J.; Allardyce, R. A.; Shaw, G. M. *Applied Occupational and Environmental Hygiene* **2003**, *18*, 759-763.
13. Custer, T. G.; Kato, S.; Fall, R.; Bierbaum, V. M. *Int J Mass Spectrom* **2003**, *223-224*, 427-446.
14. Smith, D.; Diskin, A. M.; Ji, Y. F.; Spanel, P. *Int J Mass Spectrom* **2001**, *209*, 81-97.

2.0 EXPERIMENTAL METHODOLOGY

2.1 EXPERIMENTAL PROTOCOL

A schematic of the flowing afterglow is shown in Figure 2.1. The flowing afterglow consists of three regions: ion generation, reaction, and detection. An electrical current is passed through a tungsten filament to create high energy electrons, which upon reaction with the added neutral, ultimately lead to the formation of the reagent ions. If other reagents are added to generate the reagent ion of choice, the second reagent is first added 36.3 cm from the nose cone (inlet B). Enough reagent is added to ensure that all reactant ions have been quenched. The defined flow of the neutral added at inlet B is relocated to inlet C (~100 cm from the nose cone). The sample, which is to be analyzed by the reaction with the reactant ion, is added at a fixed distance from the nose cone, depending on the experiment performed. The ions are extracted from the flow tube into the detection end through an orifice plate and a series of lenses, mass-separated by a quadrupole and directed to an electron multiplier for detection and collection by a Merlin Automation System (Extrel CMS) or by a custom-built data collection system.

Qualitative product, rate coefficient, and branching ratio determinations were performed to fully characterize the ion/molecule chemistry. This includes two qualitative experiments conducted on separate experimental days. An experimental day is

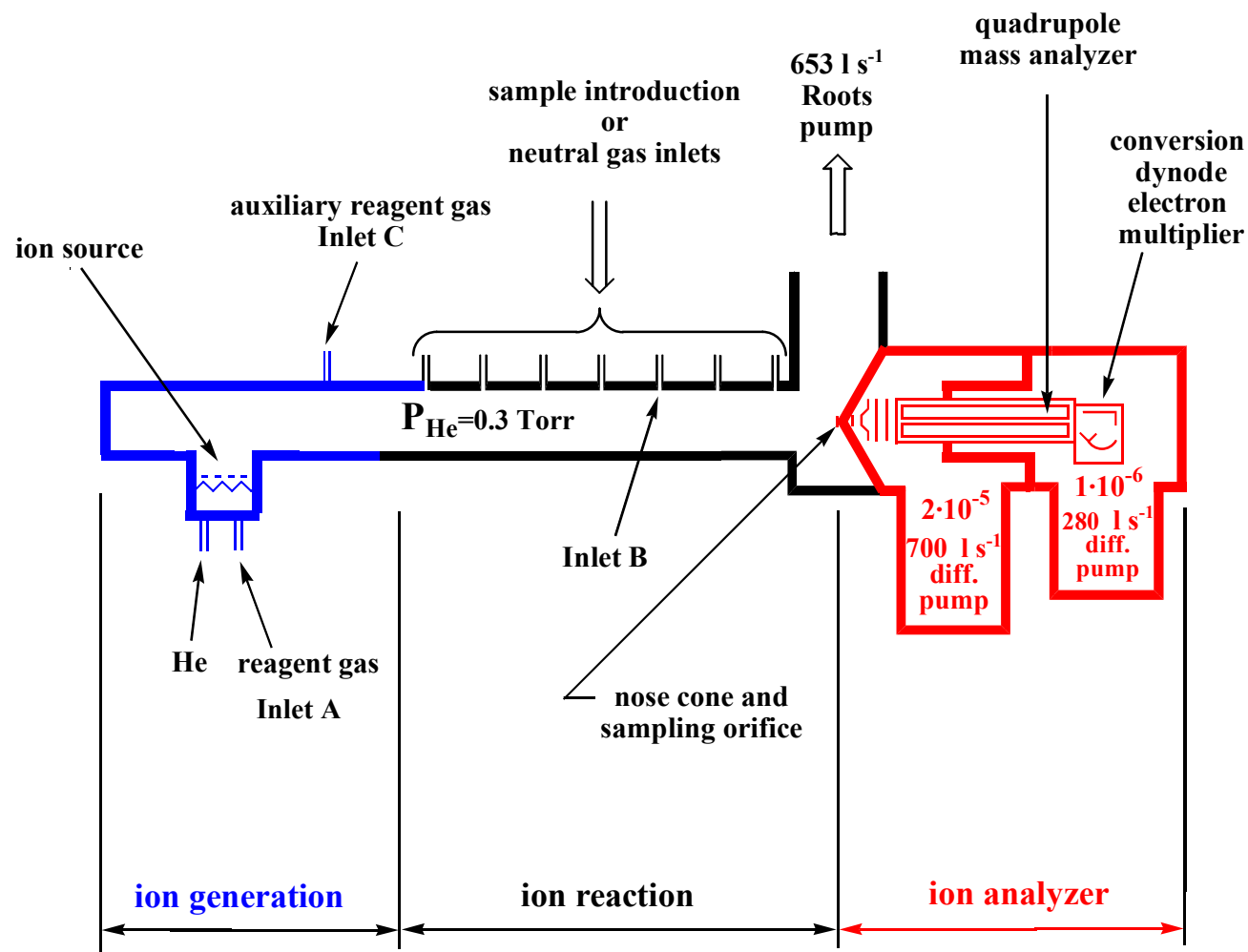


Figure 2.1 A schematic diagram of the University of Pittsburgh's FA apparatus illustrating its major sections. The pressures indicated are uncalibrated ion gauge readings for a typical experiment at a flow tube pressure of 0.3 Torr of helium (capacitance manometer measurement). The pumping speeds listed are for diffusion pumps and reflect values for air.

defined as the complete startup and shutdown of the instrument. Qualitative experiments determine the m/z values of an ion/molecule reaction. Changing the concentration of the neutral in the flow tube provides insight as to the formation of products, whether they be primary or secondary.

In addition, the rate coefficient of the ion/molecule reaction is measured. Since, the measurement of a rate coefficient is a standard and well-known experiment;^{1,2} only unique details of such measurements will be discussed. To ensure accuracy, the rate coefficient is measured a minimum of five times over two experimental days and the average of these independent measurements is reported. The error attached to a reported rate coefficient is the precision in these measurements. The accuracy of a measured rate coefficient is estimated as 20%; the primary contributor to the uncertainty are all flow measurements. The efficiency of reaction reported is defined as the ratio between the measured rate coefficient and the collisional rate coefficient. The calculation of the collisional rate coefficient is well established.³

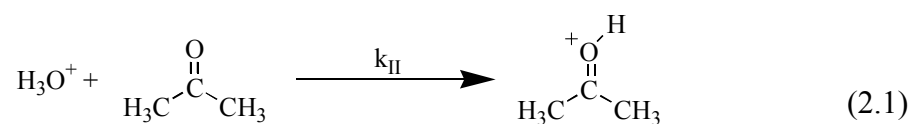
The final experiment used to characterize an ion/molecule reaction is the measurement of the branching ratio (i.e., the absolute yield of competing products). In this work, the method of measuring the branching ratio used is that is described by Anderson and coworkers.⁴ In this technique, the intensities of the reactant ion and product ions are recorded as the flow of the neutral is varied at a fixed distance (i.e., in effect, changing the extent of reaction). A plot of relative intensity of the product ions versus the extent of loss of the reagent ion is then generated. The slope of the lines of each product ion at 0% conversion is its respective branching ratio. The error in the slope is used as error in the branching ratio. If a curvature of product ion intensities is observed, then a secondary reaction must be occurring, and which either removes or adds to

that product ion. These branching ratio plots are then used to construct chemical reaction schemes.

In a VOC analysis experiment, the desired reagent ion is generated, and the sample is introduced at a fixed distance from the nosecone. Volatile organic compounds can be identified by using the following technique. The identities of the neutrals are inferred by the knowledge of the chemistry occurring in the sample and by previous fundamental ion/molecule chemistry. The VOCs can be quantitated, as described in the next section.

2.2 DERIVATION OF QUANTITATION OF THE CRMS

An example of a bimolecular ion/molecule reaction is H_3O^+ reacting with acetone to produce protonated acetone and water, having a bimolecular rate coefficient k_{II} (eq 2.1). A first



order integrated equation assuming that the hydronium ion concentration is much larger than the concentration of acetone can be written (eq 2.2), where $[\text{Acetone}]_t$ is the concentration of acetone

$$[\text{Acetone}]_t = [\text{Acetone}]_0 e^{-k_{II} [\text{H}_3\text{O}^+]_0 t} \quad (2.2)$$

at time t , $[\text{Acetone}]_0$ and $[\text{H}_3\text{O}^+]_0$ are the concentration of acetone and the hydronium at time $t=0$, respectively, and t is the reaction time.

Since a neutral species cannot be directly detected in our CRMS, we need to write the concentration of acetone at time t in terms of observable ion signals (eq 2.3). Eq 2.3 is a

$$[\text{Acetone}]_t = [\text{Acetone}]_0 - [\text{Acetone-H}^+]_t \quad (2.3)$$

mass-balanced description of the limiting reagent acetone. Substituting eq 2.3 into eq 2.2 and solving for the initial concentration of acetone leads to eq 2.4.

$$[\text{Acetone}]_0 = \frac{[\text{Acetone-H}^+]_t}{\left(1 - e^{-k_{II} [\text{H}_3\text{O}^+]_0 t}\right)} \quad (2.4)$$

When the experimental conditions are correctly chosen such that $k_{II} t [\text{H}_3\text{O}^+]_0 \ll 1$, then $1 - e^{-k_{II} [\text{H}_3\text{O}^+]_0 t}$ simplifies to $k_{II} [\text{H}_3\text{O}^+]_0 t$ and eq 2.4 can be rewritten as eq 2.5. It must be noted that in eq 2.5, the concentrations of ions cannot be measured directly. However, the count rates of the ions can be. The relation of the concentration of protonated acetone and the

$$[\text{Acetone}]_0 = \frac{[\text{Acetone-H}^+]_t}{k_{II} [\text{H}_3\text{O}^+]_0 t} \quad (2.5)$$

hydronium ion to their count rates is expressed in eq 2.6, where C is an unknown conversion factor assumed to be constant across the entire observed mass range, t is the reaction time, and $[\text{H}_3\text{O}^+]_0$ is the concentration of the hydronium ion at time t=0.

$$\frac{[\text{Acetone-H}^+]_t}{[\text{H}_3\text{O}^+]_0} = \frac{C \{\text{Acetone-H}^+\}}{C \{\text{H}_3\text{O}^+\}_0} \quad (2.6)$$

Using eq 2.7, the number density of a particular VOC in the flow tube can be determined. Relating the number density of the VOC to the number density of the bulk sample containing that VOC yields the mixing fraction of that VOC.

$$[\text{A}]_{\text{ppm}} = \frac{[\text{A}]_0}{[\text{Sample}]} 10^6 \quad (2.7)$$

It should be noted here that because the bulk sample is diluted 1000-10,000 fold when it is introduced into the helium buffer gas, the detected mixing fraction in the flow tube is considerably smaller than in the bulk sample.

2.3 EVALUATING ASSUMPTIONS

One of the assumptions mentioned in section 2.2 is that as $k_{II}[\text{H}_3\text{O}^+]t$ in $(1-e^{-(k_{II}[\text{H}_3\text{O}^+]t)})$ approaches 0, $(1-e^{-(k_{II}[\text{H}_3\text{O}^+]t)})$ can be approximated by $k_{II}[\text{H}_3\text{O}^+]t$. The assumption that $(1-e^{-(k_{II}[\text{H}_3\text{O}^+]t)})$ is effectively $k_{II}[\text{H}_3\text{O}^+]t$ under the conditions we employ to determine quantities can be evaluated by examining these two expressions using typical experimental variables. Eq 2.8 shows how reaction time is related to the experimental variables. The list of commonly used experimental conditions is shown in Table 2.1, having r , α , and R set to be 3.65 cm, 1.6, and 62365.6 cm³ Torr/mol K respectively. R is the gas constant, α is a correction factor,⁵ and r is the radius of the flow tube. Evaluating eq 2.8 using the data from Table 2.1, gives a reaction time of 6.1 ms. Evaluation of $(1-e^{-(k_{II}[\text{H}_3\text{O}^+]t)})t = 6.1$ ms and the k_{II} and $[\text{H}_3\text{O}^+]$ values noted in table 2.1

$$t = \frac{z P_{\text{He}} \pi r^2}{\alpha F_{\text{He}} R T} \quad (2.8)$$

Table 2-1 Common Experimental Conditions used for VOC analysis

Experimental Variable	Magnitude
$[\text{H}_3\text{O}^+]$	3×10^6 counts/s
k_{II}	3.9×10^{-9} cm ³ molecule ⁻¹ s ⁻¹
T	298.3 K
P_{He}	0.310 Torr
z	76.7 cm
F_{He}	5.9×10^{-3} mol/s

a value of 7.02×10^{-5} . Evaluation of $(k_{II}[\text{H}_3\text{O}^+]t)$ yields a value of 7.02×10^{-5} . In other words, under the conditions discussed in table 2.1, $(1 - e^{-(k_{II}[\text{H}_3\text{O}^+]t)}) = (k_{II}[\text{H}_3\text{O}^+]t)$.

The final assumption made is that the concentration of the reagent ion is much larger than the concentration of the VOC (e.g., $[\text{H}_3\text{O}^+] \gg [\text{Acetone}]$). This assumption will be validated in Chapter 5.

2.4 PROPAGATION OF ERRORS

The expression used with readily known variables that determines the number density of a VOC is shown in eq 2.9. Table 2.2 lists all of the errors associated with one measurement of a VOC and their sources. The errors mentioned in table 2.2 regarding the hydronium ion and $[\text{HA}^+]$ are

Table 2-2 Errors in accuracy from various measurement sources

Variable	Error (± %)	Source
k_{II}	20	Adams, N.G.; Church, M.J.; Smith, D. <i>J Phys D</i> 1975 , 8, 1409-1422.
P_{ft}	0.08	MKS Calibration
F_{he}	2.10	Wet test meter calibration by Morris on 10/21/2005.
T	2	Thermometer
r	1	Measurement by Morris on 4/3/07
$[H_3O^+]$	1	See text for explanation
$[HA^+]$	5	See text for explanation
z	6.8	Alge, E.; Adams, N. G.; Smith, D. <i>J. Phys. B</i> 1983, 16, 1433-1444.
F_{sample}	2.13	See text for description
α	3	Adams, N. G.; Church, M. J.; Smith, D. <i>J. Phys. D</i> 1975 , 8, 1409.

assumed numbers and are taken as a best case scenario for counting statistics. The user should report their own errors in counting statistics.

$$[A]_0 = \frac{\{HA^+\}_t \alpha F_{He} R T}{k_{II} \{H_3O^+\} z P_{He} A} \quad (2.9)$$

A general propagation of errors is shown in that includes covariances (eq 2.10). The following is an analysis of the variances and covariances that exist in the error analysis. The bimolecular rate coefficient (k_{II}) can be dependent on temperature and pressure. If the

$$S_x^2 = S_u^2 \left(\frac{\delta x}{\delta u} \right)^2 + S_v^2 \left(\frac{\delta x}{\delta v} \right)^2 + 2S_{uv} \left(\frac{\delta x}{\delta u} \right) \left(\frac{\delta x}{\delta v} \right) + \dots \quad (2.10)$$

rate coefficient of the ion/molecule reaction of interest is dependent on pressure, that is insignificant since the experiment is ran at a fixed pressure and temperature . Therefore, no

covariance exists with k_{II} . In the proposed experiment, the following are held or are constant and therefore no covariances exist amongst them: temperature, the reaction distance, the flow of sample, the flow of helium, and the pressure in the flow tube. Since we assume that $[H_3O^+] \gg [HA^+]$, there are no covariances amongst these two variables either. Therefore, there are no covariances present in this experiment and the error analysis can be treated without including covariances.

The flow of a sample is determined by measuring the pressure change over time as a calibrated volume (eq 2.11). The delta pressure term is determined by the reading of two separate pressures along with one time measurement.

$$F_A = - \frac{\Delta P \text{ (Torr)}}{\Delta t \text{ (s)} T \text{ (K)}} \text{ Constant} \quad (2.11)$$

An entire experiment would then comprise of eight pressure measurements along with four time measurements and one temperature measurement. The error in one time measurement using a digital stopwatch that is accurate to 0.01s is 2%. The stated error in the 1000 Torr Baratron used for pressure measurements is 0.08%. Therefore, if one uses eq 2.10, the propagated error of F_A incorporating eq 2.11 is 2.13%.

The next correction to the VOC quantitation is an end correction. An end correction is a correction to the reaction distance. An end correction is needed since the distance is not varied in this experiment. Alge and coworkers have estimated the end correction for a ring inlet (the type on our instrument) to be 1-2 cm.⁵ The error associated with the reaction distance is 6.8%.

If one uses the errors listed in table 2.3, 6.8% for the reaction distance error, 2.13% for the sample flow error, and eq 2.10, the entire propagated error in a VOC measurement is 22% if all of the errors stated above are included. There is no covariance analysis needed in this error analysis.

2.5 REFERENCES

1. Norton, R. B.; Ferguson, E. E.; Fehsenfeld, F. C.; Schmeltekopf, A. L. *Planetary Space Sci.* **1966**, *14*, 969-978.
2. Adams, N. G.; Church, M. J.; Smith, D. *J. Phys. D* **1975**, *8*, 1409.
3. Su, T.; Su, E. C. F.; Bowers, M. T. *J. Chem. Phys.* **1978**, *69*, 2243-2250.
4. Anderson, D. R.; Bierbaum, V. M.; Depuy, C. H.; Grabowski, J. J. *Int J Mass Spectrom. Ion Phys.* **1983**, *52*, 65-94.
5. Alge, E.; Adams, N. G.; Smith, D. *J. Phys. B* **1984**, *17*, 3827-3833.

3.0 FACILE TRIMETHYLSILYL TRANSFER INVOLVING ION/MOLECULE REACTIONS OF PROTONATED HEXAMETHYLDISILOXANE

3.1 INTRODUCTION

The Selected Ion Flow Tube (SIFT)¹ and Proton Transfer-Mass Spectrometer (PTR-MS) have been used to identify and quantify volatile organic compounds (VOCs).² This technique utilizes known branching ratios, rate coefficients, and products from ion/molecule reactions reported in the literature. This method has advantages over other techniques such that no conventional “calibration” methods are needed for quantitation, and analysis of VOCs can occur on-line in real-time. Readily accessible experimental variables such as the intensity of the product and reactant ions and the value of the rate coefficient are needed for quantitation.³

Three reagent ions that have been used in VOC analysis are H_3O^+ , $\text{O}_2^{+\bullet}$, and NO^+ .⁴ While each of these ions has their advantages, they all suffer from some limitations. The hydronium readily clusters with water; these cluster ions can also react with the VOCs, complicating spectral interpretation.⁵ When $\text{O}_2^{+\bullet}$ is allowed to react with VOCs, dissociative charge transfer products are formed.⁶ NO^+ can form products through hydride ion transfer, clustering, and/or charge transfer.⁶ These limitations suggest that the development of novel reagent ions, which do not complicate spectra interpretation, would be useful. If one considers the CRMS approach in general and the reagent ion in detail, it can be argued that the ideal reagent ion possesses the

following attributes: (1) only one ion is produced during the reagent ion preparation, (2) the reagent ion and product ions corresponding to the VOCs being investigated are unreactive with the major components of air and breath (e.g. O₂, N₂, CO₂, H₂O), (3) the reaction between the reagent ion and the trace VOCs ideally has an efficiency of 1, and (4) the *m/z* values observed are readily traceable back to the VOCs identity. The hydronium ion performs well for criterion 1. Smith and others have reported the ability to generate ~100 Kcps of the hydronium ion using a selected ion flow tube.⁷ The hydronium ion and its product ions do cluster with water, but do not react with other major components of air and breath since their proton affinities are less than water. The hydronium ion partially fails criterion 3 since the cluster ions are unreactive with the major components of air and breath but are reactive with water. The radical cation of oxygen fulfills criteria 1, 2, and 5. The radical cation of oxygen does cluster with water, but not as efficiently as the hydronium ion (c.f. $k_{III} = 2.9$ vs. 6.65×10^{-28} molecule⁻² cm⁶ s⁻¹, respectively).^{8,9} O₂⁺ forms multiple dissociative charge transfer products with various neutrals such as ethers and therefore fails criterion 4.^{6,10} NO⁺ performs well in criteria 1, 2, and 4. NO⁺ can produce any of three products, which could allow for differentiation of the neutrals identity.¹⁰ Most reaction efficiencies are less than 1, and therefore NO⁺ fails at criterion 5. An alternative reagent ion could be useful for VOC analysis.

Fleming has referred to the trimethylsilyl group as a “large proton”.¹¹ One could envision replacing the “protons” on the hydronium ion sequentially with a trimethylsilyl moiety. That ion should then be evaluated against the criteria stated above in hopes of finding a candidate precursor ion suitable for VOC analysis. Chen and Stone have studied the ion chemistry of the trimethylsilyl cation with various amines and ammonia using a flowing afterglow.¹² They

postulated trimethylsilyl transfer from protonated trimethylsilanol to ammonia (eq 3.1). Wojtyniak and Stone have observed trimethylsilyl transfer using a high pressure mass



spectrometer and determined relative trimethylsilyl cation affinities.¹³ Trenerry and coworkers, using an ion cyclotron resonance spectrometer, also have determined relative trimethylsilyl cation affinities within certain classes of compounds (i.e. alcohol, esters).¹⁴

Trimethylsilyl transfer chemistry can be used in competition with proton transfer to probe a neutral's identity. This chapter focuses on the formation and reaction of protonated hexamethyldisiloxane ((Me₃Si)₂OH⁺). Tobita and coworkers have studied the mass ionized kinetic energy (MIKE) studies of *m/z* 147, an electron ionized fragment of hexamethyldisiloxane.¹⁵ Li and Stone have determined the proton affinity of hexamethyldisiloxane, but no group yet has studied reactions of protonated hexamethyldisiloxane with a variety of neutrals.¹⁶ The thrust of this chapter is to understand the fundamental ion chemistry of protonated hexamethyldisiloxane and to discuss the possibility of its use as a reagent ion that can be used to detect and identify VOCs on the breath of individuals¹⁷.

3.2 EXPERIMENTAL

Our flowing afterglow has been previously described in detail;¹⁸ only details unique to this work are described here. Helium (99.997%, Valley National Gas, Wheeling, WV) is used as the

carrier gas and is further purified by passage through a trap filled with a uniform mixture of 3A, 4Å and 13X molecular sieves and immersed in liquid nitrogen. Pressures in the flow tube were selected to be in the range from 0.250 – 0.500 Torr and flow rates of helium ranged from 120 – 180 STP cm³/s.

Qualitative experiments, which determine the m/z of the products made from an ion-molecule reaction, were performed at least twice over two experimental days in order to ensure reproducibility. An experimental day is defined as the complete startup and shutdown of the instrument. Pseudo-first order conditions were used for all experiments with the ion being the limiting reagent.

Rate coefficients were measured by monitoring the change in reactant ion intensity as the concentration of the neutral was changed. Rate coefficients were measured at least five times over two experimental days, and the error reported for each rate coefficient is the precision. The accuracy of a measured rate coefficient is $\pm 20\%$ or better, and is primarily limited by errors in the absolute pressure measurements and flow measurements.¹⁹ The listed error in accuracy is a propagation of all of the errors of the experimental variables. The efficiency of reaction reported is the ratio of the measured rate coefficient to the collisional rate coefficient. The collisional rate coefficient was calculated using the variational collision complex theory as described by Su and coworkers.²⁰ Polarizabilities and dipole moments, obtained from suitable sources, were used to calculate the collisional rate coefficient.²¹ The polarizability of trimethylphosphate was calculated to be $1.60 \times 10^{-23} \text{ cm}^3$ using the group additivity method of Miller and coworkers since no polarizability has been reported in the literature.²² For the cases where no discernable reaction occurred, an upper limit of the rate coefficient was determined.

The reported branching ratios are measured twice over two experimental days using the

method described by Anderson and coworkers.²³ The reported branching ratios are averaged over separate experiments conducted on different experimental days. The branching ratio plots also can determine secondary products, which are defined as the reaction of a primary product ion with a second equivalent of the neutral in the reaction being investigated. The importance of a secondary product is revealed by the appearance of a curvature in the data points of the branching ratio plots at longer reaction times.

The following reagents were obtained from the following sources and used without further purification: acetone, acetonitrile, triethylamine, furan (99% Fisher Scientific, Pittsburgh, PA), ethyl acetate, benzene (99.9% HPLC Grade Fisher Scientific), hexamethyldisiloxane (98% Sigma-Aldrich), deuterium oxide (99.9% D MDS Isotopes), 2-methylbutane (99.7%, Fisher Scientific), cyclopentene (96% Sigma-Aldrich), methyl butyrate (\geq 98%, Sigma-Aldrich), naphthalene (99+% Scintillation Grade, Sigma-Aldrich), methane (Grade 4.0 Valley National Gas), isoprene (99% Acros Organics), ammonia (semi-conductor grade, Matheson), ethanol (100%, Aaper Alcohol and Chemical Company), acetic acid (glacial, Fisher Scientific), trimethylphosphate, dimethylsulfide, pyridine (99+%, Sigma-Aldrich), methyl mercaptan (Matheson Gas Products), diethyl ether (99.7%, JT Baker), dimethylformamide (99+%, Fisher Scientific), and diethylamine (98+%, Avocado Research Lab). Tert-butyl chloride (99% Sigma-Aldrich) was placed in a flask containing 4Å molecular sieves (Fischer Chemical) to hinder the formation of tert-butyl alcohol via a hydrolysis reaction. All liquid reagents were subject to several freeze-pump-thaw cycles each experimental day to ensure contaminants other than the neutral of interest were removed. Deionized water was also deoxygenated by pumping at room temperature. A sweeper, a piece of glassware that facilitates

volatilization of compounds, was used for trimethylphosphate and naphthalene in qualitative and branching ratio determinations.

3.3 RESULTS

3.3.1 Formation of protonated hexamethyldisiloxane

Three reagent ions: protonated methane, the hydronium ion, and the tert-butyl cation were selected to see which would be a suitable candidate to form protonated hexamethyldisiloxane. These three ions were selected because of their capability of transferring a proton to hexamethyldisiloxane (HMDSO) in addition to the exothermicity of the proton transfer reaction (see Table 3.1).

Table 3-1 Summary of the reactions of AH^+ with hexamethyldisiloxane

AH^+	k_{II} (Eff) ^a	ΔH_{rxn} (kcal/mol) ^c
CH_5^+	2.83 ^b (1.000)	-72.4
H_3O^+	2.64 ± 0.20 (0.983)	-39.7
tBu ⁺	1.16 ± 0.09 (0.680)	-10.6

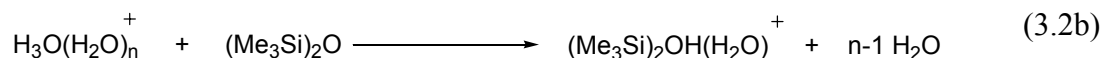
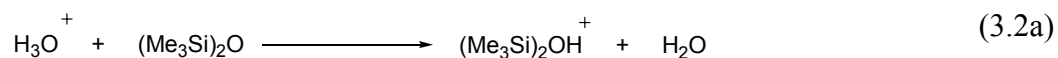
a—Units of $10^{-9} \text{ cm}^3 \text{ molecule}^{-1} \text{ s}^{-1}$. Eff = k_{obs}/k_{coll} . k_{coll} is calculated via the VTST theory of Su and Bowers.²⁰

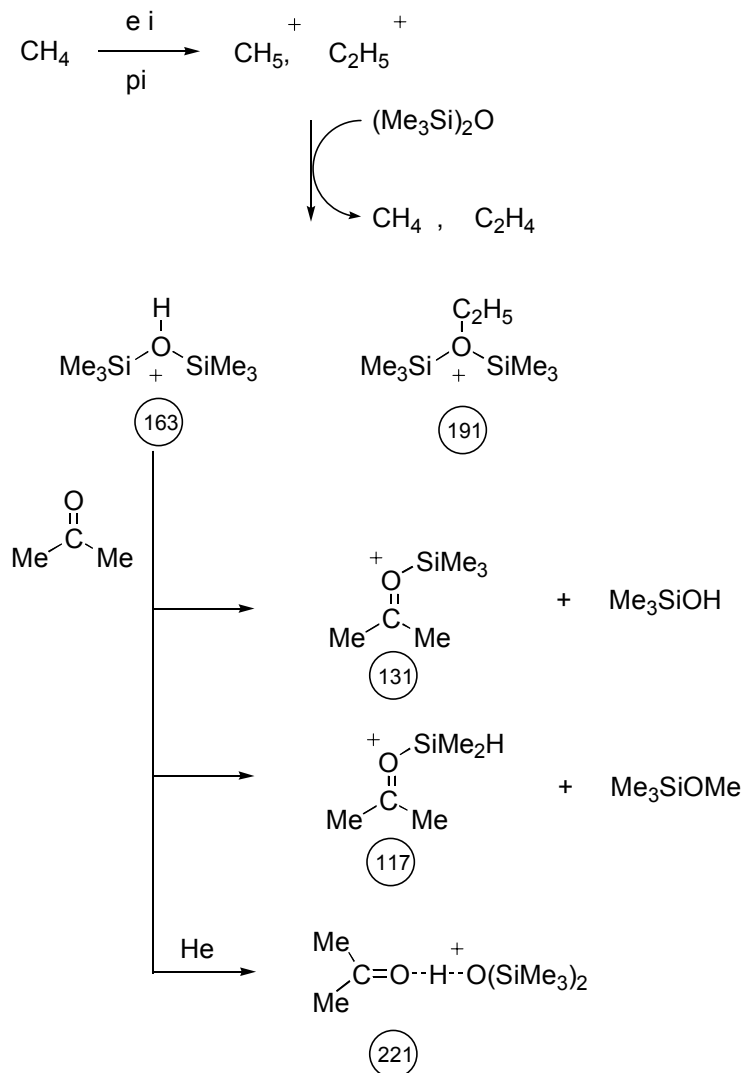
b—Assumption that $k_{coll} = k_{obs}$

c—Linstrom, P.J. (Ed.) NIST Chemistry Webbook (<http://webbook.nist.gov>, accessed 20 March 2007).

The first ion/molecule reaction explored was the reaction of CH_5^+ with HMDSO. When methane is ionized in the flowing afterglow, C_2H_5^+ is also formed.²⁴ When these ions are allowed to react with HMDSO, two m/z values are observed, 163 and 191 (Scheme 3.1). These m/z values are assigned as protonated hexamethyldisiloxane and $\text{C}_2\text{H}_5(\text{O}(\text{SiMe}_3)_2)^+$, respectively. This route of forming protonated hexamethyldisiloxane was dismissed because of the following observations. When protonated hexamethyldisiloxane was allowed to react with acetone, the following products were observed: m/z 131, 221, and 117 (also shown in Scheme 3.1). m/z 131 is assigned as the trimethylsilyl transfer product of acetone, m/z 221 is the proton-bound dimer of HMDSO and acetone, and m/z 117 was at first assigned as the proton-bound dimer of acetone. This assignment was changed when protonated hexamethyldisiloxane was allowed to react with d_6 -acetone. An unexpected mass shift of 6 Da occurred instead of the expected 12 Da. Another suitable route for the formation of protonated hexamethyldisiloxane was then explored.

The next attempt to form protonated hexamethyldisiloxane was to allow the hydronium ion to react with HMDSO. The products formed from this reaction are protonated hexamethyldisiloxane and the proton-bound dimer of water and HMDSO (eq 3.2a and b). The

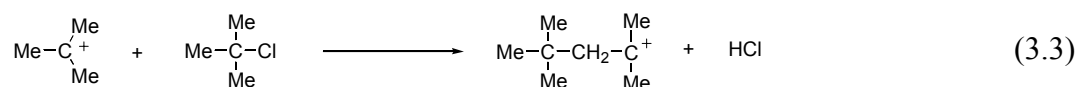




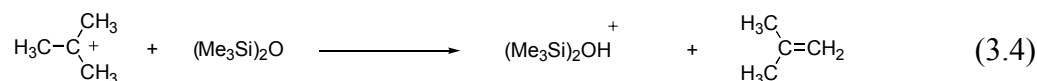
Scheme 3-1 Formation and reaction of protonated hexamethyldisiloxane via proton transfer with acetone. Note the isomeric m/z 117 formed due to the excess exothermicity of the reaction.

proton-bound dimer of water and HMDSO is formed via a solvent switching reaction with $\text{H}_3\text{O}(\text{H}_2\text{O})_n^+$ ($n=1-3$) to $(\text{Me}_3\text{Si})_2\text{OH}(\text{H}_2\text{O})^+$. $\text{H}_3\text{O}^+(\text{H}_2\text{O})_n$ is formed in the flow tube due to the reaction of the hydronium ion with excess water. Bierbaum and coworkers have characterized this clustering reaction.⁸ Since two products are formed via this reaction, a final attempt was made to form a “clean” spectrum of protonated hexamethyldisiloxane.

The final attempt to form protonated hexamethyldisiloxane was to ionize tert-butyl chloride. The tert-butyl cation (m/z 57) and $C_8H_{17}^+$ at m/z 113 are formed from this process (eq



3.3). When these complements of ions are allowed to react with HMDSO, a cleaner spectrum of protonated hexamethyldisiloxane is obtained then through the other routes of formation via the reaction stated in eq 3.4. This fulfills one of the criteria as mentioned in the introduction.



When $(\text{Me}_3\text{Si})_2\text{OH}^+$, formed via proton transfer from the tert-butyl cation, is allowed to react with acetone, an expected secondary product ion at m/z 117 is formed. d_6 -Acetone experiments show a shift of 12 Da, which indicates that the ion at m/z 117 is the proton-bound dimer of acetone. Since the tert-butyl cation generates the cleanest spectrum of protonated hexamethyldisiloxane, it was used to generate $(\text{Me}_3\text{Si})_2\text{OH}^+$ for reactions with neutrals since its ion chemistry involving acetone is well defined.

3.3.2 Reaction of protonated hexamethyldisiloxane with neutrals

A summary of the data obtained from the reaction of protonated hexamethyldisiloxane with selected neutrals is summarized in Table 3.2. When $(\text{Me}_3\text{Si})_2\text{OH}^+$ is allowed to react with 2-methylbutane, cyclopentene, benzene, methyl mercaptan, furan, isoprene, and naphthalene, no products are formed under our experimental constraints; for these reactions, an upper limit of the rate coefficient could be determined.

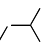

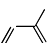

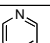
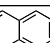
Cluster ions were observed when water, ethanol, and acetic acid were allowed to react with $(\text{Me}_3\text{Si})_2\text{OH}^+$. Plots of k_{obs} vs. pressure of helium do not exhibit any pressure dependence over 0.250 – 0.500 Torr for ethanol and acetic acid.

Acetonitrile, acetone, diethyl ether, and dimethylsulfide form both cluster and trimethylsilyl transfer products. The measured branching ratios and rate coefficients are shown in Table 3.2. Acetone forms a secondary product, which is identified by a curvature of the branching ratio (see experimental section), that is assigned as the proton-bound dimer of acetone. When the concentration of acetonitrile, diethyl ether, and dimethylsulfide were increased, no secondary products were observed.

When protonated hexamethyldisiloxane is allowed to react with ammonia and dimethylformamide, the secondary products observed are the proton-bound dimer of the base. This product is formed by a reaction of a protonated base with another equivalent of base in the presence of helium. Secondary and tertiary products formed when protonated dimethylformamide is allowed to react with one or two equivalents of dimethylformamide are the proton-bound dimer and trimer, respectively. No secondary or tertiary products are observed when trimethylphosphate is allowed to react with protonated hexamethyldisiloxane under our experimental constraints.

When pyridine is allowed to react with protonated hexamethyldisiloxane, the primary products formed are protonated pyridine and the trimethylsilyl transfer product of pyridine. Upon examination of the branching ratio plot, protonated pyridine (m/z 80) appears to react away to form the trimethylsilyl transfer product (m/z 152) in addition to forming the proton-bound dimer (m/z 159) as the concentration of pyridine is increased (Figure 3.1). In a separate

Table 3-2 Reactions of protonated hexamethyldisiloxane with neutrals

Neutral	k_{obs} (Eff) ^a	TMS T ^b		PT ^b		Other ^c
		BR ^c	$\Delta H_{rxn}^{d,e}$	BR ^c	$\Delta H_{rxn}^{d,f}$	
	$\leq 0.0009^g$ (≤ 0.001)					No Reaction
	$\leq 0.0009^g$ (≤ 0.001)				+ 19.1	No Reaction
C ₆ H ₆	$\leq 0.0002^g$ (≤ 0.001)		+20		+ 23.0	No Reaction
H ₂ O	$\leq 0.002^g$ (≤ 0.001)		+ 14		+ 37.3	100% Cluster
D ₂ O	0.0238 ± 0.0018 (0.077)					H/D Exchange/Cluster
MeSH	$\leq 0.0003^g$ (≤ 0.001)				+ 17.5	No Reaction
	$\leq 0.0002^g$ (≤ 0.001)				+ 4.8	No Reaction
	$\leq 0.008^g$ (≤ 0.007)				+ 10.3	No Reaction
EtOH	0.290 ± 0.032^h (0.175)		+2		+16.7	100% Cluster
EtOEt	0.46 ± 0.01^h (0.346)	92 ± 1 %	0		+ 4.3	8 ± 1 % Cluster
Me ₂ S	0.012 ± 0.010^h (0.009)	97 ± 1 %			+ 3.7	3 ± 1 % Cluster
MeCOMe	1.37 ± 0.10^h (0.603)	62 ± 1 %	-1		+ 8	38 ± 1 % Cluster
NH ₃	1.15 ± 0.17 (0.551)	85 ± 2 %	-4	15 ± 5 %	-1.7	
HCONMe ₂	1.88 ± 0.18 (0.705)	91 ± 4 %		9 ± 4 %	-14.7	
	1.68 ± 0.47 (0.931)	60 ± 1 %		40 ± 1 %	-19.7	
MeCN	0.25 ± 0.07^h (0.077)	9 ± 1 %			+ 16.1	91 ± 1 % Cluster
MeCO ₂ H	0.27 ± 0.06^h (0.180)				+ 15.0	100% Cluster
MeCO ₂ CH ₂ Me	1.19 ± 0.01 (0.804)	100%	-5		+ 2.6	
						No Reaction
(MeO) ₃ PO	0.53 ± 0.06 (0.254)	98 ± 1 %		2 ± 1 %	-9.7	
(Et) ₂ NH	0.73 ± 0.02 (0.581)	6 ± 1 %		94 ± 1 %	-25.3	
Et ₃ N	0.45 ± 0.06 (0.352)			100%	-32.4	

a—Units of $10^{-9} \text{ cm}^3 \text{ molecule}^{-1} \text{ s}^{-1}$. Eff = k_{obs}/k_{coll} . k_{coll} is calculated via the VTST theory of Su and Bowers.

b—TMST = trimethylsilyl transfer PT = proton transfer

c—Branching Ratios (BR) measured at 0.3 Torr flow tube pressure.

d—trimethylsilyl affinity of trimethylsilanol estimated by appearance or non-appearance of trimethylsilyl transfer product.

e—Linstrom, P.J. (Ed.) NIST Chemistry Webbook.

f—Upper limit of reactivity estimated by using highest flow of neutral introduced during qualitative reactions

g—Rates measured at 0.3-0.5 Torr flow tube pressure.

h—Polarizability of neutral estimated using the method obtained from Miller and coworkers

qualitative study, protonated pyridine (formed via proton transfer from the tert-butyl cation)

forms the trimethylsilyl transfer product when allowed to react with HMDSO.

The primary products that are formed when diethylamine is allowed to react with protonated hexamethyldisiloxane are protonated diethylamine and the trimethylsilyl transfer product as shown in Figure 3.2. A downward curvature is observed in the proton transfer product, while an upward curvature is observed with the trimethylsilyl product. An upward curvature is observed in the proton-bound dimer of diethylamine. This suggests that both the trimethylsilyl transfer product and the proton-bound dimer are secondary products arising from the reaction of protonated diethylamine with an equivalent of a neutral. No curvatures are observed in the trimethylsilyl transfer product when protonated hexamethyldisiloxane is allowed to react with the other neutrals (data not shown).

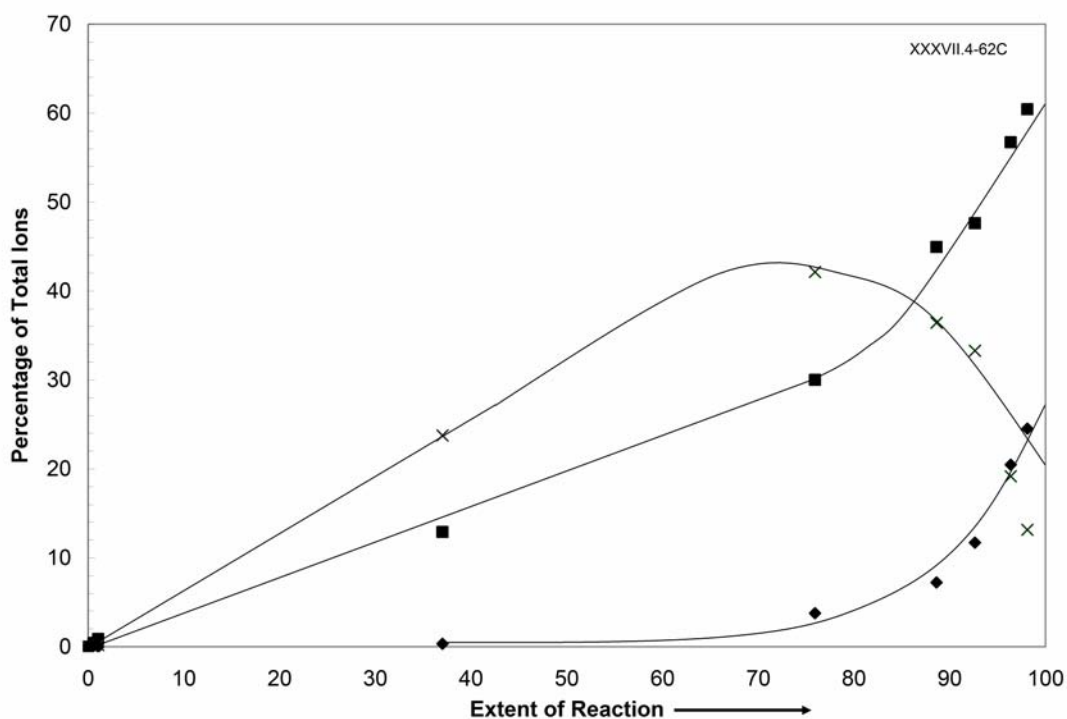


Figure 3.1 A branching ratio plot of the reaction of protonated hexamethyldisiloxane with pyridine. Note the disappearance of protonated pyridine (m/z 80, x) and formation of the trimethylsilyl transfer product (m/z 152, ■) and the proton-bound dimer of pyridine (m/z 159, ◆).

Only primary products are observed when protonated hexamethyldisiloxane is allowed to react with deuterium oxide, triethylamine, and ethyl acetate. $(\text{Me}_3\text{Si})_2\text{OH}^+$ performs H-D exchange with deuterium oxide along with clustering. $(\text{Me}_3\text{Si})_2\text{OH}^+$ reacts with triethylamine to form a proton transfer product.

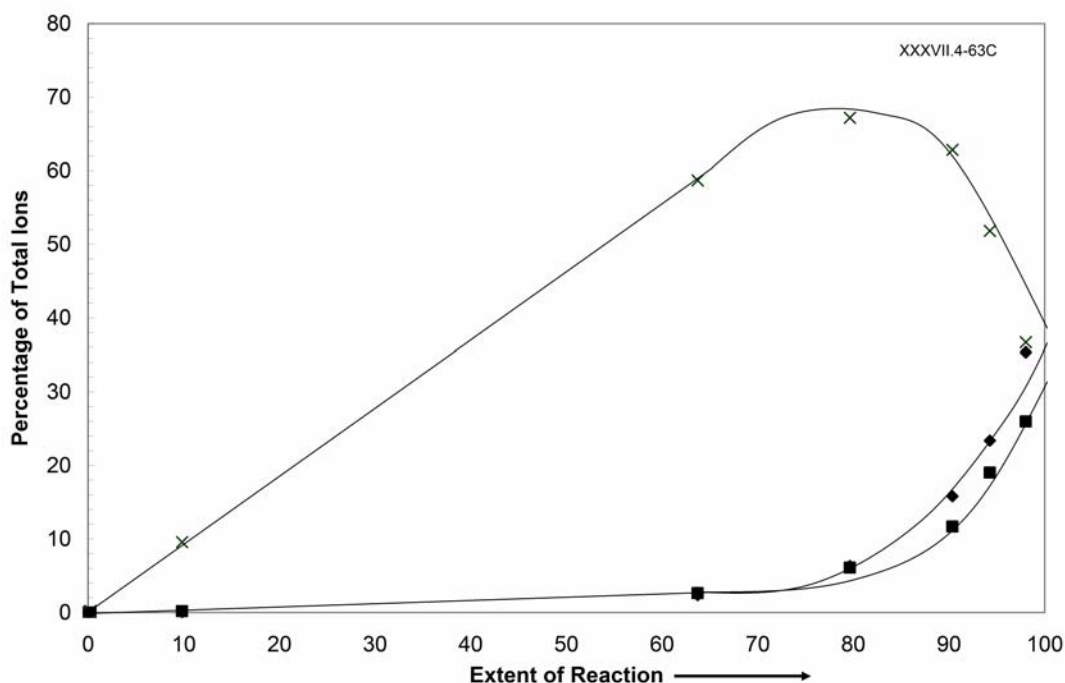


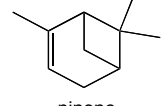
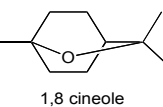
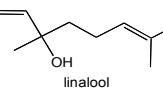
Figure 3.2 A branching ratio plot of the reaction of protonated hexamethyldisiloxane with diethylamine. Note the disappearance of protonated diethylamine (m/z 74, \times), and formation of the trimethylsilyl transfer product (m/z 146, \blacksquare) and the proton-bound dimer of diethylamine (m/z 147, \blacklozenge).

3.3.3 Terpenoids

When pinene, 1,8—cineole, and linalool were allowed to react with protonated hexamethyldisiloxane, proton transfer, water loss, and/or a loss of an R group are observed. When pinene is allowed to react with protonated hexamethyldisiloxane, protonated pinene is observed. The rate coefficient for the reaction was measured, but no collisional rate coefficient should be calculated since the data needed could not be found in the literature. When 1,8—cineole is allowed to react with protonated hexamethyldisiloxane, protonated cineole and a water

loss product is observed. The rate coefficient was measured and the collisional rate coefficient was calculated. When linalool was allowed to react with protonated hexamethyldisiloxane, protonated linalool, a water loss product, and an R loss is observed. No rate coefficient was measured for the reaction of protonated hexamethyldisiloxane due to the inability of achieving a suitable decrease of reactant ion.

Table 3-3 Reaction of protonated hexamethyldisiloxane with selected terpenes

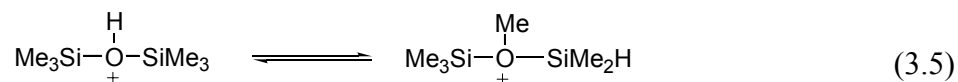
B	$(\text{Me}_3\text{Si})_2\text{OH}^+$				H_3O^+			
	k_{obs} Eff	M+H ⁺	M-H ₂ O ⁺	m/z 81	k_{obs} Eff	M+H ⁺	M-H ₂ O ⁺	m/z 81
 pinene	0.16 ± 0.02 X.XX	1.00				α 0.62 ^a β 0.57	0.00 ^a	α 0.38 ^a β 0.43
 1,8 cineole	1.26 ± 0.15 0.90	0.94 ± 0.03	0.06 ± 0.03		2.6 ^b 0.87	0.07 ^b	0.91 ^b	
 linalool		0.05 ± 0.01	0.89 ± 0.01	0.06 ± 0.01	3.0 ^b 0.94	0.04 ^{b,c}	0.56 ^{b,c}	0.30 ^{b,c}

a--Wang, T.; Spanel, P.; Smith, D. *Int J Mass Spectrom* **2003**, 228, 117-126. BR range due to reaction with either α or β pinene
 b--Amelynck, A.; Schoon, N.; Kuppens, T.; Bultinck, P.; Arijs, E. *Int. J. Mass Spectrom.* **2005**, 247, 1-9.
 c--Other products detected <0.1

3.4 DISCUSSION

When protonated hexamethyldisiloxane, formed via proton transfer from CH_5^+ , is allowed to react with acetone, a trimethylsilyl transfer product and a product at m/z 117 is observed (Scheme 3.1). This product was initially assigned as the proton-bound dimer of acetone. When d_6 -acetone was allowed to react with protonated hexamethyldisiloxane, an unexpected 6 Da shift

occurred instead of the expected 12 Da shift. When hexamethyldisiloxane, formed via proton transfer from the tert-butyl cation, was allowed to react with d_6 -acetone, an expected 12 Da mass shift occurs. The discrepancy amongst the two results can be explained if protonated hexamethyldisiloxane isomerizes (eq 3.5). The proton transfer reaction between CH_5^+ and



HMDSO is 72 kcal/mol exothermic, while the proton transfer reaction between the tert-butyl cation and HMDSO is only 10 kcal/mol exothermic (see Table 3.1). This extra energy supplied to the ion would allow for this isomerization to take place. Isomerization of silicon containing ions in the gas-phase is not unprecedented. Ignatyev and Sundius have studied the isomerization of Me_3Si^+ using the B2YLP 6-31G** level of theory.²⁵ They concluded that a methyl group transfer followed by a hydrogen atom transfer takes ~ 70 kcal/mol of energy to occur, which is consistent with our observations. Tabita and coworkers studied the unimolecular decomposition of m/z 147 ($\text{Me}_3\text{SiOSiMe}_2^+$) using mass analyzed ion kinetic energy (MIKE) spectrometry.²⁶ The methyl groups present on m/z 147 scrambled before any unimolecular decomposition occurred, which was confirmed using half-deuteriated m/z 147. This information suggests that isomerization of protonated hexamethyldisiloxane can occur, given the correct amount of excess energy.

Calculating the enthalpy of trimethylsilyl transfer from protonated hexamethyldisiloxane to a base B at first seemed to be trivial. Initial calculations used the heat of formation of HMDSO obtained from the literature (-186 ± 1 kcal/mol).^{27,28} When this value was used to calculate the enthalpy of reaction, the observed trimethylsilyl transfer channels were endothermic. The trimethylsilyl transfer channels are observed, however, and therefore the enthalpies of reaction should be, at a maximum, thermoneutral. Using a correlation between known trimethylsilyl

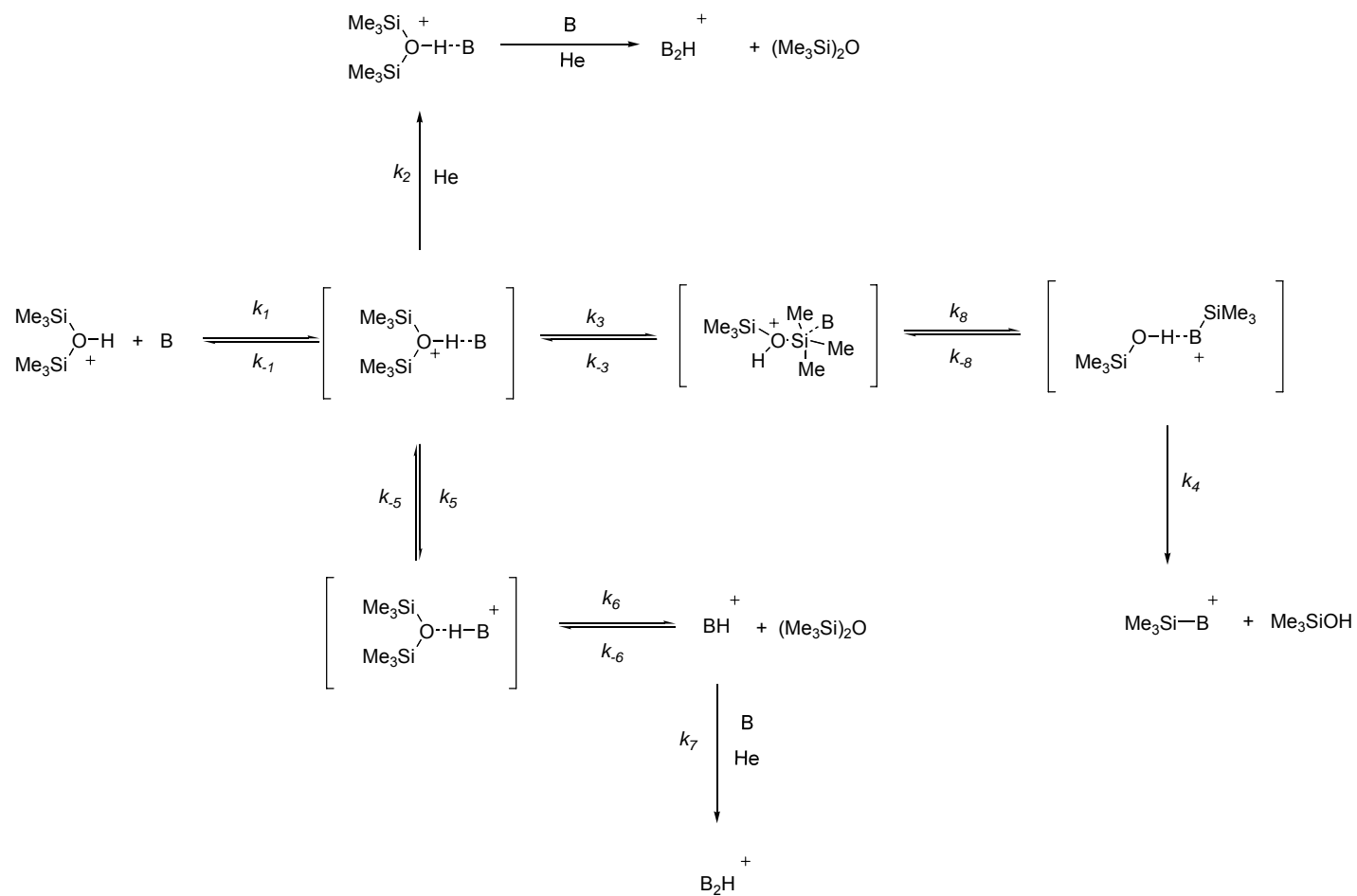
affinities obtained from Stone and our observations (see Table 3.2), we can estimate the heat of formation of HMDSO and the trimethylsilyl affinity of trimethylsilanol.²⁹ Since it is observed that trimethylsilyl transfer occurs with acetone but not with benzene, an estimate to the heat of formation of HMDSO, assuming that the enthalpy of reaction of all trimethylsilyl transfers are at least thermoneutral, is ≥ -167 kcal/mol. Using the known trimethylsilyl cation affinities of diethylether and ethanol, we can estimate the trimethylsilyl affinity of trimethylsilanol to be 44 ± 3 kcal/mol.

The reaction of protonated hexamethyldisiloxane with a base B is shown in Scheme 3.2. The two interact to form an ion neutral complex at a rate k_1 . If no reaction is observed, as in the case of 2-methylbutane, benzene, cyclopentene, etc. then the complex returns to reactants through k_{-1} . It is then assumed that $k_{-1} > k_1$ in that particular case. Once the initial complex is formed, it may be stabilized by a third body (i.e. helium) to form a cluster product through k_2 (e.g. ethanol). The initial complex may also transfer a trimethylsilyl group to the base B and form the trimethylsilyl product through k_3 (e.g. ethyl acetate). The initial ion neutral complex has a third route in which a proton is transferred to B to form $B-H^+$ through k_5 and k_6 . An example is the reaction of protonated hexamethyldisiloxane and triethylamine. A base may also go through a combination of pathways. For example, when protonated hexamethyldisiloxane is allowed to react with ammonia, pathways k_5 , k_6 , and k_3 , k_4 are favored, but not k_2 .

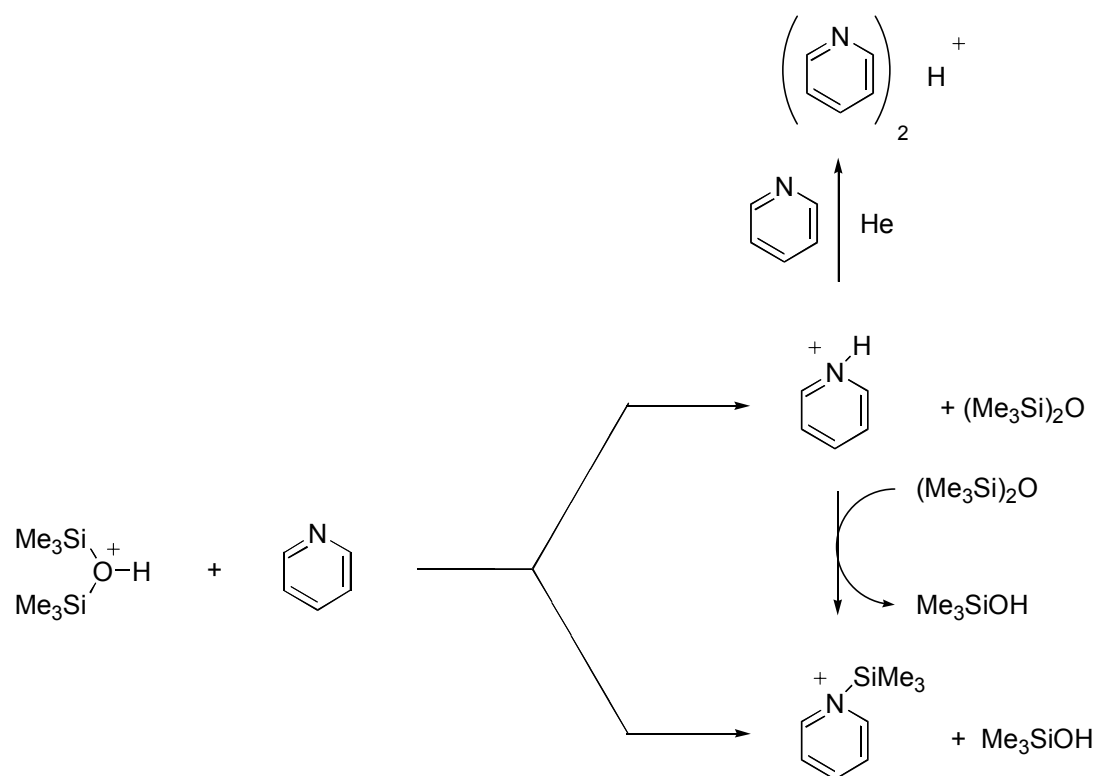
The same scheme also addresses the observation of secondary products. A proton-bound dimer of a base B can be formed by solvent switching with a cluster ion formed via pathway k_2 or by further clustering of the protonated base formed via pathway k_6 . The unusual formation of a secondary trimethylsilyl transfer product is discussed below.

Inspection of the branching ratio plots for the reaction of protonated hexamethyldisiloxane with pyridine (Figure 3.2) or diethylamine (Figure 3.3) reveals an apparent anomaly. The primary products for the reaction are clearly these from proton transfer (m/z 80) and from trimethylsilyl transfer (m/z 152). At longer reaction times, protonated pyridine reacts away to form both the proton-bound dimer of pyridine (m/z 159) and additional trimethylsilylated pyridine (Scheme 3.3). This later product must be coming from the reaction of the primary product, protonated pyridine, with excess hexamethyldisiloxane (present in the flow tube from the reaction used to form protonated hexamethyldisiloxane). Thus this latter “secondary” reaction is not a classic secondary reaction (i.e., it is not formed from the reagent ion and two sequential reactions with the neutral of interest). Confirmation of the m/z 152 forming reaction in Scheme 3.3 was obtained by an independent experiment in which protonated pyridine (formed from the reaction of the tert-butyl cation with pyridine) was allowed to react with hexamethyldisiloxane to produce the trimethylsilyl transfer product. The exchange of a proton for a trimethylsilyl group in an ion/molecule encounter has previously been noted by Hendewerk and coworkers and serves to further establish the similarity of these two groups.³⁰ This dual transfer reaction starts with an endothermic proton transfer reaction followed by an exothermic trimethylsilyl transfer reaction. This hypothesis can only be true if the overall enthalpy of reaction is thermoneutral or exothermic. A similar “secondary” product is observed when protonated hexamethyldisiloxane is allowed to react with diethylamine. This “secondary” product was confirmed in a separate experiment when the reaction of protonated diethylamine (formed via proton transfer from the tert-butyl cation) with hexamethyldisiloxane.

The proton transfer products react with neutrals to form proton-bound dimers in the case of acetone, diethylamine, ammonia, and pyridine. The formation of a proton-bound dimer of



Scheme 3-2 Reaction of protonated hexamethyldisiloxane with a base B. The primary products formed are proton transfer, trimethylsilyl transfer, and/or cluster ion formation. A secondary product of a proton-bound dimer can be formed from either the protonated neutral or the cluster ion.

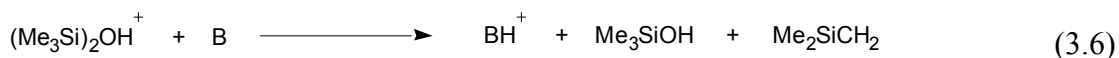


Scheme 3-3 The reaction of protonated hexamethyldisiloxane with pyridine forming the primary products of protonated pyridine and the trimethylsilyl transfer product. An unconventional secondary product of protonated pyridine reacting with an equivalent of hexamethyldisiloxane is formed in addition to the proton-bound dimer of pyridine.

acetone, pyridine, and ammonia has been reported in the literature and is thermodynamically accessible.³¹⁻³³ Diethylamine and ammonia form proton-bound trimers (a proposed tertiary product). The other neutrals do not form tertiary products within experimental constraints.

Trimethyl phosphate, dimethylformamide, pyridine, diethylamine, and ammonia form trimethylsilyl and proton transfer products. When triethylamine is allowed to react with $(\text{Me}_3\text{Si})_2\text{OH}^+$, a proton transfer product is formed. It is interesting to note that efficiency of the measured rate coefficient decreases as the yield of the proton transfer product increases. The

proton transfer reaction also becomes increasingly exothermic. It is well known that if the proton transfer reaction is exothermic, the kinetics are near the collisional limit;³⁴ however, there are known exceptions. Stone and Chen have observed that the efficiency of reaction decreases when protonated trimethylsilanol is allowed to react with ammonia and triethylamine (c.f. 0.75 and 0.51, respectively).³⁵ The explanation offered is that the different polarizabilities of ammonia and triethylamine will produce different collision cross sections and therefore will affect the efficiency of reaction. The polarizabilities of ammonia, diethylamine, and triethylamine are 2.81, 10.2, and 13.2 X 10⁻²⁴ cm³, respectively. The larger polarizabilities of diethylamine and triethylamine, when compared to ammonia, would account for our observations and also concur with the hypothesis of Stone and Chen.³⁵ An alternative explanation is that the reaction produces elimination products (eq 6) instead of the proposed proton transfer reaction. Since a mass spectrometer can only detect ionic species, this



possibility should be explored. The enthalpies of elimination reactions involving triethylamine and diethylamine are +30 and +36 kcal/mol, respectively. The endothermic reactions elucidate this possibility, leaving the former hypothesis as an explanation of the decrease in reaction efficiency.

Deuterium oxide performs a H-D exchange reaction with (Me₃Si)₂OH⁺ as well as clustering even though the deuteron transfer reaction is 37 kcal/mol endothermic. Slight H-D exchange with an endoergic proton (deuteron) transfer reaction has been observed by Smith and coworkers.³⁶ Using a selected ion flow tube, Smith and coworkers studied the reaction of the ammonium ion with deuterium oxide. They observed slight scrambling and measured a rate coefficient of ~3 X 10⁻¹² cm³ molecule⁻¹ s⁻¹. Smith and coworkers' hypothesis is that the lifetime

of the intermediate is sufficiently long for H-D exchange to occur. Our results can be rationalized using the same hypothesis since the measured rate coefficient is $2 \times 10^{-11} \text{ cm}^3 \text{ molecule}^{-1} \text{ s}^{-1}$ and we observe H-D exchange.

Protonated hexamethyldisiloxane can be evaluated against the five criteria outlined in the introduction. Protonated hexamethyldisiloxane can be formed in high yield ($\sim 10^6$ cps) that fulfills criterion 1, and since only one ion is formed on a linear scale that should fulfill criterion 2. Protonated hexamethyldisiloxane is unreactive with water, but no studies have been conducted on its reactivity with N_2 , CO_2 , etc. (criterion 3). The unique capability of this ion to be unreactive with some compounds, while also generating unique product ions could ease identification of compounds (criterion 4). The hydronium ion only gives insight into the compounds' mass and not its identity, and the oxygen radical cation produces multiple product ions for each compound, which complicates interpretation of spectra. Only NO^+ allows some insight into a neutral's identity. Protonated hexamethyldisiloxane fails in criterion 5 since most reactions are less than unit efficiency.

When protonated hexamethyldisiloxane is allowed to react with the selected terpenoids, less fragmentation occurs than when the hydronium ion is used. This is attributed to the fact that the proton affinity of hexamethyldisiloxane is greater than water. This would then suggest that protonated hexamethyldisiloxane is a better candidate for the determination of terpenoids.

3.5 CONCLUSIONS

The formation of protonated hexamethyldisiloxane has been investigated with protonated methane, the hydronium ion, and the tert-butyl cation. Protonated methane and C_2H_5^+ are

formed via ionization of methane, and these react with hexamethyldisiloxane (HMDSO) to form $(\text{Me}_3\text{Si})_2\text{OH}^+$ and $(\text{Me}_3\text{Si})_2\text{OEt}^+$. It is hypothesized that $(\text{Me}_3\text{Si})_2\text{OH}^+$ isomerizes as confirmed by d_6 -acetone experiments. The hydronium ion is used to form $(\text{Me}_3\text{Si})_2\text{OH}^+$, but two products of $(\text{Me}_3\text{Si})_2\text{OH}^+$ and $(\text{Me}_3\text{Si})_2\text{OH}^+(\text{H}_2\text{O})$ are formed; therefore, the criterion of one reactant ion is not fulfilled due to the fact that other ions such as $\text{H}_3\text{O}^+(\text{H}_2\text{O})$ are present. Proton transfer from the tert-butyl cation was selected since it created the cleanest spectrum of $(\text{Me}_3\text{Si})_2\text{OH}^+$. When protonated hexamethyldisiloxane was allowed to react with the selected neutrals, the following outcome(s) were observed: 1) proton transfer, 2) trimethylsilyl transfer, 3) cluster ion, and/or 4) no reaction within experimental constraints. No proton transfer was observed if the reaction was endothermic. As the proton transfer reaction becomes more exothermic, the rate slows due to the increase in the polarizabilities of the neutrals. The observation of trimethylsilyl transfer is supported by the observations in the literature and by the inferred trimethylsilyl affinity of trimethylsilanol. H-D exchange is observed when $(\text{Me}_3\text{Si})_2\text{OH}^+$ is allowed to react with deuterium oxide. The small reaction efficiency (0.07) is due to the endothermic proton transfer between D_2O and HMDSO.

The secondary reactions observed were the formation of proton-bound dimers from cluster ions or protonated ions of acetone, ammonia, dimethylformamide, and diethylamine. A secondary product is also observed from the reaction of protonated pyridine and diethylamine with excess HMDSO, forming additional trimethylsilyl transfer product. A dual transfer reaction of a proton and a trimethylsilyl group is hypothesized to account for this observation. It is important to note all of the secondary and tertiary reactions observed are not important to VOC analysis, since the concentration of sample added is much lower than the ion concentration. The ability of this ion to form different products with varying branching ratios could serve as a

fingerprint in VOC detection. It also seems to be a good candidate for terpenoids detection due to its high proton affinity.

3.6 REFERENCES

1. Smith, D.; Spanel, P. *Rap. Comm. Mass Spectrom.* **1996**, *10*, 1183-1198.
2. Lagg, A.; Taucher, J.; Hansel, A.; Lindinger, W. *Int J Mass Spectrom Ion Proc* **1994**, *134*, 55-66.
3. Spanel, P.; Pavlik, M.; Smith, D. *Int J Mass Spectrom Ion Proc* **1995**, *145*, 177-186.
4. Smith, D.; Diskin, A. M.; Ji, Y. F.; Spanel, P. *Int J Mass Spectrom* **2001**, *209*, 81-97.
5. Spanel, P.; Smith, D. *J. Phys. Chem.* **1995**, *99*, 15551-15556.
6. Spanel, P.; Smith, D. *J. Chem. Phys.* **1996**, *104*, 1893-1899.
7. Spanel, P.; Smith, D. *Rap. Comm. Mass Spectrom.* **2001**, *15*, 563-569.
8. Bierbaum, V. M.; Golde, M. F.; Kaufman, F. *J Chem Phys* **1976**, *57*, 3491.
9. Young, C. E.; Falconer, W. E. *J Chem Phys* **1972**, *57*, 918-929.
10. Spanel, P.; Smith, D. *Int J Mass Spectrom* **1998**, *172*, 239-247.
11. Fleming, I. *Chem. Soc. Rev.* **1981**, *10*, 83-111.
12. Wojtyniak, A. C. M.; Stone, J. A. *International Journal of Mass Spectrometry and Ion Processes* **1986**, *74*, 59-79.
13. Wojtyniak, A. C. M.; Stone, J. A. *Int J Mass Spectrom Ion Proc* **1986**, *74*.
14. Trenerry, V. C.; Klass, G.; Bowie, J. H.; Blair, I. A. *J Chem Res, Syn* **1980**, *11*, 386-387.
15. Tobita, S.; Tajima, S.; Okada, F.; Mori, S.; Tabei, E.; Umemura, M. *Org. Mass Spectrom.* **1990**, *25*, 39-43.
16. Li, X.; Stone, J. A. *J. Am. Chem. Soc.* **1989**, *111*, 5586-5592.
17. Phillips, M.; Herrero, J.; Krishnan, S.; Zain, M.; Greenberg, J.; Cataneo, R. N. *J Chrom B: Biomed Sci Appl* **1999**, *729*, 75-88.
18. Melley, S. J.; Grabowski, J. J. *Int J Mass Spectrom Ion Proc* **1987**, *81*, 147-164.
19. Adams, N. G.; Smith, D. *Int J Mass Spec Ion Phy* **1976**, *21*, 349-359.
20. Su, T.; Su, E. C. F.; Bowers, M. T. *J. Chem. Phys.* **1978**, *69*, 2243-2250.
21. Lide, D. R., Ed. *CRC Handbook*; 3rd Electronic Edition ed.; CRC Press: Boca Raton, FL, 2000.
22. Miller, K. J.; Savchik, J. A. *Journal of the American Chemical Society* **1979**, *101*, 7206-7213.
23. Anderson, D. R.; Bierbaum, V. M.; Depuy, C. H.; Grabowski, J. J. *Int J Mass Spectrom. Ion Phys.* **1983**, *52*, 65-94.
24. Field, F. H.; Munson, M. S. B. *Journal of the American Chemical Society* **1965**, *87*, 3289-3294.
25. Ignatyev, I. S.; Sundius, T. *Organometallics* **1998**, *17*, 2819-2824.
26. Tobita, S.; Tajima, S.; Okada, F.; Mori, S.; Tabei, E.; Umemura, M. *Organic Mass Spectrometry* **1990**, *25*, 39-43.
27. Good, W. D.; Lacina, J. L.; DePrater, B. L.; McCullough, J. P. *Journal of Physical Chemistry* **1964**, *68*, 579-586.

28. Pedley, J. B.; Rylance, J. *Sussex-N.P.L. Computer Analysed Thermochemical Data: Organic and Organometallic Compounds* University of Sussex, 1977.
29. Stone, J. A. *Mass Spec. Rev.* **1997**, *16*, 25-49.
30. Hendewerk, M. L.; Weil, D. A.; Stone, T. L.; Ellenberger, M. R.; Farneth, W. E.; Dixon, D. A. *J Amer Chem Soc* **1982**, *104*, 1794-1799.
31. Meot-Ner, M. *Journal of the American Chemical Society* **1984**, *106*, 1265.
32. Davidson, W. R.; Sunner, J.; Kebarle, P. *Journal of the American Chemical Society* **1979**, *101*, 1675.
33. Payzant, J. D.; Cunningham, A. J.; Kebarle, P. *Canadian Journal of Chemistry* **1973**, *51*, 3242.
34. Bohme, D. K.; Ausloos, P., Ed.; Plenum Publishing Co.: New York, NY, 1974.
35. Chen, Q.-F.; Stone, J. A. *Int J Mass Spectrom Ion Proc* **1997**, *165/166*, 195-207.
36. Ausloos, P.; Lias, S. G. *Journal of the American Chemical Society* **1981**, *103*, 3641-3647.

4.0 PROTONATED TRIMETHYLSILANOL: ITS CAPACITY AS A TRIFUNCTIONAL REAGENT ION

4.1 INTRODUCTION

The selected ion flow tube (SIFT) and proton transfer mass spectrometer (PTR-MS) have been widely used for volatile organic compound (VOC) identification and quantification.^{1,2} These techniques commonly use the hydronium ion as the chemical ionization reagent ion. The hydronium ion transfers a proton to VOCs having a proton affinity (PA) larger than water forming the protonated neutral ($M+H^+$). Since only the mass of the neutral is inferred to the user, the assignment of the neutrals' identity is not straightforward. Prior knowledge of the chemistry occurring in the sample is needed to hypothesize the compounds identity. A study might only focus on one particular VOC to simplify the identification process.³ Attempts to circumvent this limitation have been made using other reagent ions such as O_2^{+} and NO^+ in conjunction with the hydronium ion in hopes that the ion complement will provide insight into the neutrals' identity.⁴

Other attempts employed gas chromatograms coupled to the PTR-MS. This technique allows one to identify neutrals by retention time and by m/z . A drawback of this technique is that the quantitation must be corrected since there is sample loss through the gas chromatograph. This correction goes against the unique aspects of this technique that no conventional calibration is needed other than experimental variables. A final example of identifying neutrals' identity are to vary the electric field on the drift tube on the PTR-MS to measure the ions' drift velocity.

This has been demonstrated by Lindinger and coworkers to differentiate and identify isoprene.² The search for a reagent ion that provides definite identification of the neutrals is needed.

This study investigates the chemistry of protonated trimethylsilanol. Orlando and coworkers⁵ and Clemens and Munson⁶ have investigated the chemistry of protonated trimethylsilanol using a gas chromatograph coupled with a mass spectrometric chemical ionization source. Clemens and Munson found that when acetone or tetrahydrofuran were introduced into an ion source containing water, tetramethylsilane, and methane that proton transfer and trimethylsilyl transfer occurred.⁶ They hypothesized that trimethylsilyl transfer and proton transfer occurred via reaction with protonated trimethylsilanol ($\text{Me}_3\text{SiOH}_2^+$). Wojtyniak and Stone, using a high pressure ionization source, determined that trimethylsilyl transfer occurred when protonated trimethylsilanol was allowed to react with methanol.⁷

This study uses the flowing afterglow to investigate various ways to generate the trimethylsilyl cation and to form protonated trimethylsilanol. Once protonated trimethylsilanol is generated, this ion is allowed to react with VOCs postulated to be present in “normal” human breath.⁸ In addition to this list, other neutrals having various functionalities are added to explore this ion’s reactivity. The primary and secondary products of the reactions are discussed, along with the rationale behind using this ion for the purpose of VOC analysis.

4.2 EXPERIMENTAL

The flowing afterglow apparatus has been previously described;⁹ only details relevant to this work will be described. Helium 99.997% (Valley National Gas, Wheeling, WV) was used as the carrier gas. The helium gas was further purified by immersing a uniform mixture of 3A, 4A, and 13X molecular sieves in liquid nitrogen. Flow tube pressures were selected between 0.3 – 0.5 Torr and helium flows ranged from 100-180 STP cm^3/s . The neutral of interest was

ionized in our ion source and allowed to react with a neutral downstream. If more than one neutral was added downstream of the ion source, control experiments were employed to ensure that all previous reactions have been quenched before exploring the reaction of interest.

All experiments were conducted under pseudo-first-order conditions in which the ion was the limiting reactant. Three types of experiments were performed in this study: qualitative, kinetic, and branching ratio measurements. Qualitative experiments detect the products from ion molecule reactions. Two qualitative experiments were conducted for the same ion molecule reaction over two experimental days. An experimental day is defined as the complete startup and shutdown of the flowing afterglow. Kinetic experiments determine the rate coefficient of an ion/molecule reaction. At least five experiments over two experimental days were performed for each ion/molecule reaction studied. If a cluster ion was observed in the qualitative experiment, a plot of observed rate coefficient versus pressure was constructed. The reported error is the precision in measurements. The accuracy of each rate was around 20%. The collisional rate coefficient was calculated using the variational collision complex theory as described by Su and coworkers.¹⁰ Polarizabilities and dipole moments if known were obtained from suitable sources.¹¹ The polarizability of trimethylphosphate was calculated using the group additivity of Miller and coworkers.¹² Branching ratio experiments were conducted twice over two experimental days using the method described by Anderson et al.¹³ A curvature in the branching ratio plot can indicate the formation of secondary products. A secondary product is the product from the reaction of a primary product ion with a neutral. An isotopic correction was applied to the branching ratio data analysis of the reaction of protonated trimethylsilanol with deuterium oxide. The H/D exchange product is isobaric to the ²⁹Si isotope of protonated trimethylsilanol (8.5 percent normalized to *m/z* 91).

The following reagents were obtained from the following sources and used without any further purification: acetone, acetonitrile, triethylamine, furan (99% Fisher Scientific, Pittsburgh, PA), ethyl acetate, benzene (99.9% HPLC Grade Fisher Scientific), tetramethylsilane (99.9+% Sigma-Aldrich), trimethylsilyl chloride (98% Sigma-Aldrich), hexamethydisilane

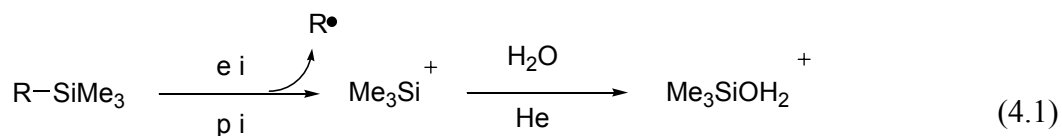
(98% Sigma-Aldrich), deuterium oxide (99.9% D MDS Isotopes), 2-methylbutane (99.7%, Fisher Scientific), cyclopentene (96% Sigma-Aldrich), naphthalene (99+% Scintillation Grade, Sigma-Aldrich), isoprene (99% Acros Organics), ammonia (semi-conductor grade, Matheson), ethanol (100%, Aaper Alcohol and Chemical Company), acetic acid (glacial, Fisher Scientific), trimethylphosphate, dimethylsulfide, pyridine (99+%, Sigma-Aldrich), diethyl ether (99.7%, JT Baker), dimethylformamide (99+%, Fisher Scientific), oxygen (99.9% Valley National Gas, Wheeling, WV), diethylamine (98+%, Avocado Research Lab), α -pinene ($\geq 99\%$, Sigma-Aldrich), 1,8-cineole (99%, Sigma-Aldrich), and linalool (97%, Sigma-Aldrich). Deionized water was obtained in house. All liquid reagents were subject to several freeze-pump-thaw cycles each experimental day to ensure contaminants were removed. A sweeper, which aides volatilization of neutrals, was used for trimethylphosphate, naphthalene, linalool, pinene, and 1,8-cineole for qualitative and branching ratio experiments using helium as the sweeper gas.

4.3 RESULTS

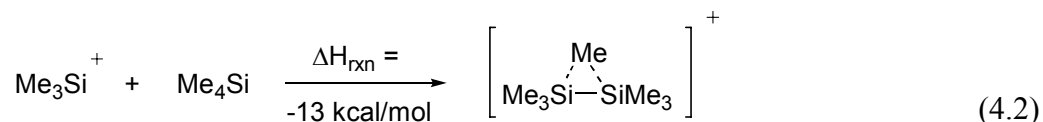
4.3.1 Reaction of protonated trimethylsilanol with neutrals

The first step in exploring the reactions of protonated trimethylsilanol with various neutrals was to form a clean spectrum of protonated trimethylsilanol. Electron and chemical ionization of trimethylsilyl containing neutrals was explored to see if this would produce an ideal protonated trimethylsilanol and/or the trimethylsilyl cation spectrum.

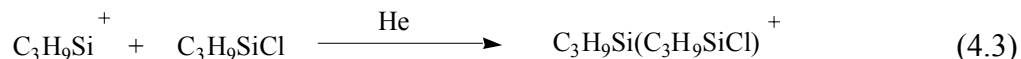
When tetramethylsilane, trimethylsilyl chloride, and hexamethyldisilane were ionized, the trimethylsilyl cation is formed in addition to other ions depending on the neutral ionized (eq 4.1). When the trimethylsilyl cation is allowed to react with tetramethylsilane, methylated



R = Me, Cl, SiMe₃



hexamethyldisilane is formed (eq 4.2). When trimethylsilyl chloride is ionized, an ion containing the trimethylsilyl cation and trimethylsilyl chloride is formed in addition to the other ions described above (eq 4.3). The radical cation of hexamethyldisilane is observed in addition



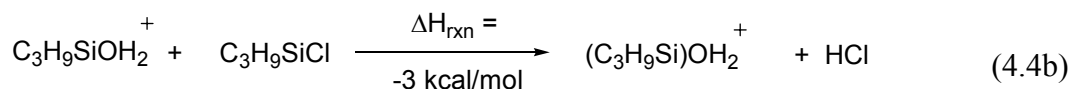
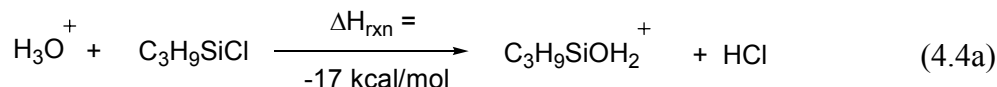
to the ions mentioned above when hexamethyldisilane is ionized. This route of forming protonated trimethylsilanol was discarded. Chemical ionization was investigated next since less neutral is introduced in our apparatus downstream than at the ion source.

Various attempts were made to form the trimethylsilyl cation via chemical ionization. The tert butyl cation, generated via ionization of tert butyl chloride, was allowed to react with tetramethylsilane in an attempt to form the trimethylsilyl cation (Table 4.1). No products were observed within experimental constraints.

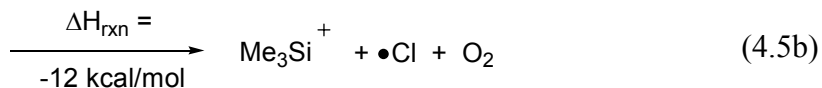
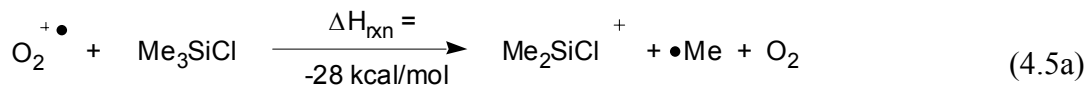
Table 4-1 Summary of the reactions of M⁺ to form the trimethylsilyl cation

M ⁺	k _{II} (Eff) ^a	ΔH _{Rxn} (kcal/mol) with Me ₄ Si ^b	ΔH _{Rxn} (kcal/mol) with Me ₃ SiCl ^b	ΔH _{Rxn} (kcal/mol) with Me ₆ Si ₂ ^b
H ₃ O ⁺		-0.09	-17.87	-38.81
tBu ⁺	≤ 0.008 ^c	+26.42	+38.75	+17.81
O ₂ ⁺⁺	2.14 ± 0.33 (0.926) ^d	-39.05	-10.82	-42.61
a--Rate coefficient of the reaction of M ⁺ with tetramethylsilane. Units of 10 ⁻⁹ cm ³ molecule ⁻¹ s ⁻¹ . Eff = k _{obs} /k _{coll} . k _{coll} is calculated via the VTST theory of Su and Bowers.				
b--Linstrom, P.J. (Ed.) NIST Chemistry Webbook.				
c--Upper limit measured using highest flow of neutral introduced.				
d--Polarizability calculated using Lorenz-Lorentz Equation (index of refraction = 1.3591, density = 0.648 g/cc)				

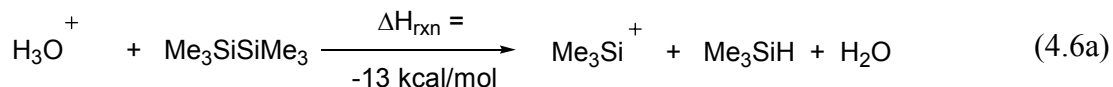
The hydronium ion was then explored as another candidate to ultimately form protonated trimethylsilanol. Water was ionized to form the hydronium ion and its hydrates (i.e. $\text{H}_3\text{O}^+(\text{H}_2\text{O})_n$, $n=0-3$). When trimethylsilyl chloride was allowed to react with the hydronium ion and its hydrates, protonated trimethylsilanol and its cluster ion was observed in addition to protonated hexamethyldisiloxane (Eq 4.4a and b).

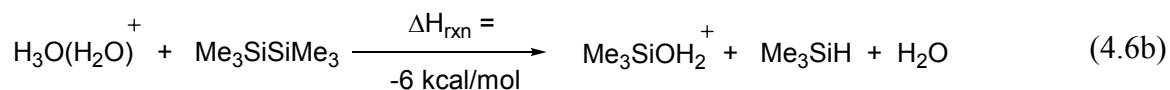


The radical cation of oxygen was used as the next possible candidate to react with trimethylsilyl chloride; it is known that this ion can form dissociative charge transfer products with other neutrals.¹⁴ When trimethylsilyl chloride was allowed to react with the radical cation of oxygen, protonated trimethylsilanol, Me_2SiCl^+ (m/z 93), and the cluster ion of the trimethylsilyl cation with trimethylsilyl chloride were formed (eq 4.5a-b).

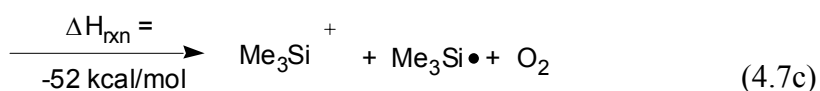
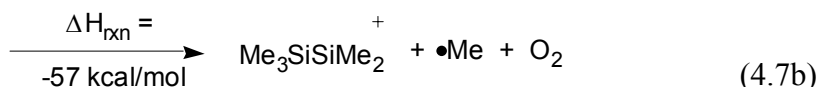


The next neutral explored was hexamethyldisilane. When the hydronium ion was allowed to react with hexamethyldisilane, the trimethylsilyl cation, protonated trimethylsilanol, m/z 147, and protonated hexamethyldisiloxane were observed (eq 4.6a-b). The reaction of the oxygen radical cation with hexamethyldisilane formed m/z 146, 131, and 73, which is the radical



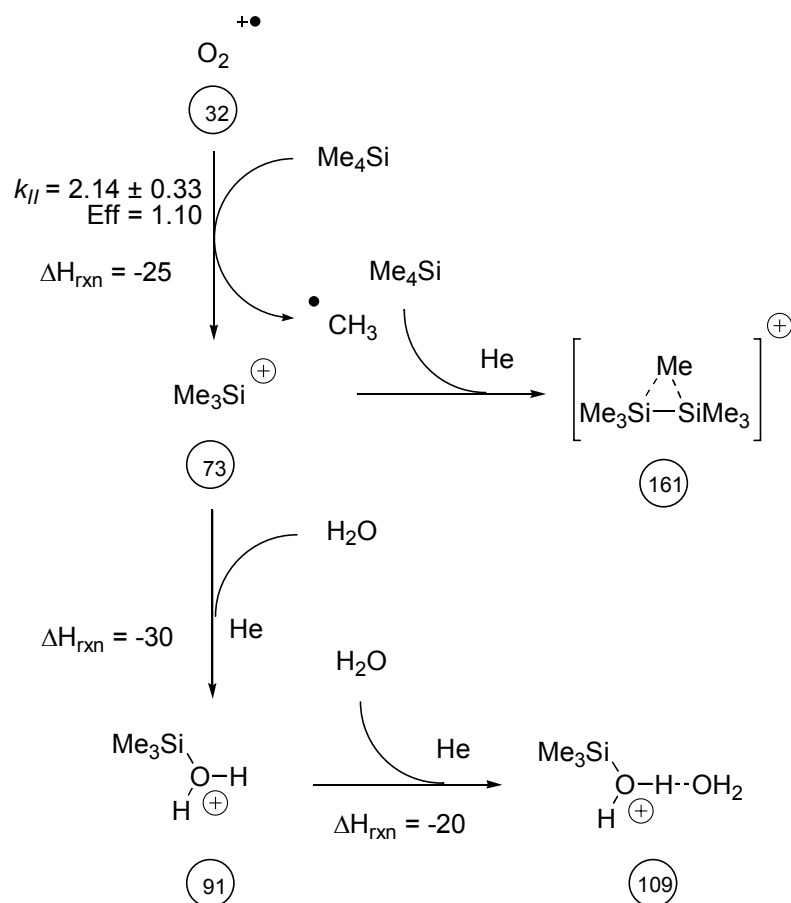


cation of hexamethyldisilane, the methyl radical loss of m/z 146, and the trimethylsilyl cation, respectively (eq 4.7a-c).



A final attempt to form the trimethylsilyl cation was to electron ionize oxygen, forming the radical cation of oxygen. The oxygen radical cation then was allowed to react with tetramethylsilane to form the trimethylsilyl cation. Protonated trimethylsilanol was also observed as a product due to the presence of adventitious water (Scheme 4.1). As the concentration of tetramethylsilane was increased, m/z 161 was observed. Water was then introduced further downstream to quench the trimethylsilyl cation. m/z 109 was observed and the intensity of m/z 161 decreased when water was added to the flow tube. A typical spectrum of protonated trimethylsilanol is shown in Figure 4.1. This method of forming the trimethylsilyl cation was the preferred method and is used to probe the reactions of protonated trimethylsilanol with the selected neutrals.

The results of the reaction of protonated trimethylsilanol with neutrals is shown in Table 4.2. When benzene was allowed to react with protonated trimethylsilanol, the trimethylsilyl transfer product and the proton bound dimer of benzene and trimethylsilanol were observed. Experimental conditions were optimized to discern whether the trimethylsilyl transfer product came from protonated trimethylsilanol or from m/z 161 ($\text{Me}_3\text{Si}(\text{Me})\text{SiMe}_3^+$). Excess



Scheme 4-1 Preferred Formation of protonated trimethylsilanol and subsequent reaction with excess water present in the flow tube. Enthalpies of reaction are in units of kcal/mol.

water was added to the flow tube to form a larger than “normal” m/z 109 ($\text{Me}_3\text{SiOH}_2^+(\text{H}_2\text{O})$) signal so that the m/z 161 was minimized. The trimethylsilyl transfer product was still observed. In a separate experiment, m/z 109 was minimized and the cluster ion was still observed. Therefore, the cluster ion and trimethylsilyl transfer products are formed by reaction with protonated trimethylsilanol.

Secondary products were observed in some of the branching ratios. When the branching ratios of diethyl ether, dimethylsulfide, ethyl acetate, dimethylformamide, and

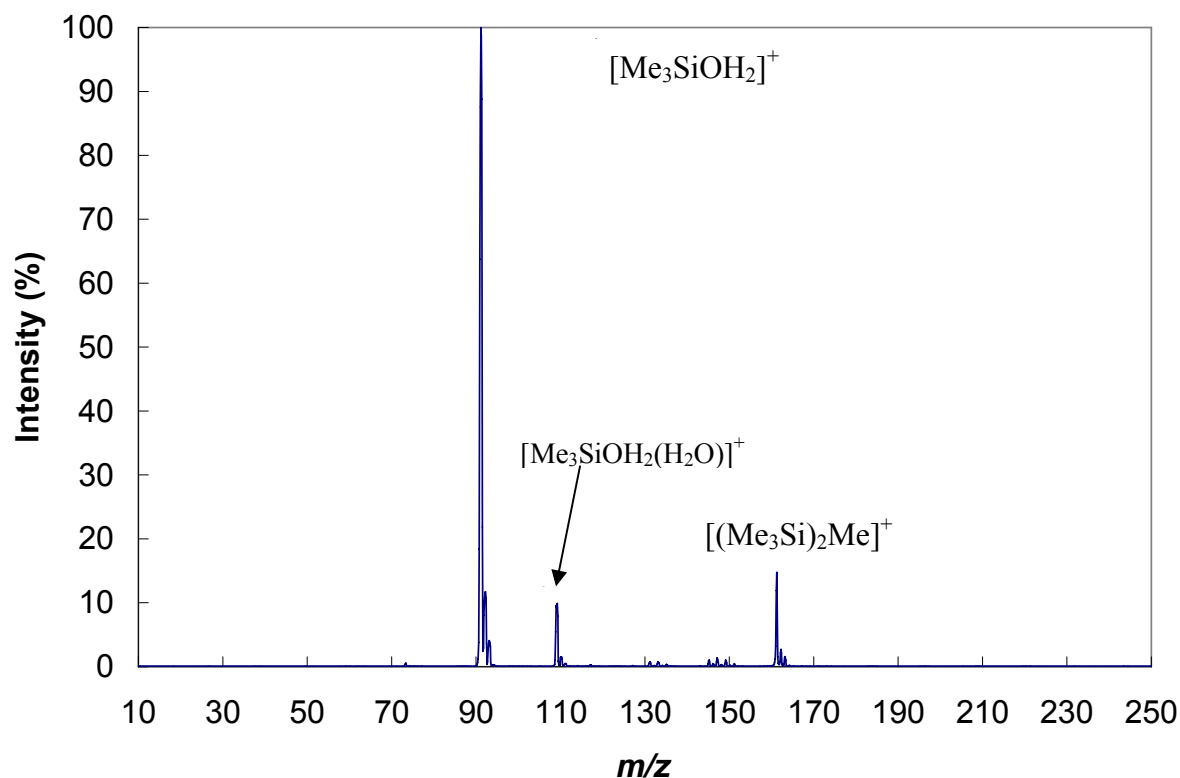
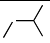
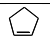
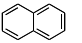

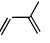
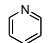


Figure 4.1 A representative spectrum of protonated trimethylsilanol. The spectrum is normalized to the intensity of protonated trimethylsilanol

pyridine were measured, the protonated base (primary product) decreases in intensity and the trimethylsilylated base's intensity increases as the concentration of the base increases (i.e. secondary products were observed). A typical example of this observed curvature is shown in Figure 4.2 of the reaction of protonated trimethylsilanol being allowed to react with dimethylformamide or pyridine. The protonated base and the trimethylsilyl transfer products are observed as primary products. The proton bound dimer and trimethylsilyl transfer product

Table 4-2 Reactions of protonated trimethylsilanol with neutrals. Shaded areas indicate where no rate coefficients were measured due to their previous measurements in the literature.

Neutral	k_{obs} (Eff) ^a	k_{obs} (Eff) ^{a,b}	TMS T ^c		PT ^c		Other ^d
			BR ^d	ΔH_{rxn} ^e	BR ^d	ΔH_{rxn} ^e	
	$\leq 0.006^f$						No Reaction
H ₂ O	0.425 ± 0.007^g (0.18)					+ 24.0	100% Cluster
D ₂ O	0.735 ± 0.085^g (0.34)						55 ± 4 % H/D Exchange 45 ± 4 % Cluster
C ₆ H ₆	0.051 ± 0.022^g (0.03)		74 ± 1 %	+ 6		+ 9.7	26 ± 2 % Cluster
	0.013 ± 0.005^g (0.01)		82 ± 1 %			+ 5.8	18 ± 1 % Cluster
EtOH	1.29 ± 0.18^g (0.72)		97 ± 1 %	-11.8		+ 3.4	3 ± 1 % Cluster
MeCN	3.64 ± 0.34 (1.00)		100%			+ 2.8	
MeCO ₂ H	1.87 ± 0.01^g (1.00)		87 ± 2 %			+ 1.7	13 ± 2 % Cluster
			39 ± 2 %		55 ± 3 %	- 2.9	6 ± 1 % Cluster
	0.53 ± 0.09 (0.45)		38 ± 2 %		62 ± 2 %	- 3.0	
MeCOMe	2.20 ± 0.37 (0.88)	1.78 ± 0.07 (0.71)	86 ± 3 %	-14.8	14 ± 3 %	- 5.0	
	0.37 ± 0.07 (0.31)		9 ± 1 %		91 ± 1 %	- 8.5	
EtOEt	1.05 ± 0.03 (0.71)		68 ± 3 %		32 ± 3 %	- 9.0	
Me ₂ S	1.07 ± 0.16 (0.66)		5 ± 1 %		95 ± 1 %	- 9.6	
MeCO ₂ CH ₂ Me	1.79 ± 0.21 (1.00)		20 ± 4 %	-18.7	80 ± 3 %	- 10.7	
NH ₃		1.56 ± 0.01 (0.75)	21 ± 2 %	-16.3	79 ± 2 %	- 15.0	
HCONMe ₂	1.63 ± 0.15 (0.55)		20 ± 3 %		80 ± 3 %	- 23.1	
(MeO) ₃ PO ^h	0.34 ± 0.09 (0.15)		41 ± 3 %		59 ± 3 %	- 23.9	
	1.35 ± 0.35 (0.67)		31 ± 2 %		69 ± 3 %	- 33.0	
(Et) ₂ NH	1.13 ± 0.17 (0.81)				100%	- 38.6	
Et ₃ N		0.75 ± 0.06 (0.51)			100%	- 45.1	

a--Units of 10⁻⁹ cm³ molecule⁻¹ s⁻¹. Eff = k_{obs}/k_{coll} . k_{coll} is calculated via the VTST theory of Su and Bowers. NR = No reaction observed.

b--Rate coefficient measured by Chen, Q.-F.; Stone, J. A. *Int. J. Mass Spectrom. Ion Proc.* **1997**, 165/166, 195-207. 8 trials

c--TMST = trimethylsilyl transfer. PT = proton transfer.

d--branching ratios measured at 0.3 Torr

e-- ΔH_{rxn} (units of kcal/mol). Linstrom, P.J. (Ed.) NIST Chemistry Webbook.

f--Upper limit of rate estimated from flow of neutral

g--Rate measured at pressures from 0.3 - 0.5 Torr. No pressure dependence on overall rate found.

h--Polarizability calculated using the group additivity of Miller and coworkers

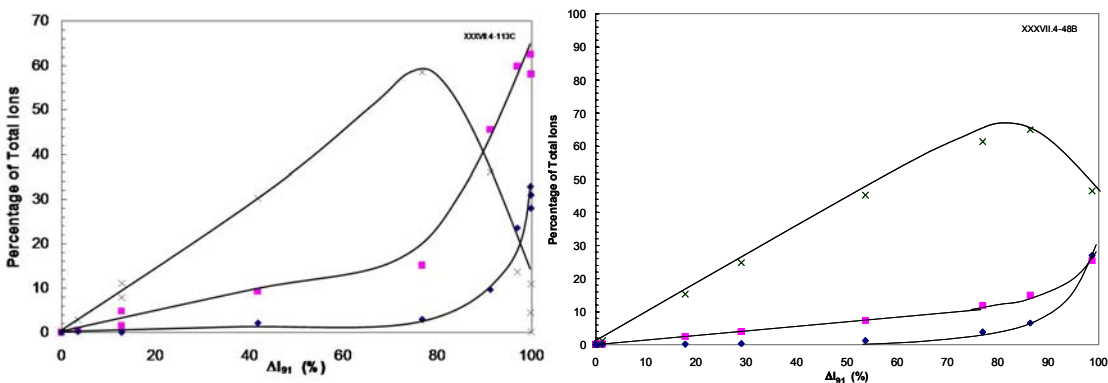


Figure 4.2 Branching Ratio plots indicating the appearance of a secondary trimethylsilyl transfer product. The reaction of protonated trimethylsilanol with either dimethylformamide (left) or pyridine (right) demonstrates the reaction of protonated base (x) to form the trimethylsilyl transfer product (■) and the proton-bound dimer (□).

increase indicating that they are being formed as secondary products. Protonated dimethylformamide or pyridine are decreasing in intensity indicating that it is reacting away to form secondary products.

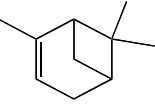
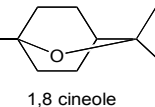
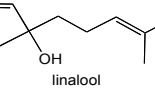
4.3.2 Protonated trimethylsilanol with terpenes

When protonated trimethylsilanol was allowed to react with the selected terpenes, proton transfer, a neutral water loss, and/or an R group loss is observed (Table 4.3). When protonated trimethylsilanol is allowed to react with pinene, only proton transfer is observed. The experimental rate coefficient was able to be measured, but the collisional rate coefficient could not be calculated due to the fact that there is no known dipole moment for the compound. When 1,8—cineole is allowed to react with protonated trimethylsilanol, both protonated trimethylsilanol and a water loss product are observed (0.68 and 0.32, respectively). Finally

when linalool is allowed to react with protonated trimethylsilanol, all three products are formed. No trimethylsilyl transfer products are observed.

Table 4-3 Observations when protonated trimethylsilanol is allowed to react with selected terpenes.

Known literature data are shown for comparison.

B	Me ₃ SiOH ₂ ⁺				H ₃ O ⁺			
	<i>k</i> _{obs} Eff	M+H ⁺	M-H ₂ O ⁺	<i>m/z</i> 81	<i>k</i> _{obs} Eff	M+H ⁺	M-H ₂ O ⁺	<i>m/z</i> 81
 pinene	0.63 ± 0.17 X.XX	1.00				α 0.62 ^a β 0.57	0.00 ^a	α 0.38 ^a β 0.43
 1,8 cineole	1.72 ± 0.18 1.00	0.68 ± 0.03	0.32 ± 0.03		2.6 ^b 0.87	0.07 ^b	0.91 ^b	
 linalool		0.01 ± 0.01	0.96 ± 0.01	0.03 ± 0.01	3.0 ^b 0.94	0.04 ^{b,c}	0.56 ^{b,c}	0.30 ^{b,c}

a--Wang, T.; Spanel, P.; Smith, D. *Int J Mass Spectrom* **2003**, 228, 117-126. BR range due to reaction with either α or β pinene
 b--Amelynck, A.; Schoon, N.; Kuppens, T.; Bultinck, P.; Arijs, E. *Int. J. Mass Spectrom.* **2005**, 247, 1-9.
 c--Other products detected <0.1

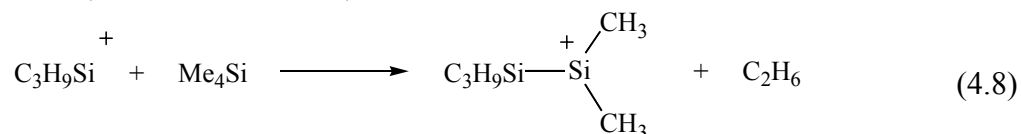
4.4 DISCUSSION

4.4.1 Non terpenoid compounds

The ionization of Me₃SiCl, Me₄Si, and Me₃SiSiMe₃ was determined to be an unsatisfactory method of producing the trimethylsilyl cation due to the fact that a larger amount of neutrals has to be added to produce a sufficient spectrum. This excess then is allowed to react with the ions formed and produces unwanted ions. When C₄H₉⁺ and H₃O⁺(H₂O) (n=0-2) was allowed to react with Me₃SiCl, Me₄Si, and Me₃SiSiMe₃, no reaction and large amounts of

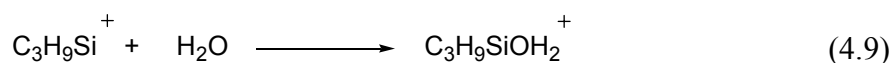
$\text{Me}_3\text{SiOH}_2^+(\text{H}_2\text{O})$ were formed, respectively. The best conditions and preferred method of forming protonated trimethylsilanol was to allow $\text{O}_2^{+\bullet}$ to react with tetramethylsilane. This ion complement was allowed to react with water. The enthalpy of reaction to produce the trimethylsilyl cation is 29 kcal/mol exothermic for tetramethylsilane. The proton-bound dimer of trimethylsilanol and water was not observed (m/z 109). When trimethylsilyl chloride was used as the neutral, m/z 181 is observed, which is assigned as the cluster ion between trimethylsilyl cation and trimethylsilyl chloride.

When tetramethylsilane was used as the neutral to form the trimethylsilyl cation, m/z 161 and 131 were observed. Stone assigned m/z 161 as methylated hexamethyldisilane (eq 4.1b).¹⁵ m/z 131 has been tentatively assigned in the literature, but it is certainly a product of the reaction of the trimethylsilyl cation with tetramethylsilane. We assign m/z 131 as $(\text{C}_3\text{H}_9)_2\text{SiSi}(\text{C}_3\text{H}_9)_2^+$ (eq 4.8). We have decided to use the chemical ionization reaction of the radical cation of oxygen with tetramethylsilane as the first step to form protonated trimethylsilanol. Tetramethylsilane has been used as a neutral to form the trimethylsilyl cation by Clemens and Munson, Lin and coworkers, and Stone.^{5,16,17}



After the trimethylsilyl cation was formed (via dissociative charge transfer from $\text{O}_2^{+\bullet}$ to tetramethylsilane), water was added to the flow tube to form protonated trimethylsilanol and to quench the trimethylsilyl cation. The proton-bound dimer of protonated trimethylsilanol and water was also observed, but to a much lesser extent than when the hydronium ion was used (10% vs. 40% respectively, normalized to Me_3Si^+). Stone has also observed this proton-bound dimer of trimethylsilanol and water.⁷ m/z 161 is still observed, but it is a minor reactant ion since the formation of m/z 161 was intercepted by the addition of water. The trimethylsilyl affinity of water is larger than tetramethylsilane, which also accounts for the lower yield of m/z 161.¹⁸

Upon inspection of the absence and presence of proton transfer, a discrepancy was found in the reported proton affinity of trimethylsilanol. Stone and coworkers reported the proton affinity (PA) to be 183.7 kcal/mol.¹⁹ Later reports from the same group stated the PA to be 192 kcal/mol.²⁰ Our observations of the absence or presence of PT places the PA of trimethylsilanol to be 191 ± 3 kcal/mol, which is in agreement with Stone. Using this value and the enthalpy of formation of trimethylsilanol, one can determine the heat of formation of protonated trimethylsilanol. Using this method, Stone found the heat of formation of protonated trimethylsilanol to be + 57 kcal/mol.¹⁸ Using this heat of formation to calculate the thermochemistry of the trimethylsilyl transfer reactions studied, all the trimethylsilyl transfer reactions would be exothermic with the exception of benzene. An alternative method used by us was to calculate the heat of formation of protonated trimethylsilanol using eq 4.9. The enthalpy of formation of water²¹ and the trimethylsilyl cation affinity of water are known.⁷ However, the

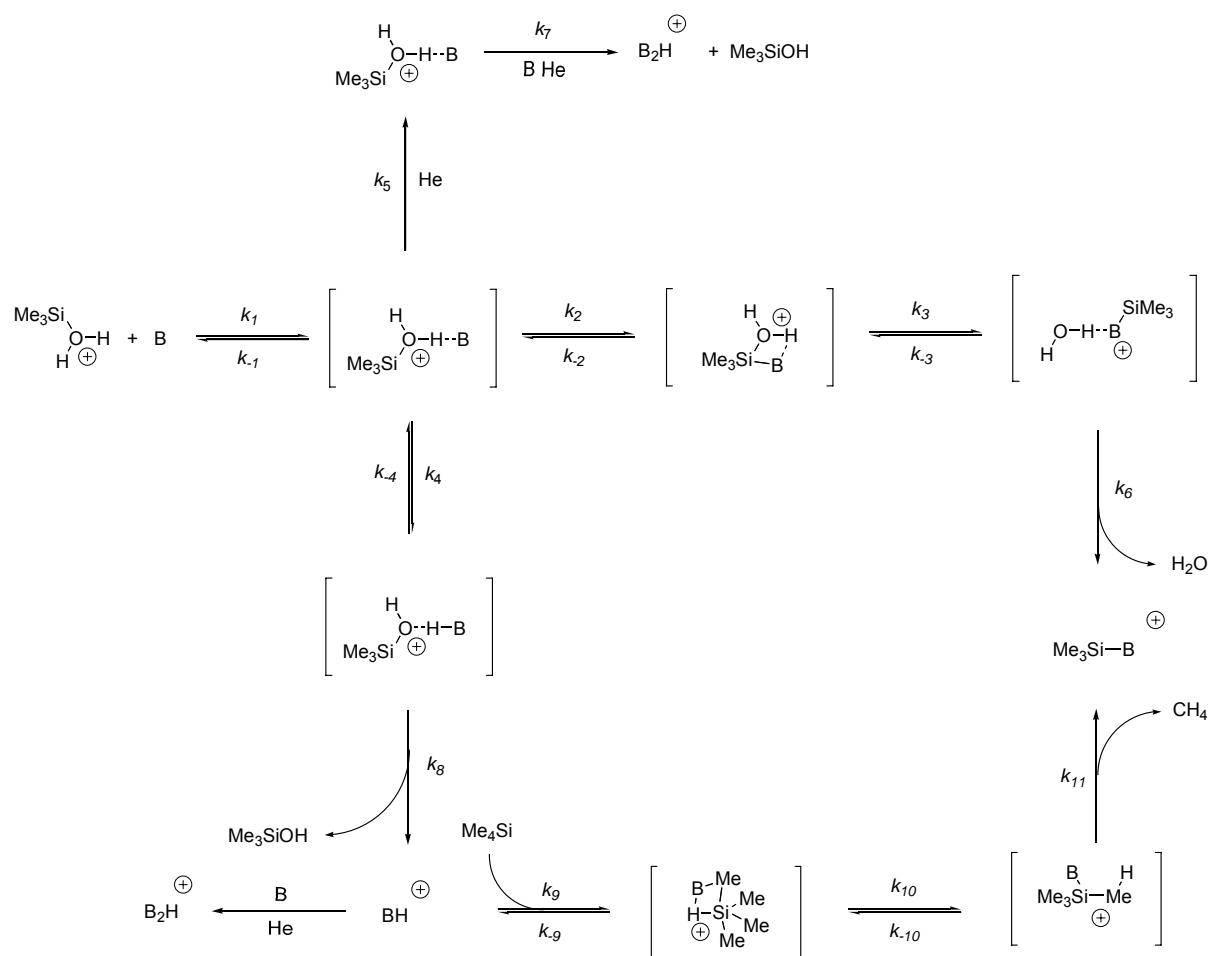


enthalpy of formation of the trimethylsilyl cation also has uncertainty. Walsh has estimated the heat of formation to be 145 kcal/mol with an error of at least 5 kcal/mol.²² This uncertainty comes from differing values by other workers such as Szepes and Baer, which found the heat of formation of the trimethylsilyl cation to be 150 kcal/mol using the dissociation of hexamethyldisilane.²³ Therefore, if the heat of formation of protonated trimethylsilanol is calculated using the later method outlined, the heat of formation is $+ 62 \pm 5$ kcal/mol. The enthalpy of reaction of trimethylsilyl transfer of protonated trimethylsilanol with benzene is now only slightly endothermic within error (6 ± 5 kcal/mol endothermic). The other enthalpies of trimethylsilyl transfer of protonated trimethylsilanol with the other neutrals remain exothermic (neutrals who have known trimethylsilyl cation affinities).

The reaction of protonated trimethylsilanol with a base B is shown in Scheme 4.2. The initial formed ion/molecule complex can revert to reactants through k_{-1} (e.g. 2-

methylbutane). The complex can alternatively be stabilized by a third body (He) to form the cluster ion (e.g. water, deuterium oxide). A third option is that the initial complex can transfer a

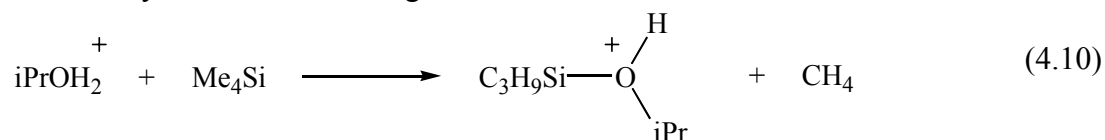
Scheme 4-2 Reaction of protonated trimethylsilanol with a base B



trimethylsilyl group to B (e.g. MeCN). The fourth and final possibly pathway is that the initial ion/molecule complex can transfer a proton to B, forming (B+H⁺).

This scheme also addresses the formation of secondary products. The cluster ion formed via routes k_1 and k_5 can react with another equivalent of B to form B_2H^+ via solvent switching.

The protonated base formed via routes k_2 and k_4 can react with another equivalent of B to form the proton-bound dimer of B (B_2H^+). Curvatures of the trimethylsilyl transfer product ($B+SiMe_3^+$) were observed when the branching ratios of diethylether, ethyl acetate, dimethylformamide, trimethyl phosphate, and pyridine. All of the branching ratios listed above follow the general trend of having the proton transfer product ($B+H^+$) react away to form a secondary trimethylsilyl transfer product. Stone has observed the reaction of protonated isopropanol with tetramethylsilane which forms the trimethylsilyl transfer product (eq 4.10).⁷ Stone also observed the same type of products when the reactions of protonated methanol and ethanol with tetramethylsilane were investigated.



This observation can explain the curvatures in the plots. The absence or presence of this secondary reaction can be explained for all the neutrals investigated. Up to naphthalene, no proton transfer products are observed, and the hypothesis described above agrees with neutrals up to acetic acid. There is insufficient data to indicate whether the trimethylsilyl transfer product is a secondary product when protonated trimethylsilanol was allowed to react with acetone, ammonia, naphthalene, and furan. Diethylamine and triethylamine do not form any secondary trimethylsilyl transfer products. The reaction is inferred to be endothermic. Further evidence that the reaction is endothermic is that the trimethylsilyl transfer between protonated tertbutyl amine and tetramethylsilane is 1 kcal/mol endothermic.^{21,24} Tertbutyl amine (223 kcal/mol) has around the same proton affinity as pyridine (222 kcal/mol).²¹ Therefore, since diethylamine and triethylamine have higher proton affinities, then the trimethylsilyl transfer reaction involving tetramethylsilane is endothermic and is inferred to not react.

When protonated trimethylsilanol is allowed to react with 2-methylbutane, no reaction was observed. While the PA of this neutral is unknown, we can safely assume that the PA of this neutral is less than all of the other neutrals. Therefore, a proton transfer product can be ruled out.

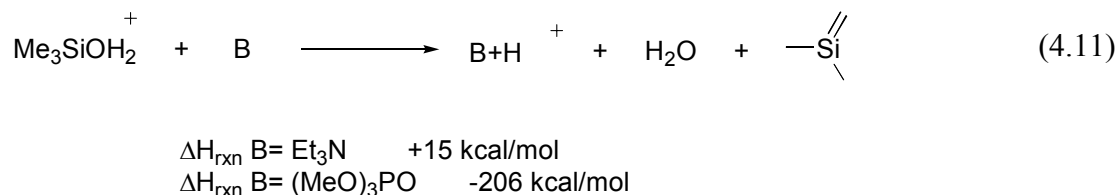
No known trimethylsilyl cation affinity (TMSA) exists for this neutral. To date, no known reactions of alkanes with protonated trimethylsilanol have been reported in the literature.

Water and deuterium oxide form cluster ions with protonated trimethylsilanol. H/D exchange also occurs with deuterium oxide. This reaction indicates that there are two exchangeable hydrogens for m/z 91 (assigned as protonated trimethylsilanol), and four exchangeable hydrogens for m/z 109 (assigned as the hydrate of protonated trimethylsilanol). The rate of reaction with deuterium oxide is faster than water within error. Deuterium oxide and protonated trimethylsilanol interact to form the ion/molecule complex (k_1) as shown in Scheme 4.1. The complex is stabilized in this case by collisions with helium (k_5) to form the cluster ion again in both cases. The original ion-molecule complex also exchanges a deuterium from the deuterium oxide (k_2), and returns to the reactant ion through k_{-2} and k_{-1} . Even though only clustering is observed when water is allowed to react with protonated trimethylsilanol, hydrogen exchange can occur and obviously would not be observed. Since both neutrals appear to follow the same reaction pathways, the observed difference in rate coefficients must be attributed to a primary isotope effect ($k_D/k_H = 2/1$).

Trimethylsilyl transfer and proton transfer products are observed when furan, acetone, isoprene, diethyl ether, dimethylsulfide, ethyl acetate, ammonia, trimethylphosphate, and pyridine react with protonated trimethylsilanol. The amount of trimethylsilyl and proton transfer product varies from neutral to neutral. This is due to many factors such as the proton and trimethylsilyl affinity of the neutral. The lowest known trimethylsilyl affinity of all neutrals studied is benzene which is: 23.9 kcal/mol.⁷ The highest known trimethylsilyl affinity of all neutrals studied is ethyl acetate (48.7 kcal/mol).⁷ The general trend of no reaction, cluster, trimethylsilyl transfer and cluster, proton transfer and trimethylsilyl transfer, and proton transfer follows the thermochemistry of trimethylsilyl affinity along with proton affinity of the neutrals.

Benzene has a low trimethylsilyl affinity⁷ in addition to a low proton affinity²¹ compared to the proton affinity of trimethylsilanol. The differences of rate are attributed to the trimethylsilyl affinities of the neutrals incorporated with their proton affinities. If one ranks the

known trimethylsilyl affinities versus the efficiency of reaction, one sees that the increasing trimethylsilyl affinities correspond to an increase of efficiency. No trimethylsilyl transfer is observed with diethylamine and triethylamine. Diethylamine's efficiency is unit efficient within error. Stone and Chen have stated that the efficiency of the reaction of protonated trimethylsilanol with triethylamine is slower due to the polarizability of triethylamine.¹⁶ Trimethylphosphate's rate is slower than the other neutrals that have comparable proton affinities such as dimethylformamide and pyridine. This trend is consistent with other trimethylsilyl containing ions investigated by this group such as protonated hexamethyldisiloxane.²⁵ The rationale is that this trimethylphosphate's calculated polarizability ($1.29 \times 10^{-23} \text{ cm}^3$)¹² is around the same as triethylamine's ($1.31 \times 10^{-23} \text{ cm}^3$).¹¹ Protonated trimethylsilanol's interaction with these neutrals are hindered compared to the other neutrals such as pyridine which has a polarizability of $9.5 \times 10^{-24} \text{ cm}^3$.¹¹ An alternative explanation is that the E₂ reaction could be thermochemically accessible (eq 4.11). The thermochemistry indicates that the E₂ reaction is



thermochemically assessable for trimethylphosphate, but not for triethylamine.

The advantage of using $\text{Me}_3\text{SiOH}_2^+$ vs H_3O^+ is that this ion can differentiate amongst isobaric neutrals. For example isoprene and cyclopentene are isobaric. As shown in Table 4.2, the branching ratios of these compounds are different for isoprene and furan, even though they have the same products (trimethylsilyl transfer and proton transfer). When cyclopentene is allowed to react with protonated trimethylsilanol, a cluster ion along with a trimethylsilyl transfer product is produced. Therefore, one can discern between three isobaric neutrals having different functionality assuming that the sample only contains furan or isoprene.

4.4.2 Terpenoids

As shown in table 4.3, it has been shown that protonated trimethylsilanol reacts with the three selected terpenes. Less fragmentation occurs (i.e. water loss or R group loss) when protonated trimethylsilanol is used as the reagent ion than when the hydronium ion is used. It is postulated that since the proton affinity of trimethylsilanol is greater than water, then less fragmentation would be observed, which is confirmed.

4.5 CONCLUSIONS

Various methods of forming protonated trimethylsilanol have been investigated. Direct ionization of tetramethylsilane, trimethylsilyl chloride, or hexamethyldisilane was ruled out due to the large amount of secondary products formed due to an excess amount of neutral added. Various chemical ionization techniques were employed. Using the hydronium ion to form protonated trimethylsilanol was also ruled out due to the large formation of the proton bound dimer of water and trimethylsilanol due to large amount of water added to the ionization source. The radical cation of oxygen being allowed to react with tetramethylsilane and further addition of water was found to be the cleanest method out of all investigated to form protonated trimethylsilanol.

When protonated trimethylsilanol was allowed to react with the representative neutrals, the following primary products were observed: clustering, trimethylsilyl transfer, and/or proton transfer. Trimethylsilyl transfer products were also observed as secondary products via reaction of the protonated base with tetramethylsilane. Triethylamine and diethylamine do not form this product due to inferred thermochemistry using tert butyl amine.

Protonated trimethylsilanol can differentiate between isobaric species such as isoprene, furan, and cyclopentene without the need of any further modifications of the apparatus or the use of other reagent ions. The reaction of protonated trimethylsilanol with isobaric neutrals should be investigated along with its capability of its use as a reagent ion for VOC analysis.

It is interesting to note that protonated trimethylsilanol would be a better candidate for VOC analysis of terpenoids since less fragmentation is observed.

4.6 REFERENCES

1. Smith, D.; Spanel, P. *Rap. Comm. Mass Spectrom.* **1996**, *10*, 1183-1198.
2. Hansel, A.; Jordan, A.; Holzinger, R.; Prazeller, P.; Vogel, W.; Lindinger, W. *Int J Mass Spectrom Ion Proc* **1995**, *150*, 609-619.
3. Abbott, S. M.; Elder, J. B.; Spanel, P.; Smith, D. *Int J Mass Spectrom* **2003**, *228*, 655-665.
4. Smith, D.; Diskin, A. M.; Ji, Y. F.; Spanel, P. *Int J Mass Spectrom* **2001**, *209*, 81-97.
5. Orlando, R.; Allgood, C.; Munson, B. *Int J Mass Spectrom Ion Proc* **1989**, *92*, 93-109.
6. Clemens, D.; Munson, B. *Anal. Chem.* **1985**, *57*, 2022-2027.
7. Wojtyniak, A. C. M.; Stone, J. A. *International Journal of Mass Spectrometry and Ion Processes* **1986**, *74*, 59-79.
8. Phillips, M.; Herrero, J.; Krishnan, S.; Zain, M.; Greenberg, J.; Cataneo, R. N. *J Chrom B: Biomed Sci Appl* **1999**, *729*, 75-88.
9. Melley, S. J.; Grabowski, J. J. *Int J Mass Spectrom Ion Proc* **1987**, *81*, 147-164.
10. Su, T.; Su, E. C. F.; Bowers, M. T. *J. Chem. Phys.* **1978**, *69*, 2243-2250.
11. Lide, D. R., Ed. *CRC Handbook*; 3rd Electronic Edition ed.; CRC Press: Boca Raton, FL, 2000.
12. Miller, K. J.; Savchik, J. A. *Journal of the American Chemical Society* **1979**, *101*, 7206-7213.
13. Anderson, D. R.; Bierbaum, V. M.; Depuy, C. H.; Grabowski, J. J. *Int J Mass Spectrom. Ion Phys.* **1983**, *52*, 65-94.
14. Glosik, J.; B., R. A.; Twiddy, N. D.; Adams, N. G.; Smith, D. *J. Phys. B: Atom. Molec. Phys.* **1978**, *11*, 3365-3379.
15. Wojtyniak, A. C. M.; Li, X.; Stone, J. A. *Can. J. Chem.* **1987**, *65*, 2849-2854.
16. Chen, Q.-F.; Stone, J. A. *Int J Mass Spectrom Ion Proc* **1997**, *165/166*, 195-207.
17. Lin, Y.; Ridge, D. P.; Munson, B. *Organic Mass Spectrometry* **1991**, *26*, 550-558.
18. Stone, J. A. *Mass Spec. Rev.* **1997**, *16*, 25-49.
19. Stone, J. A.; Wojtyniak, A. C. M.; Wytenburg, W. *Can. J. Chem.* **1986**, *64*, 575-576.
20. Li, X.; Stone, J. A. *Canadian Journal of Chemistry* **1988**, *66*, 1288.

21. Lidstrom, P. J.; Mallard, W. G., Eds. *NIST Chemistry WebBook, NIST Standard Reference Database Number 69*; March 2003 ed.; National Institute of Standards and Technology: Gaithersburg MD, 20899, 2003.
22. Walsh, R. *Journal of Physical Chemistry* **1986**, *90*, 389-394.
23. Szepes, L.; Baer, T. *Journal of the American Chemical Society* **1984**, *106*, 273-278.
24. Lias, S. G.; Bartmess, J. E.; Liebman, J. F.; Holmes, J. L.; Levin, R. D.; Mallard, W. G. *J Phys Chem Ref Data* **1988**, *17*..

5.0 ION/MOLECULE REACTION STUDIES USING THE TRIMETHYLSILYL CATION

5.1 INTRODUCTION

The chemistry of the trimethylsilyl cation, which has been referred to as a “large proton”,¹ has been explored with organic compounds.^{2,3} Various groups have studied the reactivity of the trimethylsilyl cation with neutrals. For example, Bowie and Blair studied the reaction of the trimethylsilyl cation with ketones, carboxylic acids, ethers, and other neutrals using the ICR technique.⁴⁻⁶ Bowie and Blair determined that adducts are formed with the trimethylsilyl cation along with other products that lost an R group (e.g. methane). Orlando and coworkers coupled gas chromatography with chemical ionization to study the reaction of the trimethylsilyl cation with alcohols and aliphatic ethers.^{7,8} Orlando and coworkers determined that adduct formation is observed when the trimethylsilyl cation is allowed to react with bases. In addition, they suggested that trimethylsilyl transfer occurs if impurity ions are present such as protonated trimethylsilanol. Presence of protonated trimethylsilanol could cause erroneous interpretation of results since its ion chemistry is different than the trimethylsilyl cation. The trimethylsilyl cation was studied with various amines using the flowing afterglow⁹ and other neutrals using a high pressure mass spectrometer³ by Stone and coworkers. When Chen and Stone studied the reactions of the trimethylsilyl cation with amines, they discovered that most amines produced

adducts, while more basic amines produced proton transfer and adducts. Another interesting observation is that the magnitude of the rate coefficient decreased as the proton affinity of the base increased.⁹

The reactions of the trimethylsilyl cation with neutrals can also provide insight into trimethylsilyl group transfer reactions.^{3,10} Isoprene, acetone, etc. have been found to be in the breath of humans by Phillips and coworkers.¹¹ Stone and coworkers have used trimethylsilyl group transfer reactions to find the relative trimethylsilyl cation affinities of neutrals.³ The goal of this chapter was to evaluate the chemistry of the trimethylsilyl cation with the neutrals studied with protonated hexamethyldisiloxane and protonated trimethylsilanol.

5.2 EXPERIMENTAL

The flowing afterglow apparatus has been previously described;¹² only details unique to this work will be described here. Helium, 99.997% (Valley National Gas, Wheeling, WV), was used as the carrier gas. Flow tube pressures were selected between 0.3 – 0.5 Torr with corresponding helium flows from 100-180 STP cm³/s.

Argon was ionized at the ion source. Tetramethylsilane was added 36.3 or 76.7 cm from the nose cone depending on the experiment performed. For example, if a qualitative reaction was to be performed, then the tetramethylsilane would be added 76.7 cm from the ion source to minimize formation of protonated trimethylsilanol. Protonated trimethylsilanol is formed via reaction of the trimethylsilyl cation with adventitious water. The amount of tetramethylsilane added was selected such that the argon radical cation was reacted (i.e. when no or minimal m/z 40 signal was detected). The same flow of tetramethylsilane was then added 100

cm from the nose. Neutrals of interest were introduced 16.1 – 76.7 cm from the nose cone for kinetic experiments and 36.3 cm from the nose cone for qualitative and branching ratio experiments.

All experiments were conducted under pseudo-first-order conditions in which the ion was the limiting reactant. Three types of experiments were performed in this study: qualitative, kinetic, and branching ratio. Qualitative experiments are carried out to determine the ionic products from ion/molecule reactions. These qualitative experiments were repeated on two different experimental days. An experimental day is defined as the complete startup and shutdown of the flowing afterglow. Kinetic experiments are carried out to determine the rate of an ion/molecule reaction. At least five experiments over two experimental days were performed for each ion/molecule reaction studied. A plot of observed rate coefficient versus pressure was examined to determine if the reaction exhibited pressure dependence. For kinetic experiments, the reported error is the precision of the measurements. The accuracy of a rate coefficient measurement has previously been determined to be $\pm 20\%$. The collisional rate coefficient, used to determine reaction efficiency, was calculated using variational collision complex theory as described by Su and coworkers.¹³ Polarizabilities and dipole moments were obtained from standard sources.¹⁴ Branching ratio experiments were conducted twice over two experimental days and analyzed using the method described by Anderson and coworkers.¹⁵ Branching ratio plots will reveal the formation of secondary products via curves in the yield vs. extent-of-reaction lines. A secondary product is that formed from the reaction of a primary product ion with the neutral being studied.

Reagents were obtained from the following sources and used without further purification: acetone, acetonitrile, triethylamine, furan (99% Fisher Scientific, Pittsburgh, PA), ethyl acetate,

benzene (99.9% HPLC Grade Fisher Scientific), tetramethylsilane (99.9+% Sigma-Aldrich), deuterium oxide (99.9% D MDS Isotopes), 2-methylbutane (99.7%, Fisher Scientific), cyclopentene (96% Sigma-Aldrich), naphthalene (99+% Scintillation Grade, Sigma-Aldrich), isoprene (99% Acros Organics), ammonia (semi-conductor grade, Matheson), ethanol (100%, Aaper Alcohol and Chemical Company), acetic acid (glacial, Fisher Scientific), trimethylphosphate, dimethylsulfide, pyridine (99+%, Sigma-Aldrich), diethyl ether (99.7%, JT Baker), dimethylformamide (99+%, Fisher Scientific), argon (99.9% Valley National Gas, Wheeling, WV), and diethylamine (98+%, Avocado Research Lab). Deionized water was obtained in-house. All liquid reagents were subject to several freeze-pump-thaw cycles each experimental day. A sweeper, which facilitates introduction of semi-volatile neutrals via a flow of helium, was used for trimethylphosphate and naphthalene for qualitative and branching ratio experiments.

5.3 RESULTS

A typical reactant ion spectrum of the trimethylsilyl cation is shown in Figure 5.1. The products formed from this reaction are the trimethylsilyl cation (m/z 73), protonated trimethylsilanol (m/z 91), methylated hexamethyldisilane ($\text{Me}_3\text{Si}(\text{Me})\text{SiMe}_3^+$, m/z 161), and m/z 131 ($\text{Me}_3\text{SiSiMe}_2^+$). Protonated trimethylsilanol is formed via reaction of the trimethylsilyl cation with adventitious water. The amount of protonated trimethylsilanol formed varied from day to day (20-50% relative to the trimethylsilyl cation).

When the trimethylsilyl cation was allowed to react with the neutrals as shown in Table 5.1, the following reactions were observed: hydride ion transfer, adduct formation, proton transfer, and/or the loss of methane or propane. A majority of neutrals form the adduct only.

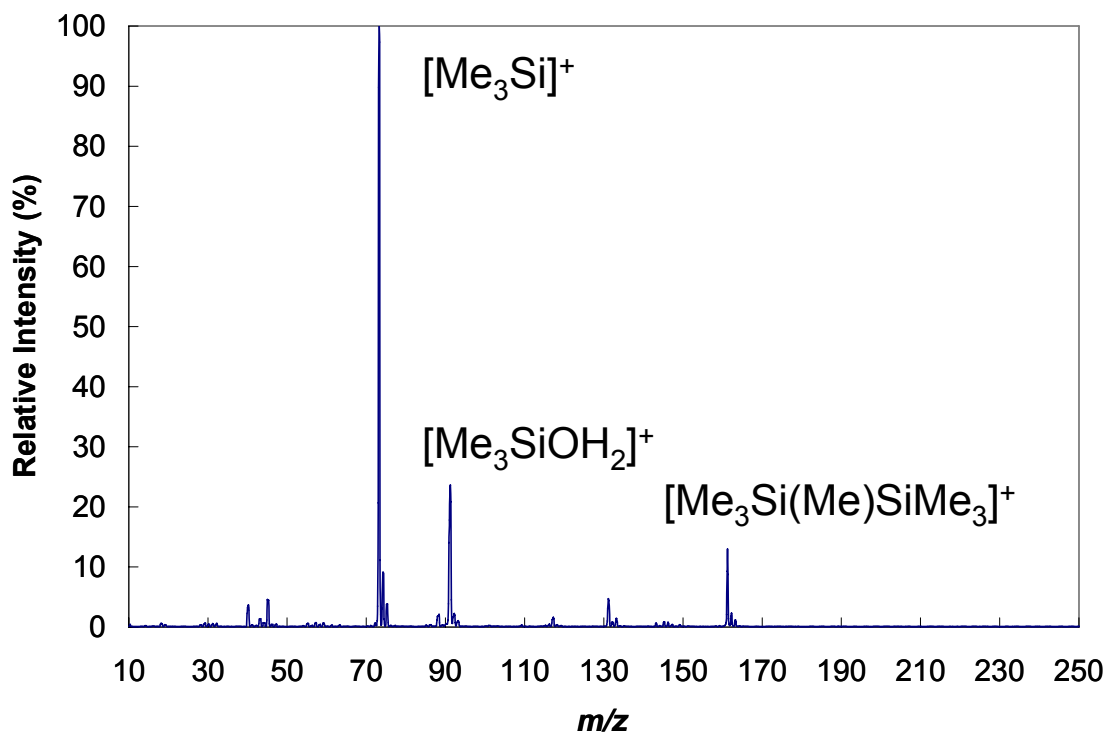


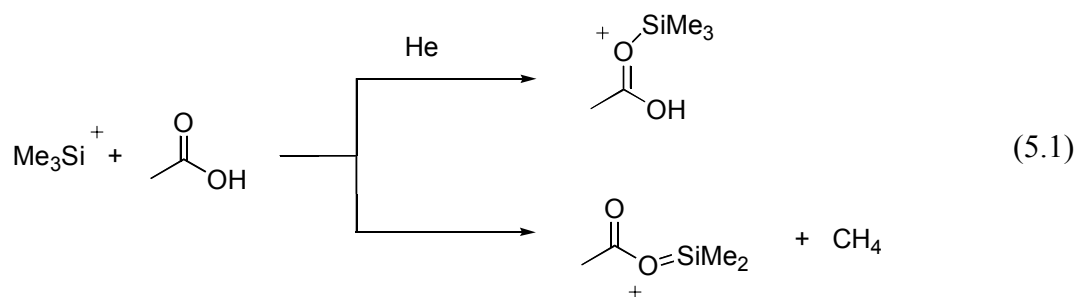
Figure 5.1 Typical spectrum of the trimethylsilyl cation formed from the reaction of Ar^+ with Me_4Si .

Hydride ion transfer is observed when 2-methylbutane and cyclopentene are allowed to react with the trimethylsilyl cation.

When the trimethylsilyl cation is allowed to react with diethylether, the adduct product is observed. In addition to this observed product, we hypothesize that the hydride transfer product also occurs. The hydride ion transfer product's m/z value is the same as the reactant ion (m/z 73). One could use an analogous ether or use a deuteriated ether to provide proof for this hypothesis. The former option was chosen, and the qualitative reaction of the trimethylsilyl cation with

tetrahydrofuran was studied. Hydride ion transfer and adduct formation was observed. Therefore, hydride ion transfer is assumed to occur with diethylether even though the product is isobaric with the reagent ion (i.e. Me_3Si^+).

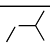

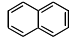

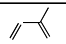
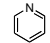
When the trimethylsilyl cation is allowed to react with acetic acid, adduct formation and methane loss products are observed (eq 5.1). A product ion, which has lost propane, is



also observed with diethylamine. In addition to propane being lost, proton transfer and adduct products are observed.

Triethylamine or diethylamine form proton transfer and adduct products when they are allowed to react with the trimethylsilyl cation. Since protonated trimethylsilanol is also present in the reactant spectrum, the issue arises whether the protonated triethylamine or diethylamine are formed via reaction with the trimethylsilyl cation or by protonated trimethylsilanol.^{3,9} Protonated trimethylsilanol reacts with both diethylamine and triethylamine to form proton transfer products. Does the presence of protonated trimethylsilanol contribute to erroneous branching ratios? To address this concern, the branching ratio was corrected for the reaction of protonated trimethylsilanol with triethylamine by subtracting the amount that would have reacted with protonated trimethylsilanol at the correct reaction time. There was no difference within error between the corrected branching and non-corrected branching ratios. Since there was no significant change in the branching ratio when the contribution of protonated trimethylsilanol

Table 5-1 Summary of the reactions of the trimethylsilyl cation with various neutrals. The dark shaded area is a rate coefficient not measured since it is present in the literature.

Neutral	k_H (Eff) ^a	k_{lit} (Eff) ^a	Adduct		PT ^b		Hydride Ion Transfer		Alkane Loss
			BR	$\Delta H_{rxn}^{c,d}$	BR	$\Delta H_{rxn}^{c,d}$	BR	ΔH_{rxn}^e	
	0.005 ± 0.003 (0.004)						100 %	+ 6 ± 5	
H ₂ O	0.99 ± 0.22 (0.42)		100%	-30.1		+ 61.5			
D ₂ O	0.71 ± 0.08 (0.32)		100%						
C ₆ H ₆	0.62 ± 0.12 (0.51)		100%	-23.9		+ 47.2			
	0.67 ± 0.08 (0.55)		93 ± 2 %			+ 43.3	7 ± 2 %	+ 2 ± 5	
EtOH	0.84 ± 0.12 (0.50)		100%	- 42.0		+ 40.9			
MeCN	1.85 ± 0.23 (0.52)		100%			+ 40.3			
MeCO ₂ H	1.56 ± 0.11 (0.91)		86 ± 4 %			+ 39.2			14 ± 4 %
			100%			+ 34.6			
	0.82 ± 0.16 (0.65)		100%			+ 34.5			
MeCOMe	1.59 ± 0.08 (0.61)	2.10 ± 0.05 ^f (0.80)	100%	-45.0		+ 32.4			
	0.92 ± 0.05 (0.72)		100%			+ 29.0			
EtOEt	0.75 ± 0.1 (0.50)		X%	-44.2		+28.5	Y% ^g	- 4 ± 5	
Me ₂ S	0.78 ± 0.17 (0.45)		100%			+ 27.9			
MeCO ₂ CH ₂ Me	1.35 ± 0.27 (0.74)		100%	-48.7		+ 26.8			
NH ₃		1.56 ± 0.78 ^f (0.73)	100%	-46.5		+ 22.5			
HCONMe ₂	1.80 ± 0.18 (0.58)		100%			+ 14.4			
(MeO) ₃ PO ^h	1.60 ± 0.22 (0.63)		100%			+ 13.6			
	1.25 ± 0.28 (0.59)		100%			+ 4.5			
(Et) ₂ NH	1.05 ± 0.33 (0.73)		66 ± 4 %		33 ± 4 %	- 1.1			1 ± 1 %
Et ₃ N	0.90 ± 0.11 (0.62)	0.72 ± 0.02 ^f (0.46)	37 ± 3 %		63 ± 3 %	- 8.2			

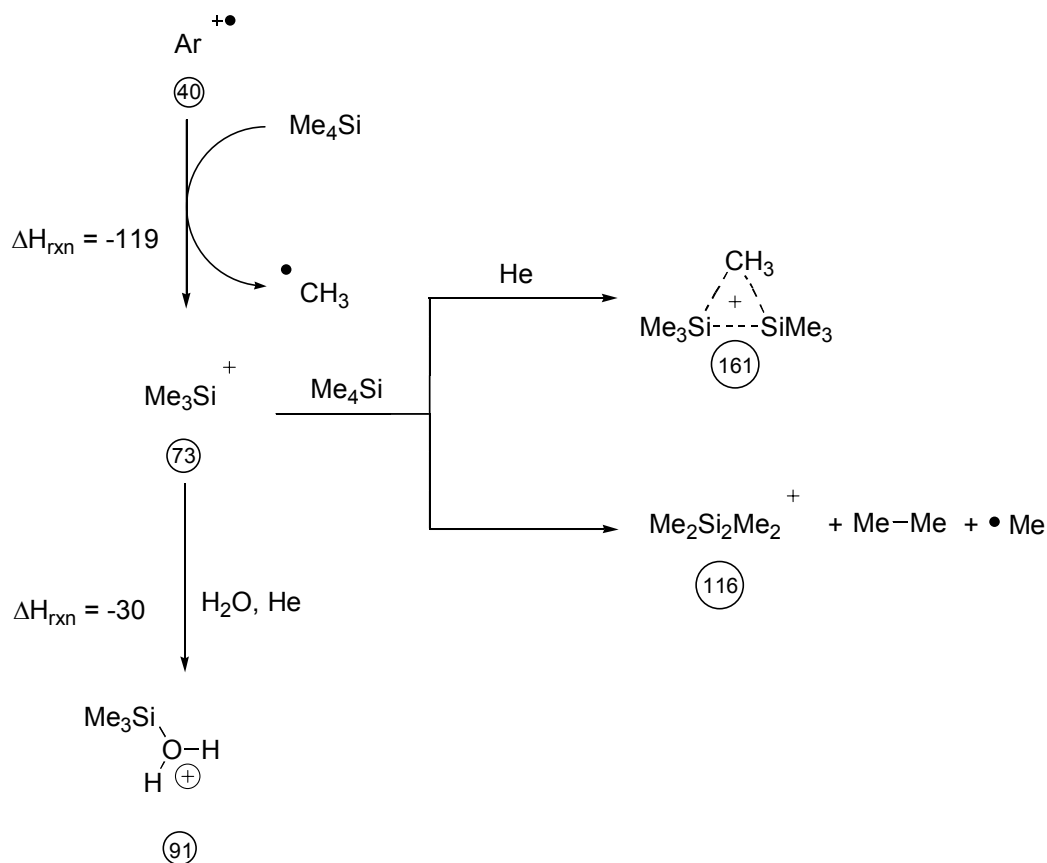
a--Units of 10⁹ cm³ molecule⁻¹ s⁻¹. Eff = k_{obs}/k_{coll} . k_{coll} is calculated via the VTST theory of Su and Bowers. NR = No reaction observed.
b--PT = proton transfer
c-- ΔH_{rxn} (units of kcal/mol). d--Linstrom, P.J. (Ed.) NIST Chemistry Webbook.
e--Lias, S.G. et al *J Phys Chem Ref Data* **1988**, 17
f--Chen, Q.-F.; Stone, J. A. *Int. J. Mass Spectrom. Ion Proc.* **1997**, 165/166, 195-207. (FA)
g--Assumed by reaction of the trimethylsilyl cation with tetrahydrofuran. Branching ratio could not be measured due to interference with the trimethylsilyl cation.
h--Polarizability calculated using the group additivity method of Miller and coworkers

was removed, no corrections were applied to the branching ratio data for the trimethylsilyl cation with diethylamine reaction.

5.4 DISCUSSION

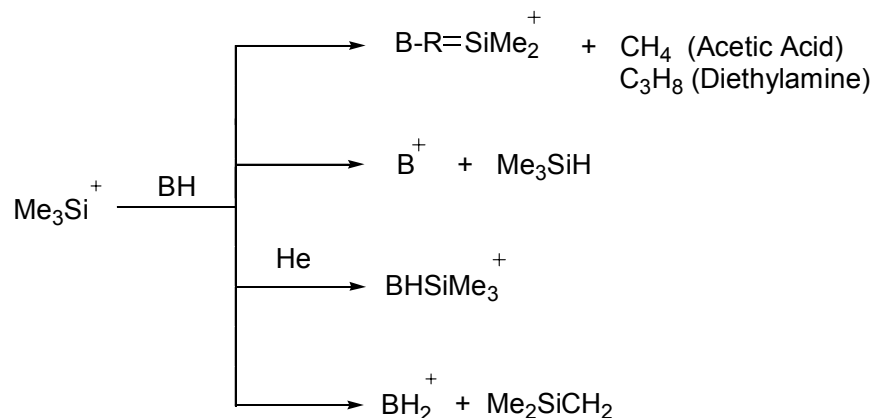
While there are no reports in the literature of using the radical cation of argon to form the trimethylsilyl cation, it is known that the radical cations of noble gases such as xenon can form charge dissociative products with neutrals.¹⁶ The ionization energy of argon is 15.8 eV and the appearance energy of the trimethylsilyl cation is ~10.6 eV.¹⁷ The dissociative charge transfer reaction is exothermic by ~5 eV (~119 kcal/mol). A scheme summarizing the principle ions observed when allowing $\text{Ar}^{+\bullet}$ to react with Me_4Si at 0.3 Torr of helium in a flowing afterglow (e.g. figure 5.1) is shown in scheme 5.1. Methylated hexamethyldisilane and m/z 131 are observed from the reaction of the trimethylsilyl cation with excess tetramethylsilane. Stone and coworkers also observed these ions.¹⁸ Protonated trimethylsilanol is a product from the reaction of the trimethylsilyl cation with adventitious water which also has been reported by Stone.⁹

The optimized trimethylsilyl cation system was allowed to react with the neutrals listed in Table 5.1 and the observed reaction channels summarized in scheme 5.2. The reaction efficiencies are all greater than 0.32, with the exception of 2-methylbutane. The reason why the efficiency of cyclopentene (0.53) is ~100 times faster than 2-methylbutane (0.004) is because when the trimethylsilyl cation is allowed to react with cyclopentene both hydride ion transfer and adduct formation is observed. Only hydride ion transfer is observed with 2-methylbutane.



Scheme 5-1 Formation of the trimethylsilyl cation and subsequent reaction with excess tetramethylsilane. All thermochemical data are in units of kcal/mol.

The derived thermochemistry of the reaction of the trimethylsilyl cation with 2-methyl butane indicates that the hydride ion transfer reaction is $+6 \pm 5$ kcal/mol endothermic. It should be noted that 150 ± 5 kcal/mol is used for the heat of formation of the trimethylsilyl cation since there are two different reported values for the heat of formation of the trimethylsilyl cation: 150 kcal/mol, as measured by Szepes and Baer,¹⁹ and ~ 145 kcal/mol, as reported by Potzinger and Ritter.²⁰ Both values are estimated, and neither include error bars.

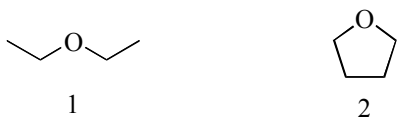


Scheme 5-2 Generalized scheme for the reaction of a base B with the trimethylsilyl cation

The hydride ion transfer reaction of the trimethylsilyl cation with 2-methylbutane is $+6 \pm 5$ kcal/mol endothermic. This slightly endothermic reaction and slow rate coefficient ($5 \times 10^{-12} \text{ cm}^3 \text{ molecule}^{-1} \text{ s}^{-1}$), can be explained by using the Arrhenius relation. Assuming that the hydride ion transfer product has an enthalpy of reaction of +1 to +6 kcal/mol and that there is no kinetic barrier to reaction, then the minimal rate that this reaction could react at is 2×10^{-10} to $5 \times 10^{-14} \text{ cm}^3 \text{ molecule}^{-1} \text{ s}^{-1}$, respectively. These rates were calculated using the Arrhenius equation, using +1 and +6 kcal/mol as the activation energy and 298K as the temperature. The collisional rate coefficient calculated using the theory as described in the experimental section was used as the preexponential factor. The polarizability of 2-methylbutane was calculated to be $9.98 \times 10^{-24} \text{ cm}^3$ using the theory of Miller and Savchik.²¹ Ausloos and Lias studied the analogous reaction of the tert-butyl cation with 2-methylbutane and observed that hydride ion transfer occurred.²² They reported the efficiency of reaction to be 0.01. The low efficiency is analogous to our observations of hydride ion transfer.

The other neutral that had an observable hydride ion transfer product was cyclopentene. The rate of reaction is ~10 times faster than 2-methylbutane. When the trimethylsilyl cation is allowed to react with ethanol, only the adduct product is formed. The rate of reaction is 0.84×10^{-9} , which is the same as cyclopentene (within error).

When diethylether was allowed to react with the trimethylsilyl cation, the adduct product was observed. It was hypothesized that the ether could have a hydride transfer product since these types of products have been observed in ethers. Smith and coworkers reported a hydride ion transfer reaction when NO^+ was allowed to react with diethylether.²³ It is hypothesized that the reaction of the trimethylsilyl cation with diethylether produces a hydride ion transfer product that is isobaric with the reactant ion (i.e. m/z 73). This is hypothesized because as the rate coefficient of this reaction was attempted to be measured, a suitable reaction of the reactant ion (i.e. Me_3Si^+) was not possible. One could ascertain whether a hydride ion transfer product occurs if the isotopic contribution to m/z 73 changes with the extent of reaction, since the ^{30}Si isotope is more abundant than ^{18}O . However, protonated diethylether (m/z 75), observed from the reaction of protonated trimethylsilanol with diethyl ether precluded this approach. Instead, the hypothesis of hydride ion transfer was tested using a cyclic ether comparable to diethylether (1), tetrahydrofuran (2). When tetrahydrofuran was



allowed to react with the trimethylsilyl cation, adduct and hydride ion transfer (less than 10%) products are observed from the qualitative experiments.

Our measured rate coefficient of the reaction of the trimethylsilyl cation with furan is $0.82 \times 10^{-9} \text{ molecule}^{-1} \text{ cm}^3 \text{ s}^{-1}$ (measured from 0.3 to 0.5 Torr). Munson and coworkers found that this reaction to be pressure dependent.²⁴ To determine whether a rate coefficient has a pressure dependence, a plot of observed rate vs. pressure is constructed, as shown in Figure 5.2. No pressure dependence was observed between 0.3 – 0.5 Torr (using an error of $\pm 20\%$). Munson and coworkers extrapolated their measured rate coefficients to zero pressure, finding a y-intercept of 1.8×10^{-11} (see figure 5.2). This value was hypothesized to be the radiative rate constant. Our value mentioned above correlates with Munson and coworker's observations since their pressure used was lower than ours, $1-10 \times 10^{-7}$ Torr vs. 0.3-0.5 Torr, respectively. Since

our rate coefficient is only 0.58 efficient, the value must lie between the minimum and maximum value. If one would continuously increase the pressure, the rate coefficient would eventually reach the collisional limit.

Acetic acid forms a product that is termed by us as an “alkane loss.” In addition to forming the adduct, acetic acid loses methane to form the structure 1 as described in Scheme 5.3. Blair and Bowie have hypothesized a loss of methane from this reaction, but did not report any transition states or structural information.⁴ It is hypothesized that a six center transition state leads to the methane loss channel (see scheme 5.3). The methane loss for acetic acid was confirmed by two experiments. The first experiment was designed to discount that this loss was due via a reaction with an excited (metastable) trimethylsilyl cation. Excess tetramethylsilane was added while the concentration of argon and acetic acid was held constant. This experiment should lead to the quenching at least some of any metastable Me_3Si^+ ions, if they existed, before they had a chance to react with acetic acid. Since the intensity of the alkane loss product did not change, as excess tetramethylsilane was added, no evidence for a metastable trimethylsilyl cation was found. The second experiment examined was the reaction of d_3 -acetic acid with the trimethylsilyl cation. We observed a 3 amu increase in the adduct and methane-loss products as compared to reaction with CH_3COOH .

When diethylamine is allowed to react with the trimethylsilyl cation, an adduct, a proton transfer, and another product which loses propane, is observed. This “alkane loss” is not observed in the other reactions.

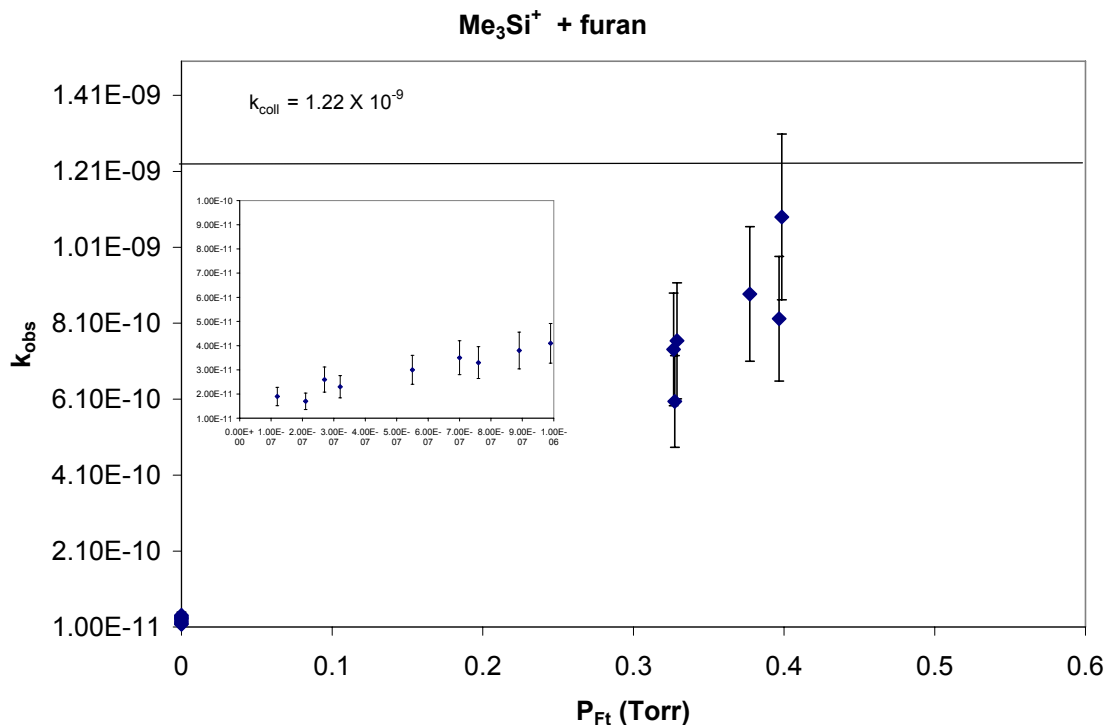
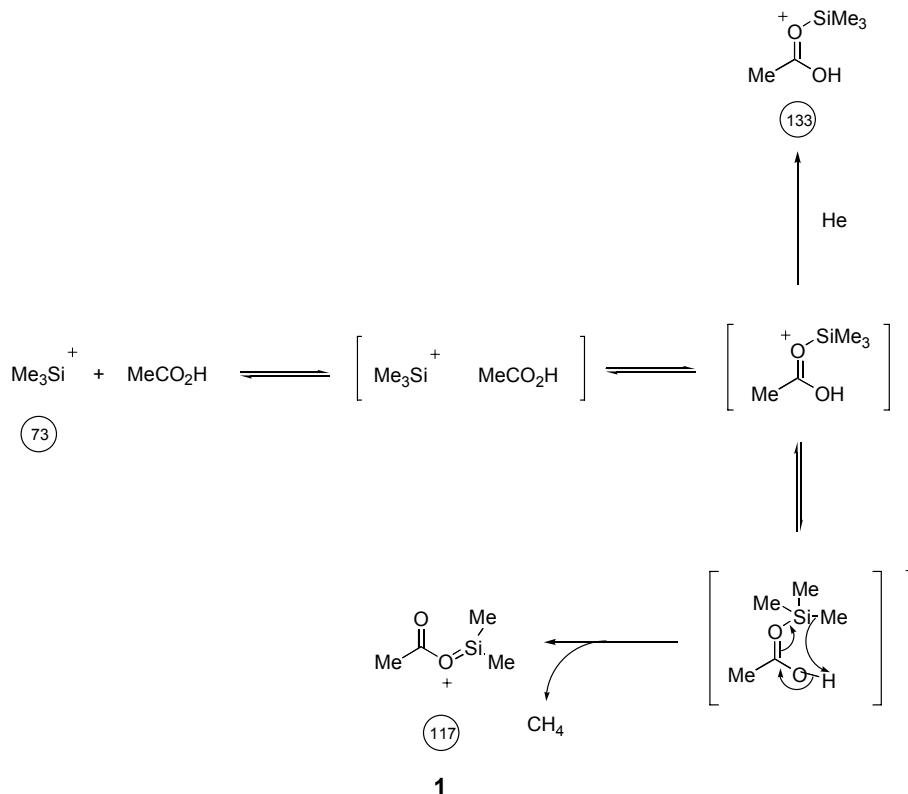


Figure 5.2 Plots of k_{obs} vs pressure. The data from 1×10^{-7} to 1×10^{-6} Torr was generated by Munson and coworkers.²⁴

The following factors should be considered to explain these “alkane losses”: whether the neutral possesses an acidic proton, what types of electron donating or withdrawing groups are on the reactant neutral, and what heteroatom is bound to the silicon atom in the adduct (i.e. bond energy). Ethanol possesses an acidic proton, but this loss is not observed. One reason why alkane loss is not observed in ethanol but is in diethylamine is that an N-Si bond (105 kcal/mol) is weaker than a O-Si bond (191 kcal/mol).¹⁴ More energy is expended if an alkane loss would occur with ethanol. An alternative explanation is that the “alkane loss” reaction with ethanol is not thermodynamically allowed, but no thermochemical data exists to prove or disprove this hypothesis.



Scheme 5-3 Hypothesized scheme of methane loss for the reaction of the trimethylsilyl cation with acetic acid

Other factors such as the type of groups attached to the heteroatom also affect the observance and yield of “alkane loss.” Neutrals possessing electron donating groups (i.e. ethanol and diethylamine) stabilize adduct formation better than electron withdrawing groups since the trimethylsilyl cation is considered a hard acid. The electron donating groups on the amine reduce the yield of the “alkane loss” versus the acidic acid product. The formation of a less stable four centered transition state present with diethylamine also explains the small yield since a four-centered transition state is not as energetically favored as a six-centered transition state with acetic acid. An electron withdrawing group on (RCO₂H) allows the alkane loss to occur since it can withdraw electrons from the trimethylsilyl moiety making the adduct less stable. This methane loss with acetic acid has been observed by Blair and Bowie.⁴ They hypothesized that the trimethylsilyl cation attacks the –OH oxygen and goes through a four-centered

intermediate. We believe attack at the carbonyl oxygen allows for a six membered transition state. The attack of the trimethylsilyl cation on the carbonyl oxygen is further stabilized via resonance. We were unable to observe this product due to the presence of protonated trimethylsilanol and its isotopomers (i.e. m/z 92 $C_3H_9^{29}SiOH_2^+$).

Blair and Bowie observed alkane loss when the trimethylsilyl cation was allowed to react with ethyl acetate.⁴ Wojtyniak and Stone did not observe the loss using ethyl acetate as the reactant neutral at 4.0 Torr.²⁵ Our observations agree with Stone's. Ethyl acetate does not have an acidic proton, which agrees with our hypothesis.

Proton transfer and adduct products are observed when diethylamine and triethylamine are allowed to react with the trimethylsilyl cation. The absence and presence of proton transfer agrees with the established proton affinity of 2-silaisobutene ($(CH_3)_2SiCH_2$) which is 226.5 kcal/mol.¹⁷

Rate coefficients have been measured by Chen and Stone for the reactions of the trimethylsilyl cation with ammonia, acetone, and triethylamine.⁹ Since our rate coefficients for acetone and triethylamine agree with Chen and Stone's within estimated errors, there was no need then to measure the rate of the trimethylsilyl cation with ammonia.

5.5 CONCLUSIONS

When the trimethylsilyl cation is allowed to react with a variety of neutrals, adduct formation, proton transfer, hydride ion transfer, and/or an "alkane loss" are observed. Even though it has been mentioned in the literature by Munson, we found no pressure dependence in the measured rate coefficient between the trimethylsilyl cation with furan. We were unable to observe hydride ion transfer with diethylether, but we were able to observe it with tetrahydrofuran, an analogous ether. Therefore we can state that is probable that hydride ion

transfer occurs when diethylethyl ether is allowed to react with the trimethylsilyl cation. Methane loss is observed as one product of the reaction of the trimethylsilyl cation with acetic acid. The presence of a metastable reactant ion was ruled out. In addition, d3-labeled acetic acid studies revealed that the methyl group of the acid is retained in the product ion. Propane is lost when diethylamine is allowed to react with the trimethylsilyl cation. The Arrhenius relation provides insight on how an endothermic reaction (i.e. the trimethylsilyl cation with 2-methylbutane) can be observed, albeit having a rate of $5 \times 10^{-12} \text{ cm}^3 \text{ molecule}^{-1} \text{ s}^{-1}$.

5.6 REFERENCES

1. Fleming, I. *Chem. Soc. Rev.* **1981**, *10*, 83-111.
2. Kadentsev, V. I.; Chuvylkin, N. D.; Stomakhin, A. A.; Kolotyorkina, N. G.; Chizhov, S. *Russ Chem Bull* **1998**, *47*, 1228-1229.
3. Stone, J. A. *Mass Spec. Rev.* **1997**, *16*, 25-49.
4. Blair, I. A.; Bowie, J. H. *Aust. J Chem.* **1979**, *32*, 1389-1393.
5. Trenerry, V. C.; Blair, I. A.; Bowie, J. H. *Aust. J Chem.* **1980**, *33*, 1143-1146.
6. Dottore, M. F.; Trenerry, V. C.; Stone, D. J. M.; Bowie, J. H. *Org. Mass Spectrom.* **1981**, *16*, 339-343.
7. Orlando, R.; Strobel, F.; Ridge, D. P.; Munson, B. *Org. Mass Spectrom.* **1987**, *22*, 597-605.
8. Orlando, R.; Ridge, D. P.; Munson, B. *Org. Mass Spectrom.* **1988**, *23*, 527-534.
9. Chen, Q.-F.; Stone, J. A. *Int J Mass Spectrom Ion Proc* **1997**, *165/166*, 195-207.
10. Li, X.; Stone, J. A. *Can. J. Chem.* **1987**, *65*, 2454-2460.
11. Phillips, M.; Herrero, J.; Krishnan, S.; Zain, M.; Greenberg, J.; Cataneo, R. N. *J Chrom B: Biomed Sci Appl* **1999**, *729*, 75-88.
12. Melley, S. J.; Grabowski, J. J. *Int J Mass Spectrom Ion Proc* **1987**, *81*, 147-164.
13. Su, T.; Su, E. C. F.; Bowers, M. T. *J. Chem. Phys.* **1978**, *69*, 2243-2250.
14. Lide, D. R., Ed. *CRC Handbook*; 3rd Electronic Edition ed.; CRC Press: Boca Raton, FL, 2000.
15. Anderson, D. R.; Bierbaum, V. M.; Depuy, C. H.; Grabowski, J. J. *Int J Mass Spectrom. Ion Phys.* **1983**, *52*, 65-94.
16. Praxmarer, C.; Hansel, A.; Jordan, A.; Kraus, H.; Lindinger, W. *Int J Mass Spectrom Ion Proc* **1993**, *129*, 121-130.
17. Lidstrom, P. J.; Mallard, W. G., Eds. *NIST Chemistry WebBook, NIST Standard Reference Database Number 69*; March 2003 ed.; National Institute of Standards and Technology: Gaithersburg MD, 20899, 2003.
18. Wojtyniak, A. C. M.; Stone, J. A. *International Journal of Mass Spectrometry and Ion Processes* **1986**, *74*, 59-79.
19. Szepes, L.; Baer, T. *Journal of the American Chemical Society* **1984**, *106*, 273-278.
20. Potzinger, P.; Ritter, A.; Krause, J. Z. *Naturforsch* **1975**, *30*, 347.
21. Miller, K. J.; Savchik, J. A. *Journal of the American Chemical Society* **1979**, *101*, 7206-7213.
22. Ausloos, P.; Lias, S. G. *Journal of the American Chemical Society* **1970**, *92*, 5037-5045.
23. Spanel, P.; Smith, D. *Int J Mass Spectrom* **1998**, *172*, 239-247.
24. Lin, Y.; Ridge, D. P.; Munson, B. *Organic Mass Spectrometry* **1991**, *26*, 550-558.
25. Wojtyniak, A. C. M.; Stone, J. A. *Int J Mass Spectrom Ion Proc* **1986**, *74*.

6.0 USING HENRY'S LAW AND THE EXPONENTIAL FLASK TO VALIDATE QUANTITATION OF THE CRMS

6.1 INTRODUCTION

The unique capability of the flowing afterglow is that the previously known ion/molecule data allows the user to quantify volatile organic compounds (VOCs) online and in realtime without any conventional calibration. Other techniques such as gas chromatography mass spectrometry (GCMS) or liquid chromatography mass spectrometry (LCMS) rely on internal or external calibrations to ensure the consistency of the measurement. While there is no actual need to perform a calibration experiment for the CRMS, this section involves control experiments that will give the researcher some sense of the errors associated with VOC quantitation.

Henry's law states that the headspace concentration of a VOC (C_{HS}) is proportional to its concentration in solution, C_{soln} (eq 6.1). The only assumption in this law is that the solute

$$C_{HS} = \frac{1}{k_H} C_{soln} \quad (6.1)$$

dissolved in the solvent must be dilute. To know the concentrations in the headspace, one must use an appropriate Henry's law constant (k_H). Henry's law constants are found in peer-reviewed lists such as the NIST chemistry webbook.¹ The use of Henry's law to determine the liquid phase concentration of a substance has been explored by Smith and coworkers by sampling the

headspace of urine.² The method used by Smith and coworkers² is used to detect known amounts of acetone and acetonitrile in deionized water solutions of 5, 50, 500, and 5000 ppm.

Another technique used for comparing quantitative results from the CRMS and theory is using an exponential dilution flask. A flask is constructed that contains a device to allow for maximum air circulation. The flask's volume is determined. A known flow of inert gas is passed through the flask. At a specified time, a known volume of gas is injected into the flask. This initial concentration and time is noted. The exponential dilution flask follows the exponential decay shown in eq 6.2. The concentration at time t, C_t , can be calculated if one

$$C_t = C_0 e^{-\frac{F t}{V}} \quad (6.2)$$

knows C_0 , the initial concentration, the flow rate, F , and the volume of the flask, V . Attempts to use to use this technique are shown later. This equation has been modeled and used by Lovelock and Ritter and Adams.^{3,4}

6.2 EXPERIMENTAL

6.2.1 Henry's Law

Standard solutions of 5, 50, 500, and 5000 ppm of acetone and acetonitrile were made in the following fashion. All glassware except for the volumetric flasks and pipettes were baked overnight at 150°C. A 500 μ L aliquot of solute was placed into a 100mL grade A volumetric flask to make a 5000 ppm solution. This 5000 ppm solution was serially diluted into a 500 ppm

solution by pipetting 10 mL (TD) aliquot of the 5000 ppm solution into another 100mL grade A volumetric flask. The same procedure was used to make 50 and 5 ppm solutions. Once these solutions were made, 20 mL of each standard in addition to duplicates of 5 ppm were placed into separate 250 mL RB flasks and sealed with a septum.

The error in volume delivery of the pipettes and flasks were determined. Gravimetric analysis was used to determine the delivery error volume via the density relation. To determine the error of volume delivery from the pipettes, the temperature of the water was measured. A volume of water was pipetted into a clean 50 mL beaker and the mass of water was determined. This was repeated 10 times for the 500 μ L and 10 mL pipettes on two separate days. The error in volume delivery for the volumetric flasks was determined by filling the flasks to the top with water past the calibration mark and removing the water down to the calibration mark. This water was placed into a beaker and weighed. The volume was then calculated using the density relation. Errors are shown in Table 6.1 and are less than 3%.

Table 6-1 Errors associated with volume delivery involving the volumetric glassware

	10mL Glass Pipette (TD)		0.5 mL glass pipette (TC)		100mL Grade A Volumetric Flask
Volume of Water Dispensed (mL)	10.0078		0.4949		99.2051
	9.9717		0.486		99.1239
	9.9859		0.4813		99.0883
	9.9881		0.4838		99.1423
	10.0068		0.4872		99.2967
	9.9877				
	9.9725				
	9.9962				
	9.9706				
	9.9865				
Avg	9.9874		0.4866		99.1713
Std dev	0.0134		0.0051		0.0819
% Std Dev	0.1345		1.0555		0.0826
Error in Accuracy (%)	0.1262		2.6800		0.8300
	Accuracy in Made Standard (%)				
5000 ppm:	2.7976				
500 ppm:	2.9205				
50 ppm:	3.0384				
5 ppm:	3.1519				

The setup of the inlet to the flowing afterglow is shown in Figure 6.1. A hypodermic syringe is cut near the handle with the plunger removed. A Cajon connector and o-ring are connected at



Figure 6.1 Setup of Headspace Collection using a 250 mL RB flask and sealed with a septum. Notice the modified hypodermic syringe.

the end. This is placed at the inlet to an arm of the vacuum rack. The port at 36.3 cm was opened and a flow of air into the flow tube is attained. A background signal with lab air introduced into the CRMS is collected, and then the septum is pierced and the headspace is sampled. The flask is removed and the lab air is collected. The same procedure is performed all the other samples. In some cases the experiment was repeated in the same day and in all cases the experiments were repeated for over two experimental days.

6.2.2 Exponential Dilution Flask

A custom-made exponential dilution flask was constructed to allow ¼” cajon connectors to attach to either end of it, allow a stir bar with minimum clearance to fit inside the device, and to have a removable septum for introducing vapors. This device is shown in figure 6.2. The volume of the flask was determined by weighing the dried empty vessel and then weighing the vessel filled with water without any air bubbles. The volume determined was 280.73 ± 0.82 mL,

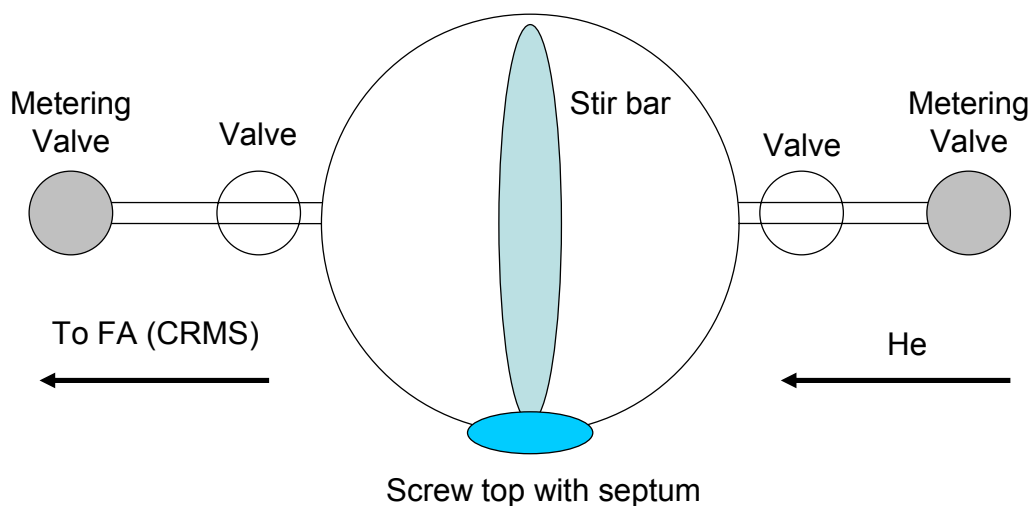


Figure 6.2 Overview of the exponential dilution flask. A known flow of helium gas is passed through the flask. A known volume of vapor is injected into the flask via the septum.

which was an average of five measurements. Helium was used as the diluent gas. The flow of helium was determined by attaching the metering valve to the vacuum rack and then disconnecting it to allow the connection to the vac rack for analysis. Another metering valve was placed at the end of the flask rack to ensure the contents of the flask was not evacuated (see figure 6.2).

6.3 RESULTS

6.3.1 Henry's Law

A plot of intensity of protonated acetonitrile (m/z 42) vs time is shown in Figure 6.3.

As indicated on the figure, the intensity of m/z 42 increased with time, after the septum

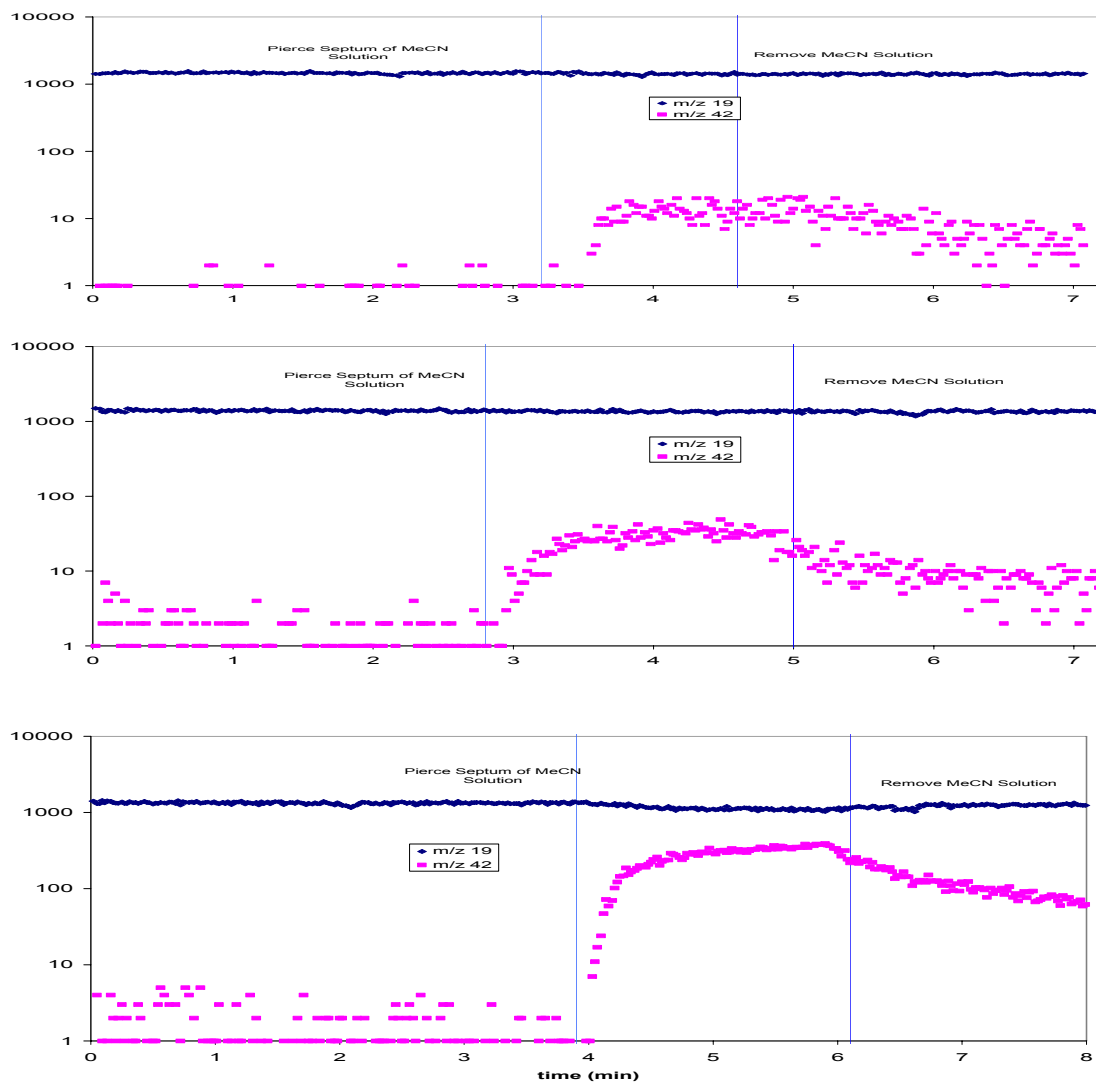


Figure 6.3 Plot of intensities of the hydronium ion (m/z 19) and protonated acetonitrile (m/z 42) vs. time as the septum is pierced and the flask removed for 50, 500, and 5000 ppm acetonitrile solutions.

is pierced. The intensity of the hydronium ion (m/z 19) and the total ion current (TIC) remains constant throughout the experiments. This must be true for pseudo first order conditions to take place (see chapter 2). A plot of the concentration of the headspace of acetonitrile vs. concentration of acetonitrile in water (M) is constructed to determine the Henry's Law constant for acetonitrile. As shown in Figure 6.4, the data points fall within the range of reported values

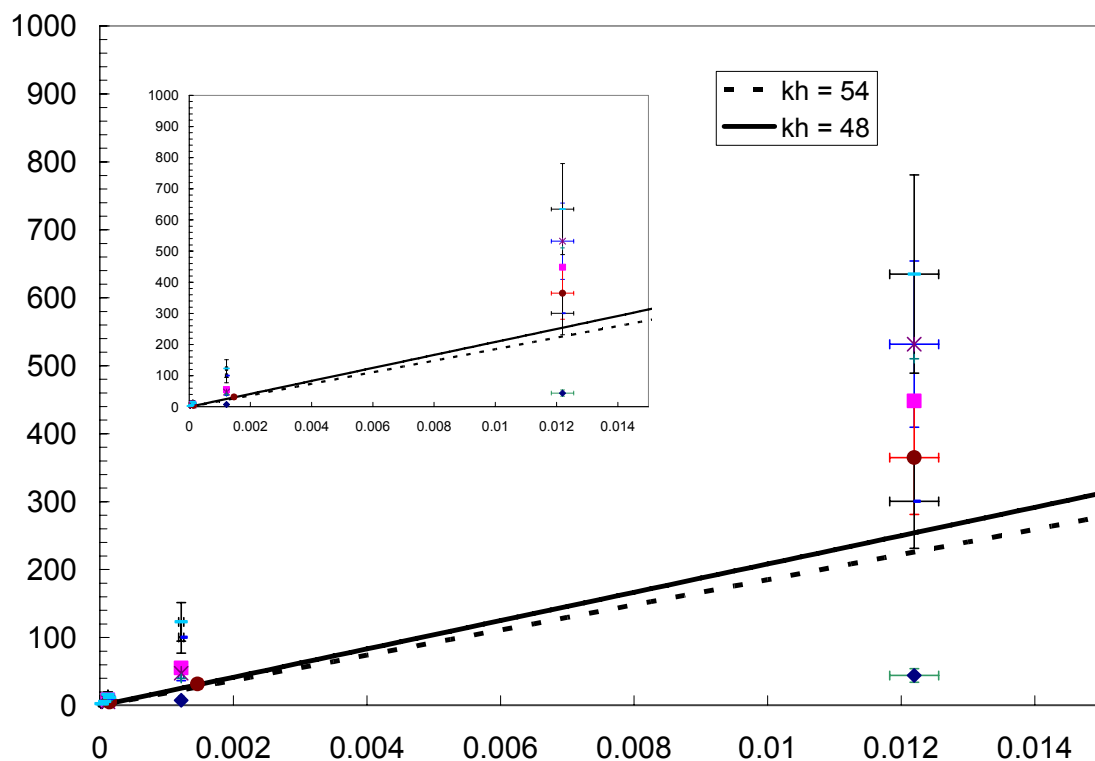


Figure 6.4 Plot of headspace concentration (ppm) vs. concentration of the liquid (M) for acetonitrile.

The inset is an expansion showing data from the 5, 50, and 500 ppm standards.

in the literature. The y error bars are the errors associated with the measurement of the headspace. The x error bars are errors associated in constructing the standards (see experimental section).

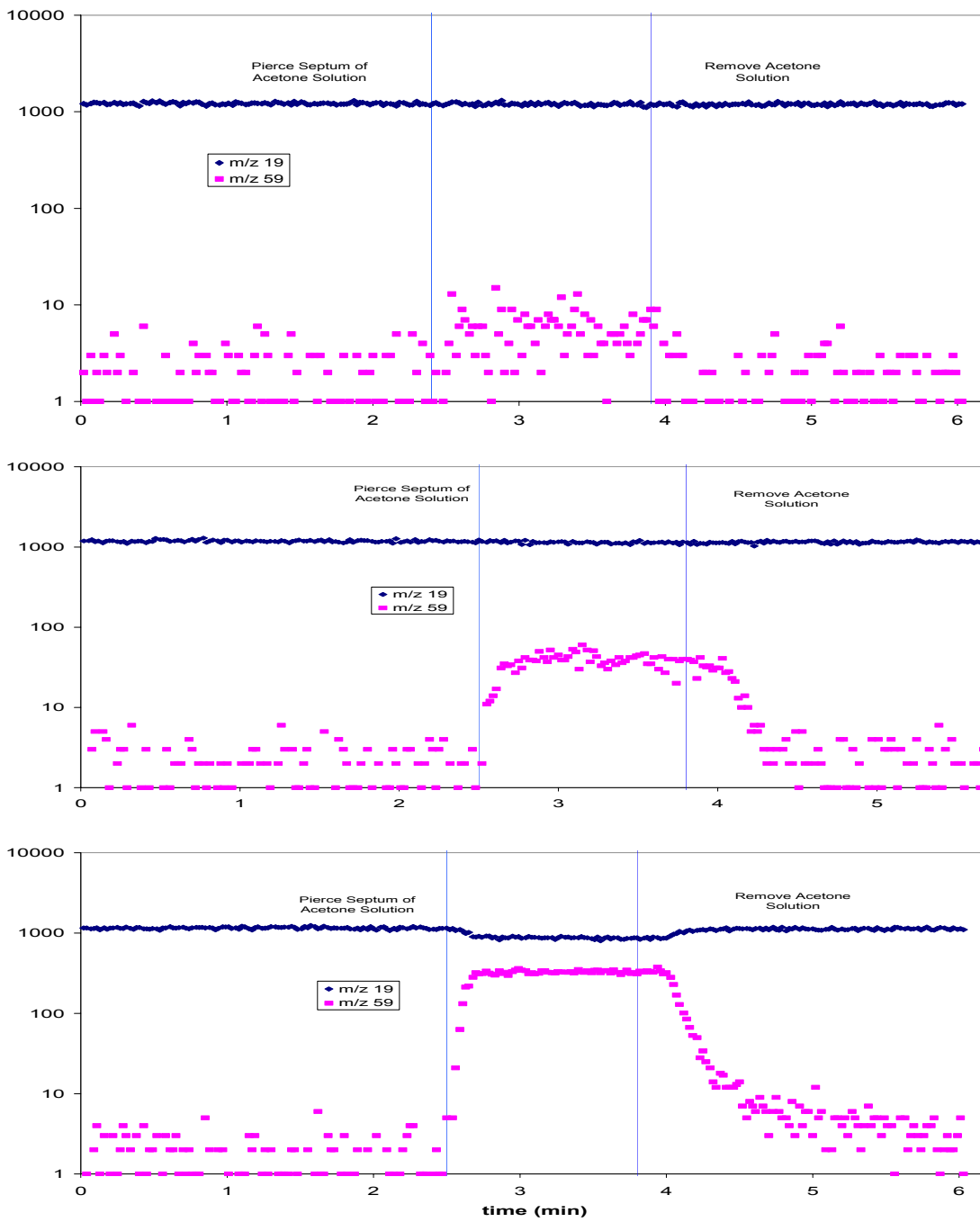


Figure 6.5 Graph of the intensity of protonated acetone (m/z 59) and the hydronium ion (m/z 19) vs. time for 50, 500, and 5000 ppm MeCN solutions.

The same type of experiments were conducted for acetone and the results are shown in figures 6.5 and 6.6.

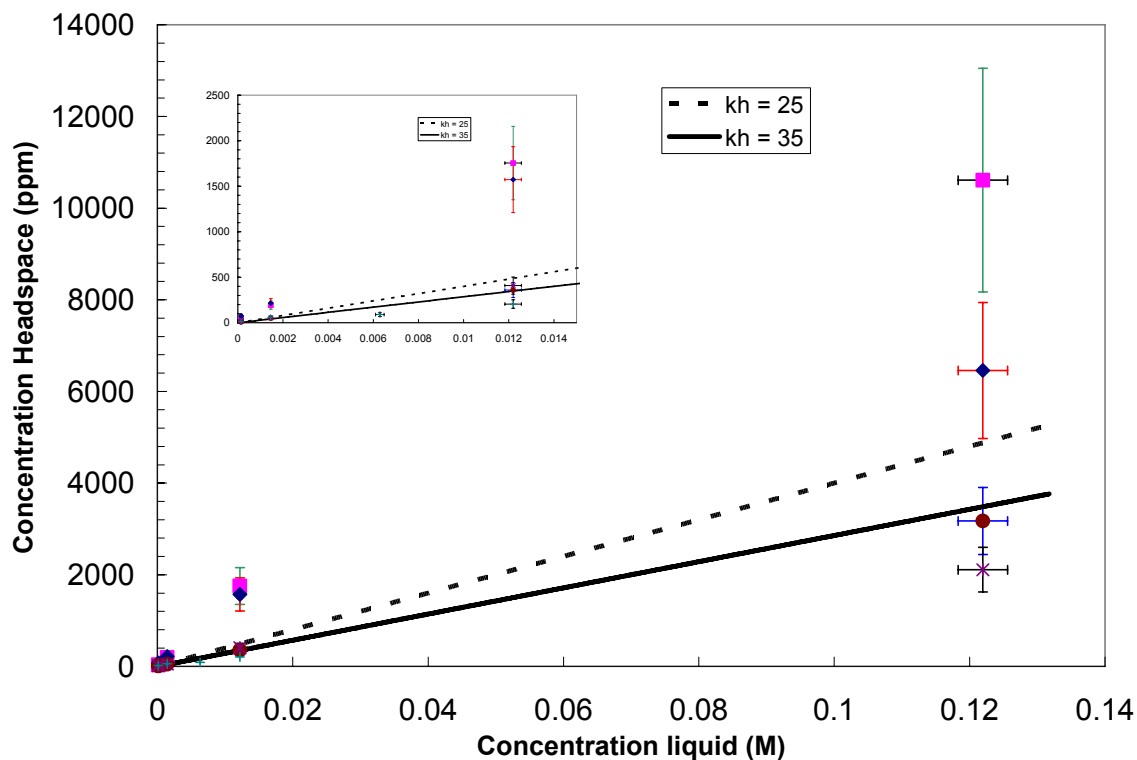


Figure 6.6 Plots of the headspace concentration (ppm) vs. the concentration of liquid (M) for acetone. See text for description of error bars.

6.3.2 Exponential Dilution Flask

A plot monitoring the introduction of ethyl acetate vapor into the flask is shown in figure 6.7. The signal due to the hydronium ion (m/z 19) is constant, while there is a noticeable increase and then decrease of m/z 89 and 90 when ethyl acetate is injected. The concentration of the CRMS is

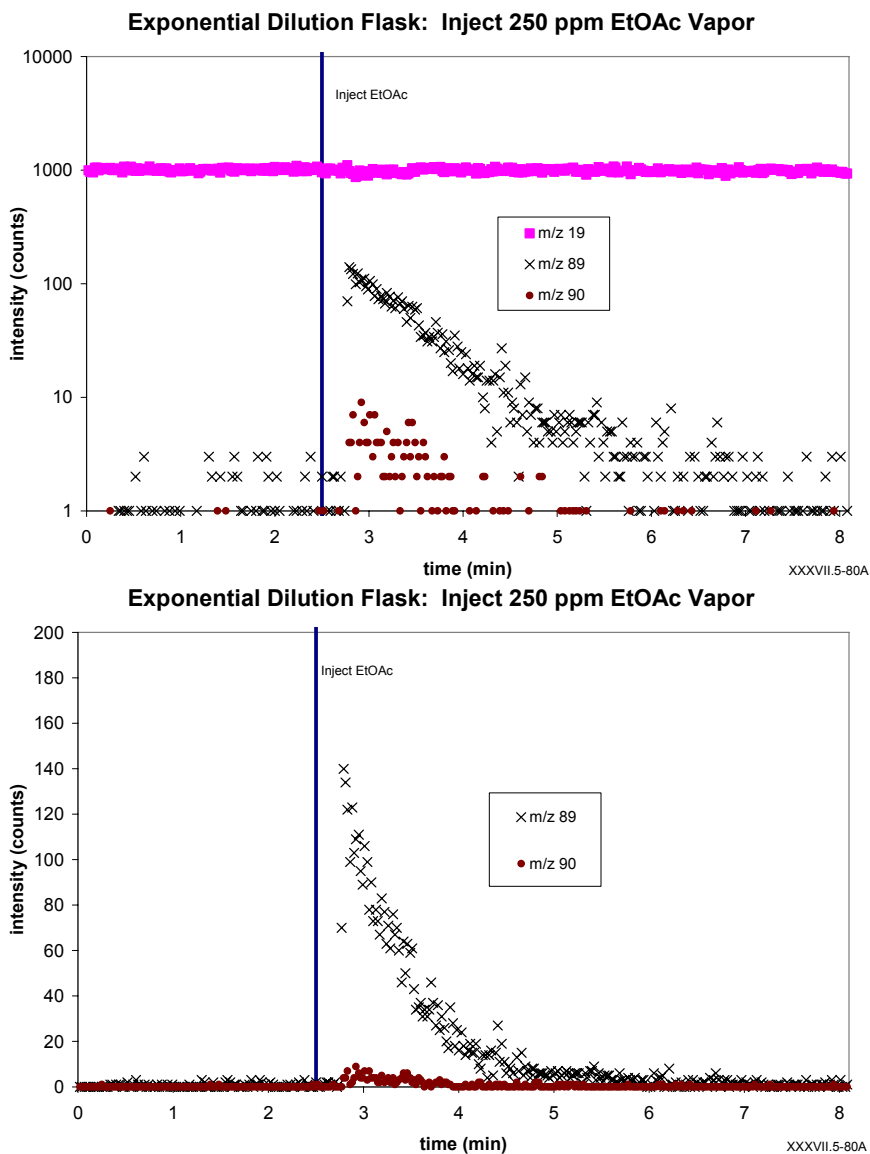


Figure 6.7 Semi logarithmic (top) and linear (bottom) graphs of ethyl acetate vapor being injected into an exponential dilution flask. m/z 19 is the hydronium ion (reactant ion), 89 is protonated ethyl acetate, and 90 is an isotopomer of protonated ethyl acetate.

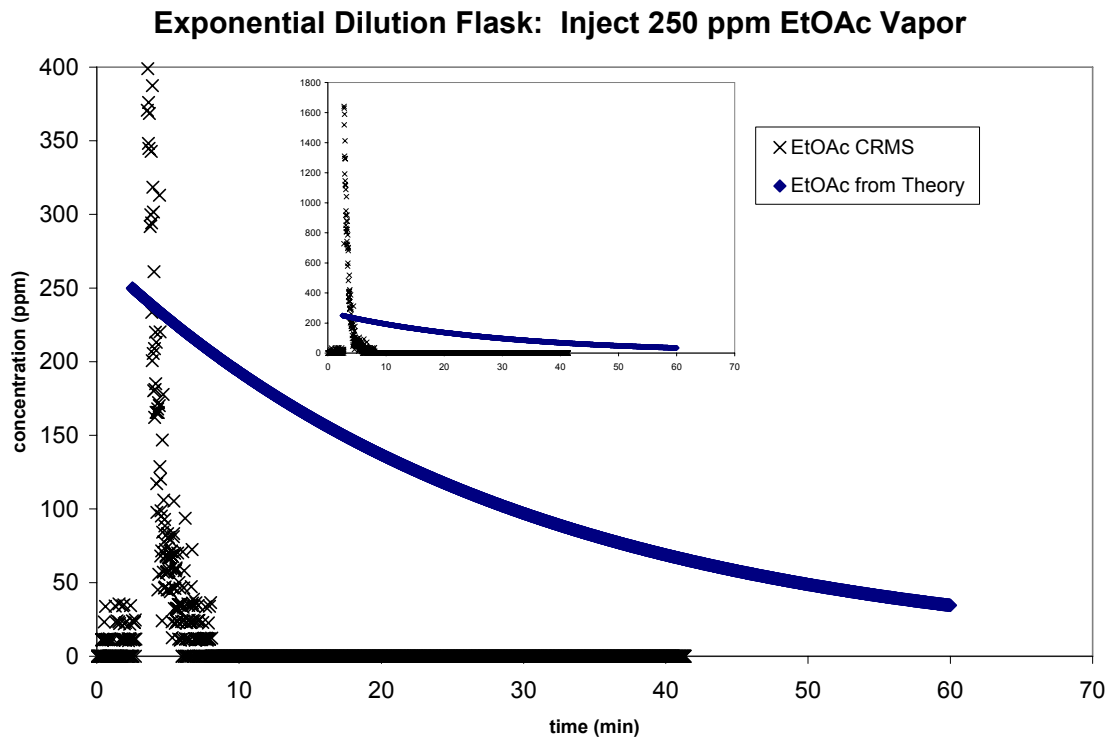


Figure 6.8 A graph comparing the concentration detected using the CRMS vs. the concentration predicted using the exponential dilution flask theory. The inset includes the full range of CRMS data. See the introduction for an explanation of exponential flask theory.

measured from known experimental variables (ch 2). The concentration decrease is modeled from eq 6.2 and other known variables such as volume of the vessel and flow rate. As is shown, the theory does not model the measured CRMS concentration (figure 6.8). The reason why there is a 10 ppm level of ethyl acetate present before any ethyl acetate is injected is because there was an experiment ran before that included ethyl acetate. There is no current explanation as to why this discrepancy exists.

6.4 DISCUSSION

6.4.1 Henry's Law

The comparisons between the measured Henry's law constant using the CRMS and the values reported in the literature are shown in Table 6.2. The values measured using the flowing afterglow were ordered in an arbitrary manner from the lowest value to the highest value. The differences between the measured Henry's law constants using the CRMS and the values reported in the literature are 6 percent for both acetone and acetonitrile. The values listed from the literature are either literature reviews or an original measurement of the value.¹ The average measured value using the CRMS agrees with the value obtained from Arijs and Brasseur (48 mol/kg/bar).⁵ Smith and coworkers have stated the error associated in measuring a Henry's law constant as 20%.² The Henry's law constant for acetone has not been measured using a flowing afterglow to date. The values measured with the CRMS agree with the average literature value within $\pm 20\%$ error that Smith reported.²

Table 6-2 Comparison of measured Henry's Law constants and constants listed in the literature. The percent difference reported is the difference between the average value measured using the flowing afterglow and the average value reported in the literature.

		Acetone		Acetonitrile	
		K _H Measured using FA	Other K _H ^a	K _H Measured using FA	Other K _H ^a
		31	30	40	53
		27	27	46	48
		25	27	52	54
		24	32	57	
			35		
			26		
			25		
			25		
			28		
Average		27	28	49	52
St Dev		3	3	7	3
% St Dev		12	12	15	6
% Difference		6		6	

a--Lidstrom, P. J.; Mallard, W. G., Eds. NIST Chemistry WebBook, NIST Standard Reference Database Number 69; March 2003 ed.; National Institute of Standards and Technology: Gaithersburg MD, 20899, 2003.

6.4.2 Exponential Dilution Flask

Various ideas have been formed as to why the theoretical concentration does not match the CRMS concentration. The first idea was that the flows of helium and diluent gas were not equal, causing erroneous results. However, this was checked and this is not the cause of the problem. Other issues which have not been addressed to date which could cause errors are whether the vessel is getting adequate mixing and if a second metering valve is needed.

6.5 CONCLUSIONS

The Henry's law constants have been measured using the CRMS and have been compared to the values listed in the literature. The values are within the range of values mentioned in the literature. These results allow the user of the CRMS to state the error associated with the CRMS.

The exponential dilution flask method was used to attempt to validate quantitation using the CRMS. While a increase and decrease was observed, the data did not match the theory and as the Henry's Law approach was useful, this dilution flask approach was abandoned.

6.6 REFERENCES

1. Lidstrom, P. J.; Mallard, W. G., Eds. *NIST Chemistry WebBook, NIST Standard Reference Database Number 69*; March 2003 ed.; National Institute of Standards and Technology: Gaithersburg MD, 20899, 2003.
2. Abbott, S. M.; Elder, J. B.; Spanel, P.; Smith, D. *Int J Mass Spectrom* **2003**, 228, 655-665.
3. Lovelock, J.E. *Anal Chem* **1961**, 33, 162-178.
4. Ritter, J.J.; Adams, N.K. *Anal Chem* **1976**, 48, 612-619.
5. Arijs, E.; Brasseur, G. *J Geophys Res* **1986**, 91D, 4003.

7.0 USING THE CRMS TO DETERMINE VOLATILE ORGANIC COMPOUNDS EMITTED FROM A GRAPHITIC BOARD COATED WITH PHENOLIC RESIN

7.1 INTRODUCTION

The flowing afterglow has the capability of quantifying and identifying multiple VOCs online and in real time. An example is using the flowing afterglow to ensure regulatory compliance. Hydrogen LLC is developing a hydrogen fuel cell membrane consisting of a graphitic board coated with phenolic resin. The process of curing the resin is to heat it from room temperature to 900°C. The company traps the VOCs that are emitted from the resin into a water trap. The goals of this project were to identify the VOCs emitted from heating the graphitic board and compare it to the VOCs emitted solely from the phenolic resin. With this data, the company would then be able to make an informed decision as to the elimination of wastes.

7.2 EXPERIMENTAL

A custom made SS chamber was used to heat the phenolic resin or graphitic board. An overview drawing of the apparatus is shown in Figure 7.1 (detailed blueprints may be found

in Appendix C). The chamber was placed inside a cylindrical copper block. The copper block has three cartridge heaters and a type J thermocouple to measure temperature. All the electrical feeds are connected to a temperature controller that was controlled via computer. The outlet of the flange is connected to a port on the flowing afterglow that was 36.3 cm from the nose cone. A picture of the apparatus around 900°C along with one set of representative temperature ramps are shown in Figure 7.2.

All mass spectral conditions along with necessary quantification information were collected. In each case, a blank was run before the graphitic board was heated. The hydronium ion was generated by the ionization of water at the ion source. Protonated hexamethyldisiloxane was generated using proton transfer from the tert butyl cation as described in chapter 3.

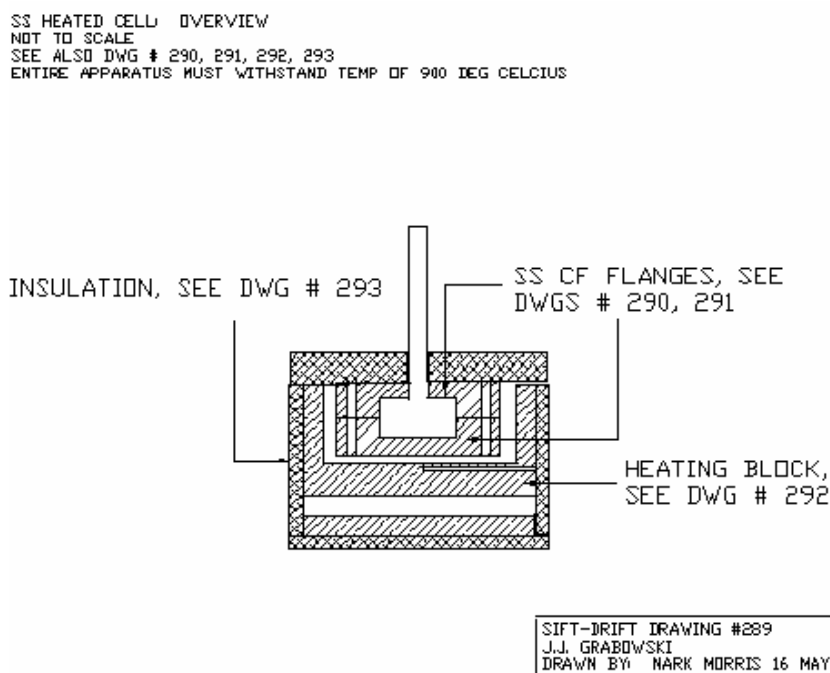


Figure 7.1 An overview drawing of the SS heated cell. Note that the drawing is not to scale. For other drawings, see appendix C.

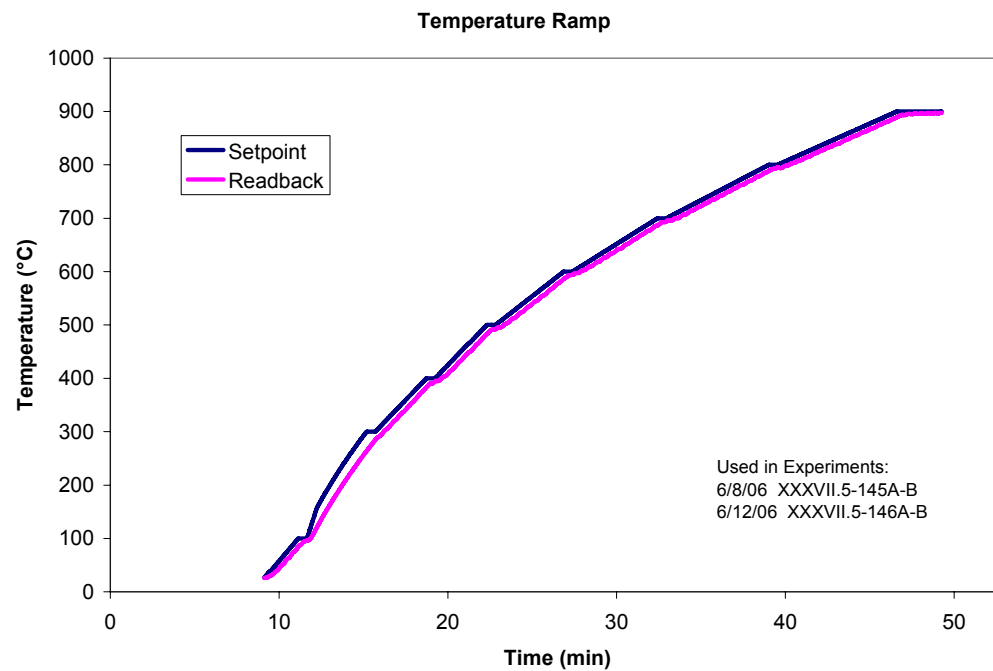
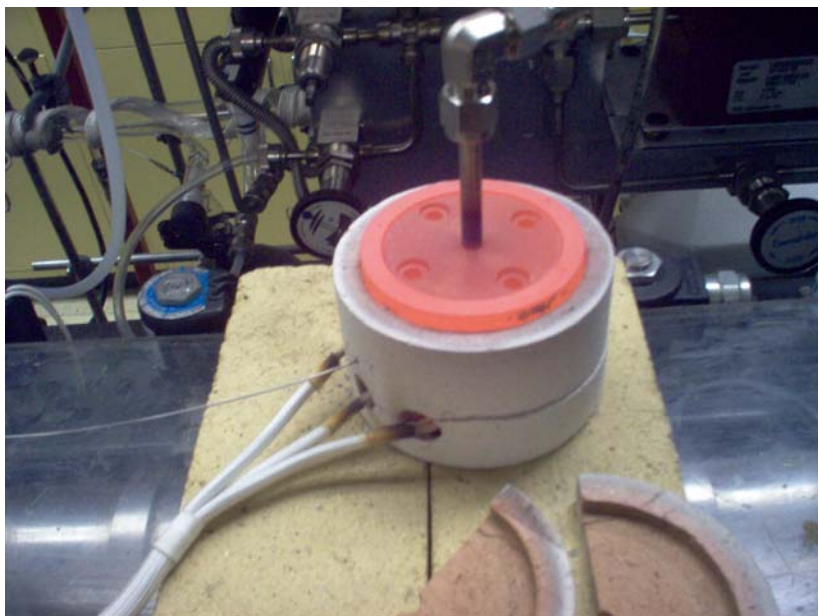


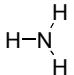
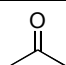
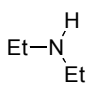
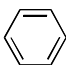
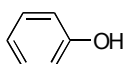
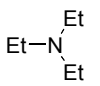
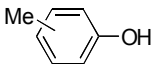
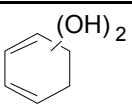
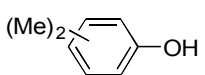
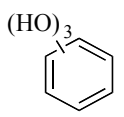
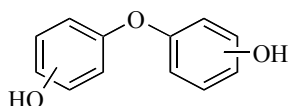
Figure 7.2 Picture of the custom made SS flange at $\sim 900^{\circ}\text{C}$ (left) and the programmed temperature ramp of the apparatus from RT- 900°C

7.3 RESULTS

When a 1.2360 g piece of graphitic board was heated from room temperature to 900°C over 40 minutes, a number of ions were detected. The top ten abundant product ions were identified: m/z 95, 113, 18, 35, 59, 102, 123, 52, 79, and 109 and the intensities of the ions vs. time are plotted in Figure 6.3, along with the blank. Hypothesized molecular formulas and compounds are shown in Table 7.1. As shown in the figure, an enormous amount of ammonia was detected. Because of that no quantitation was determined, since pseudo first order conditions must be maintained. This experiment was repeated again, with similar results. In a third experiment, a smaller piece of graphitic board (71.9 mg) was heated, and both meaningful quantification and identification were made. Figure 7.4 shows the selected ion chromatograms and total ion chromatogram for the blank and run with the piece of graphitic board. The “spikes” shown in the blank are from changes in the H_2O^{++} ion. H_2O^{++} is isobaric with NH_4^+ , an ion which was observed when a sample of graphitic board was heated. A real-time quantification is shown in Figure 7.5 along with the blank. An 8.0 mg sample of the phenolic resin used to coat the graphitic board was heated in the SS cell and the same VOCs are eluted, albeit at a smaller concentration (see Figure 7.6).

When protonated hexamethyldisiloxane was used at the reagent ion, the following product ions were observed: m/z 18, 35, 90, 107, and 181. The total ion chromatogram and selected ion chromatograms are shown in Figure 7.7. Figure 7.8 plots the intensities of m/z 18 and 90 at early elution. It is known that the branching ratio of the reaction of protonated hexamethyldisiloxane with ammonia produces 15% of NH_4^+ (m/z 18) and 85% of

Table 7-1 Hypothesized Identities of VOCs detected

<i>m/z</i>	Molecular Formula	Suggested Compound	Possible Structure
18, 35, 52	NH ₃	Ammonia	
59	C ₃ H ₆ O	Acetone	
74	C ₄ H ₁₁ N	Diethylamine	
79	C ₆ H ₆	Benzene	
95	C ₆ H ₆ O	Phenol	
102	C ₆ H ₁₅ N	Triethylamine	
109	C ₇ H ₈ O	Methyl substituted phenol	
113	C ₇ H ₁₂ O	Cyclohexadiene Diol	
123	C ₈ H ₁₀ O	Dimethyl substituted phenol	
127	C ₈ H ₁₄ O	Benzene Triol	
203	C ₁₂ H ₁₀ O ₃	Hydroxy Phenyl Ether	

Me₃Si—NH₃⁺ (*m/z* 90) (see chapter 3 for details). If one examines the intensities of *m/z* 18 and 90, the intensity of *m/z* 90 is greater than *m/z* 18, which is consistent with our observations reported in chapter 2.

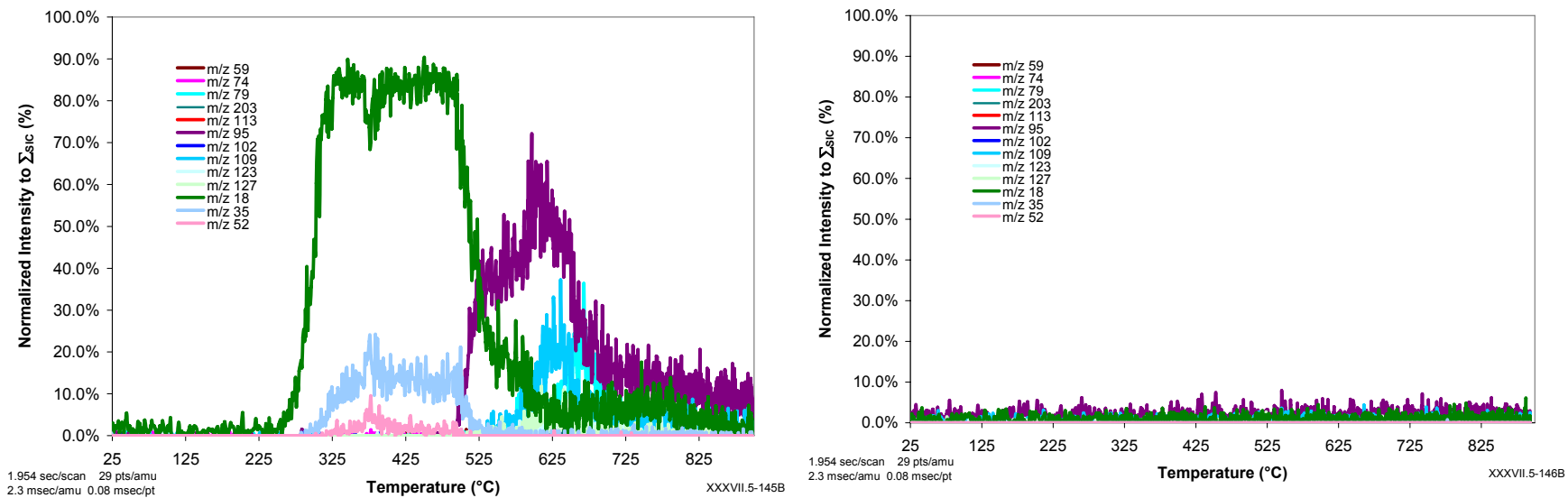


Figure 7.3 Selected ion chromatograms for the sampling of the headspace of a graphitic board from RT-900°C. The blank (right) and 1.2360 g sample (left) are normalized to the sum of the ions extracted.

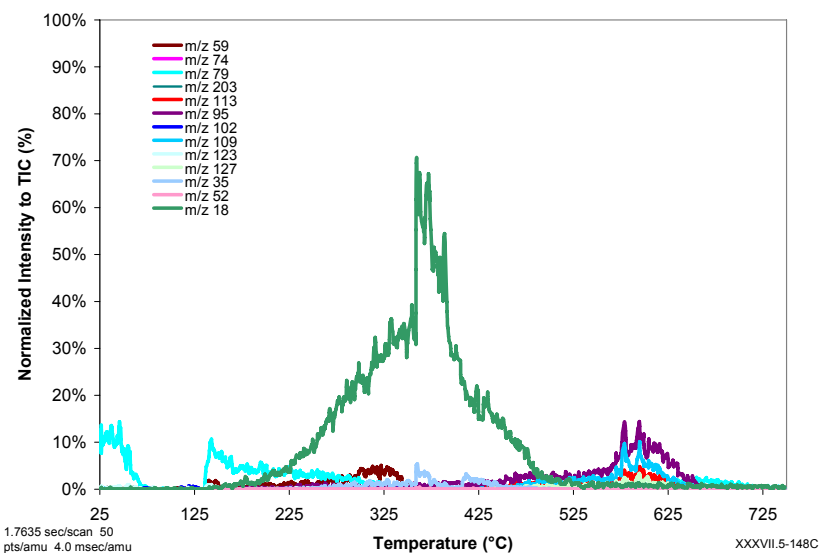
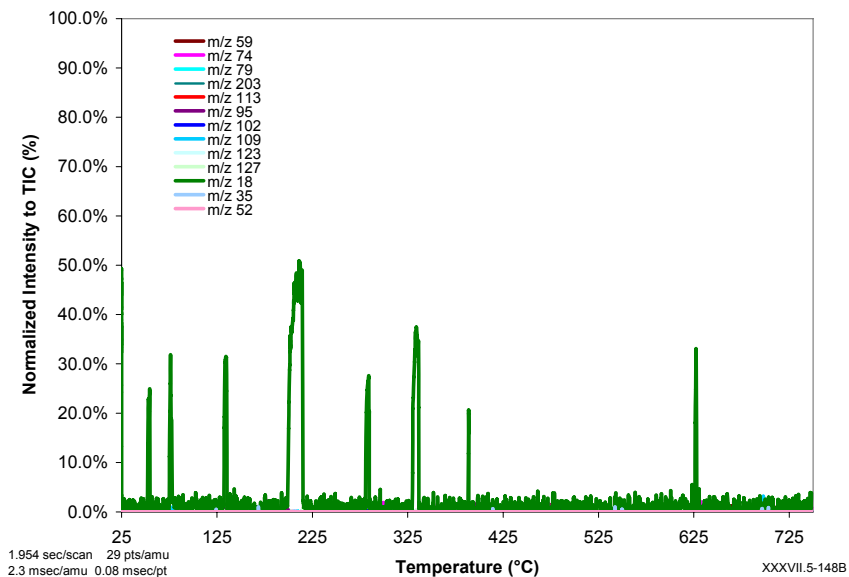


Figure 7.4 Selected ion chromatograms for the sampling of the headspace of a graphitic board from RT-900°C. The blank (left) and 71.5 mg sample (right) are normalized to the total ion current. The spikes observed on the blank are from the isobaric H_2O^+ ion (m/z 18).

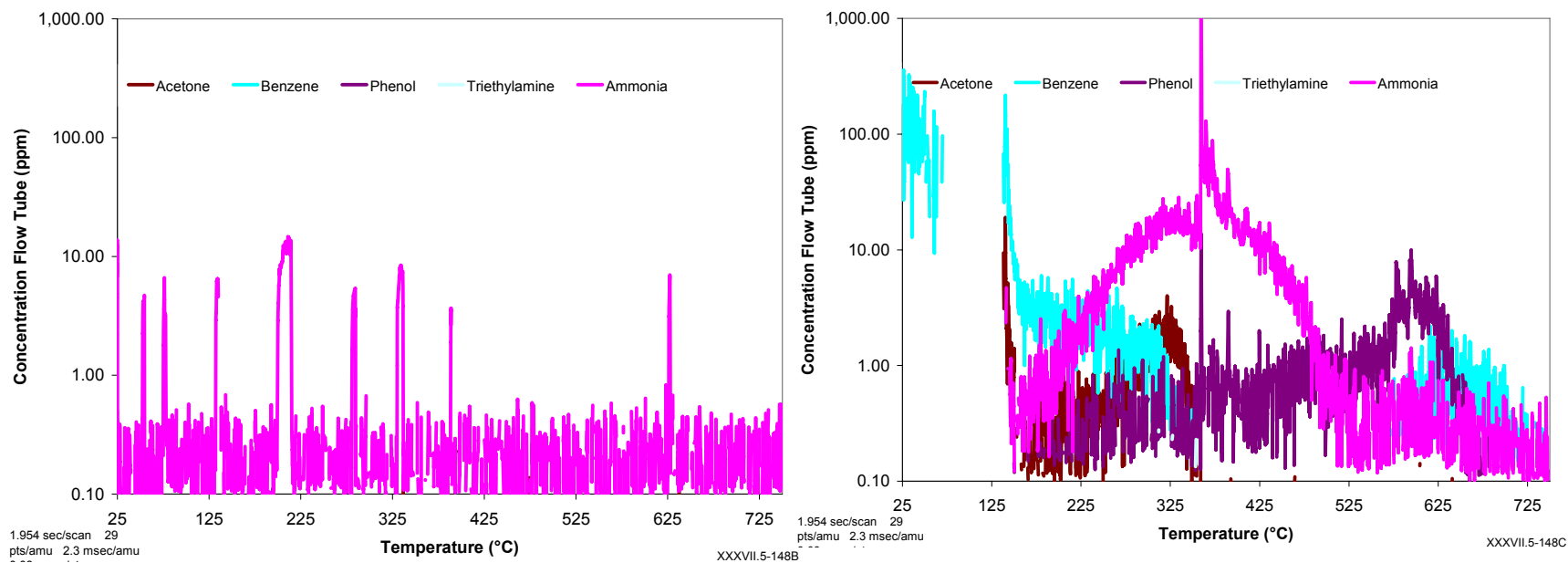


Figure 7.5 Real-time quantification of the 71.5 mg piece of graphitic board as shown in Figure 7.4 and discussed in the text. The blank (left) and 71.5 mg sample (right) are normalized to the total ion current.

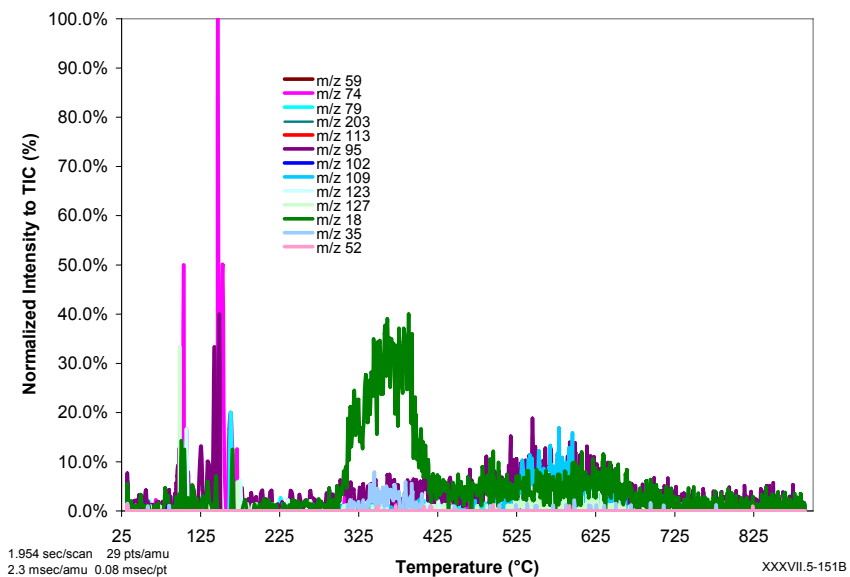
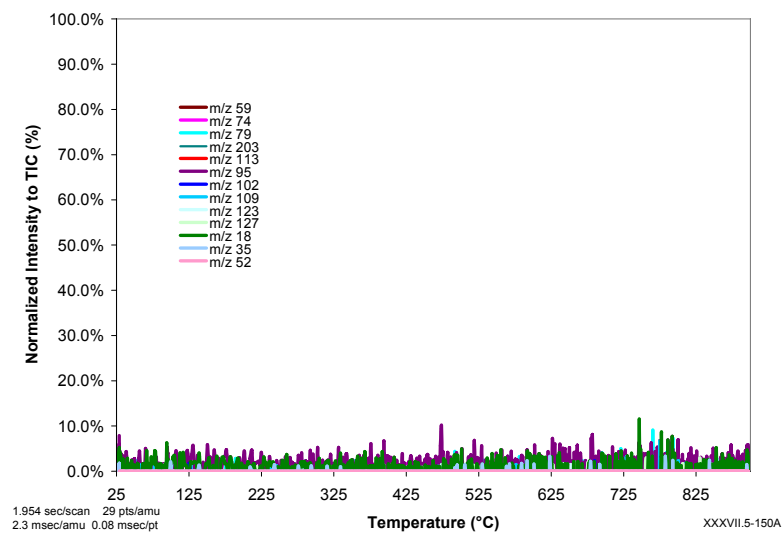


Figure 7.6 Selected Ion Chromatograms for the sampling of the headspace of a 8.0 mg sample of pure phenolic resin heated from room temperature to 900°C. The blank (left) and 8.0 mg sample (right) are normalized to the total ion current.

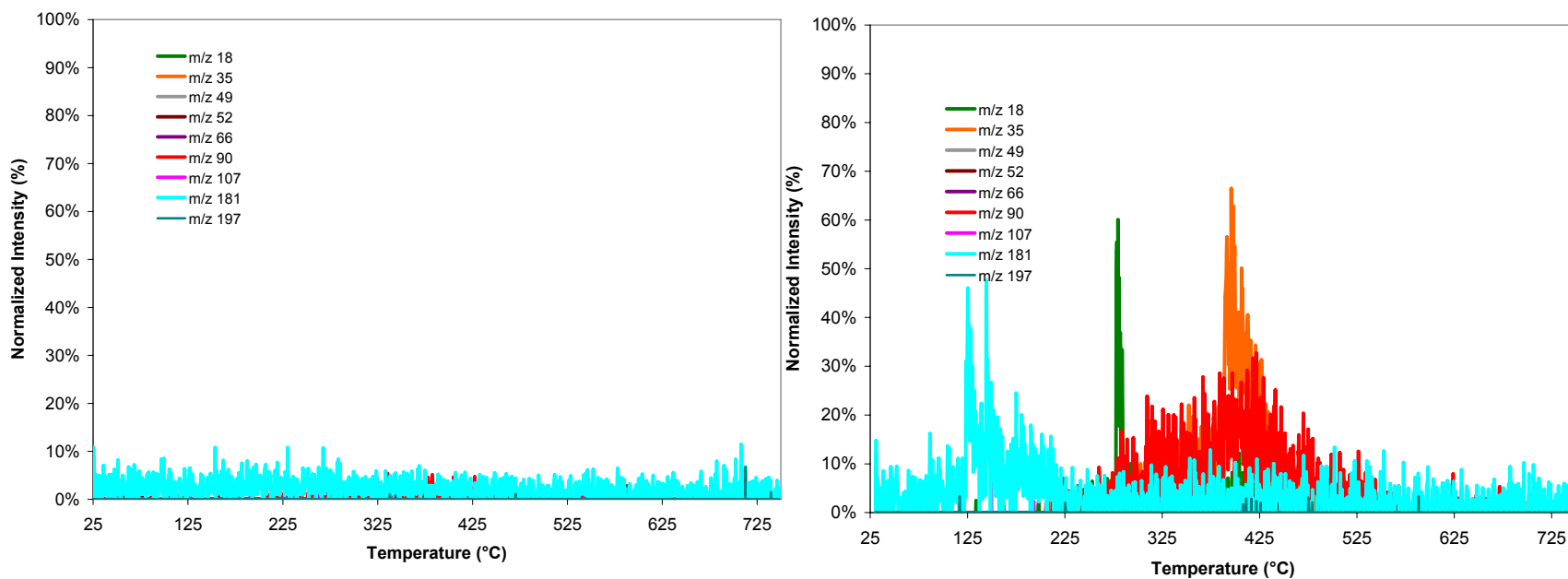
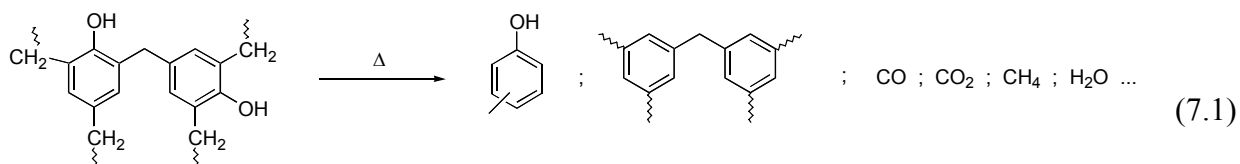
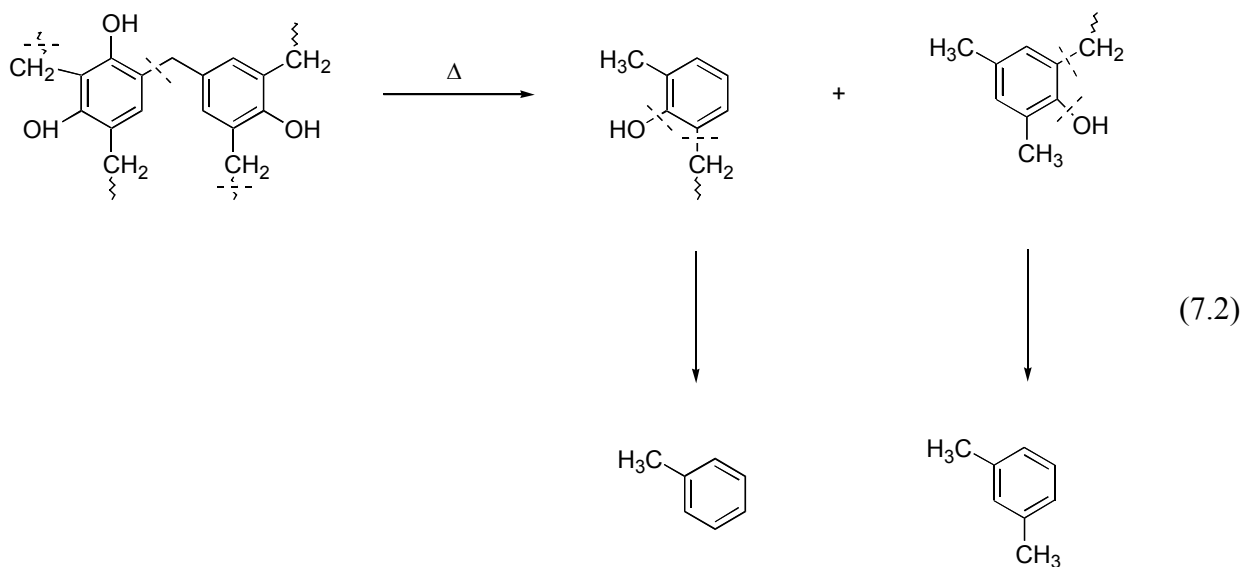


Figure 7.7 Selected ion chromatograms for the sampling of the headspace of a graphitic board from room temperature to 750 °C using protonated hexamethyldisiloxane ($\text{Me}_3\text{Si}_2\text{OH}^+$) as the reagent ion. The blank (left) and 80.6 mg sample (right) are normalized to the total ion current.

7.4 DISCUSSION

There is one publication involving thermal decomposition of phenolic resin.¹ The neutrals hypothesized to be present in the phenolic resin correlates well to what has been reported in the literature.¹ The m/z values observed at 109 and 123 are identified as methylated and dimethylated phenols which are decomposition products of the phenolic resin. Bouajila and coworkers studied the thermal degradation of phenolic resins under an inert and oxidizing atmosphere.¹ The neutrals produced from the degradation were indirectly sampled by adsorption onto a canister containing absorbent. The adsorbed neutrals were then analyzed by GCMS. The results obtained from the inert atmosphere will be used for comparison since the sample was heated under 0.3 Torr of vacuum. Bouajila and coworkers observed phenol, dimethylated phenol, and monomethylated phenol in their experiments (eq 7.1).¹ In addition, they observed xylenes and toluene (eq 7.2). The authors reason that these compounds are released by the breakup of various methylene bridges and other bridges in the phenolic resin.





Our results are consistent with the observations of Bouajula and coworkers.¹

Iwakami and coworkers have studied the thermal decomposition of hexamethylene tetramine (hexa).² Hexa is an additive to the phenolic resin to facilitate hardening. Iwakami and coworkers placed a sample of hexa into a glass ampoule that was sealed and heated to various temperatures. Once the desired temperature was reached, the headspace was sampled. Iwakami and coworkers observed that if hexa is heated to 400°C, ammonia vapor is produced along with other VOCs as shown in Table 7.2. Protonated trimethylamine and ethylene imine are observed when our phenolic resin is heated from RT to 900°C as shown in Figure 7.8. The other compounds are not observed. It should be noted that Iwakami and coworkers' experiment was performed in the absence of other substances, where our experiment was performed in the presence of phenolic resin. Iwakami and coworkers also studied the decomposition of hexa in the presence of activated carbon. They observed the amines decompose into ammonia with the

Table 7-2 Neutrals detected by Iwakami and coworkers

Trimethylamine	Dimethylamine
Methylamine	Propionitrile
Acetonitrile	Ethylene imine
Water	Ammonia
Methane	Hydrogen
Carbon Dioxide	Nitrogen and Carbon Monoxide

exception of trimethylamine. Propionitrile was not observed in our experiments. A possible explanation is that protonated propionitrile (m/z 56) is isobaric with one of the isotopes of the water clusters (i.e. $\text{H}_3^{17}\text{O}(\text{H}_2\text{O})_2^+$, m/z 55). The other neutrals that were observed by Iwakami and coworkers were not observed (e.g. hydrogen, nitrogen, etc.) since their proton affinities are less than water, which makes the proton transfer reactions endothermic.

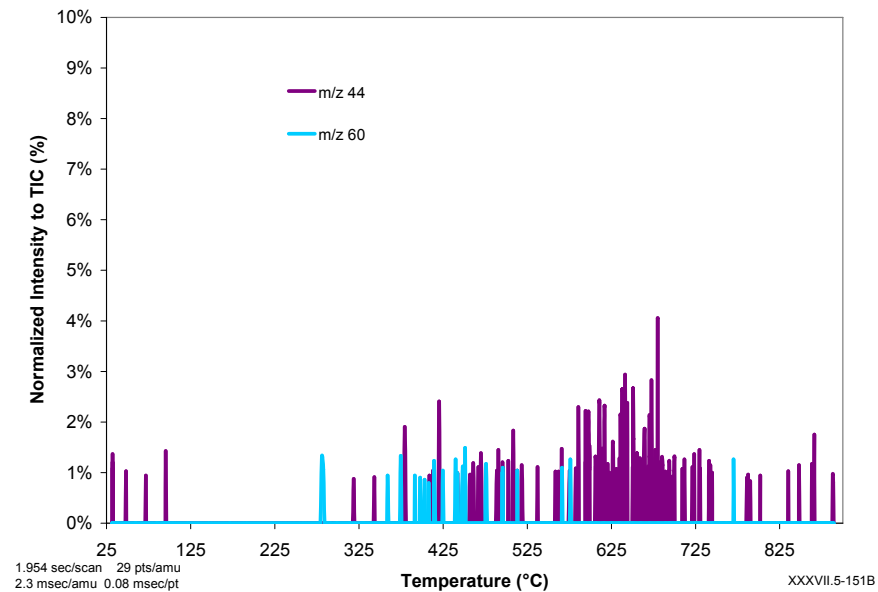
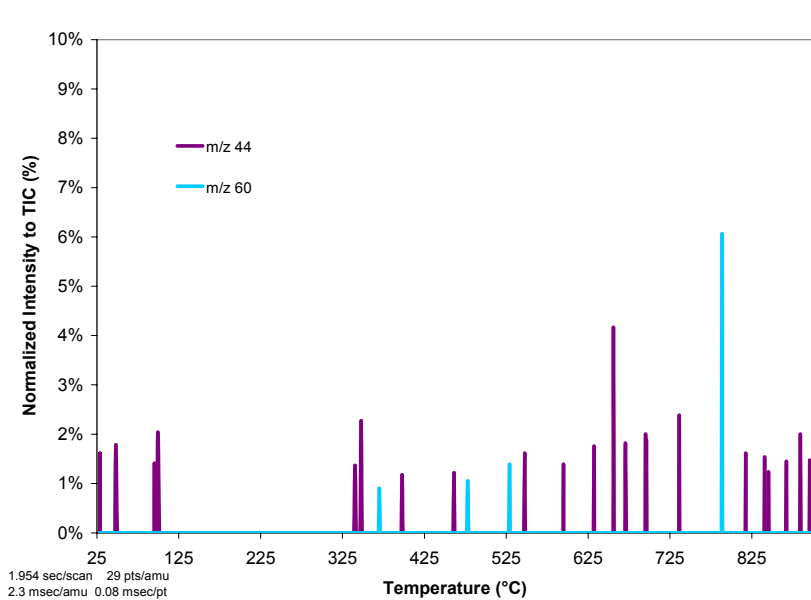


Figure 7.8 The study of VOCs that are released when 5 mg of phenolic resin is heated (right) and its blank (left). The VOCs detected correlate with the findings of Iwakami and coworkers: trimethylamine (m/z 60) and ethylenimine (m/z 44).

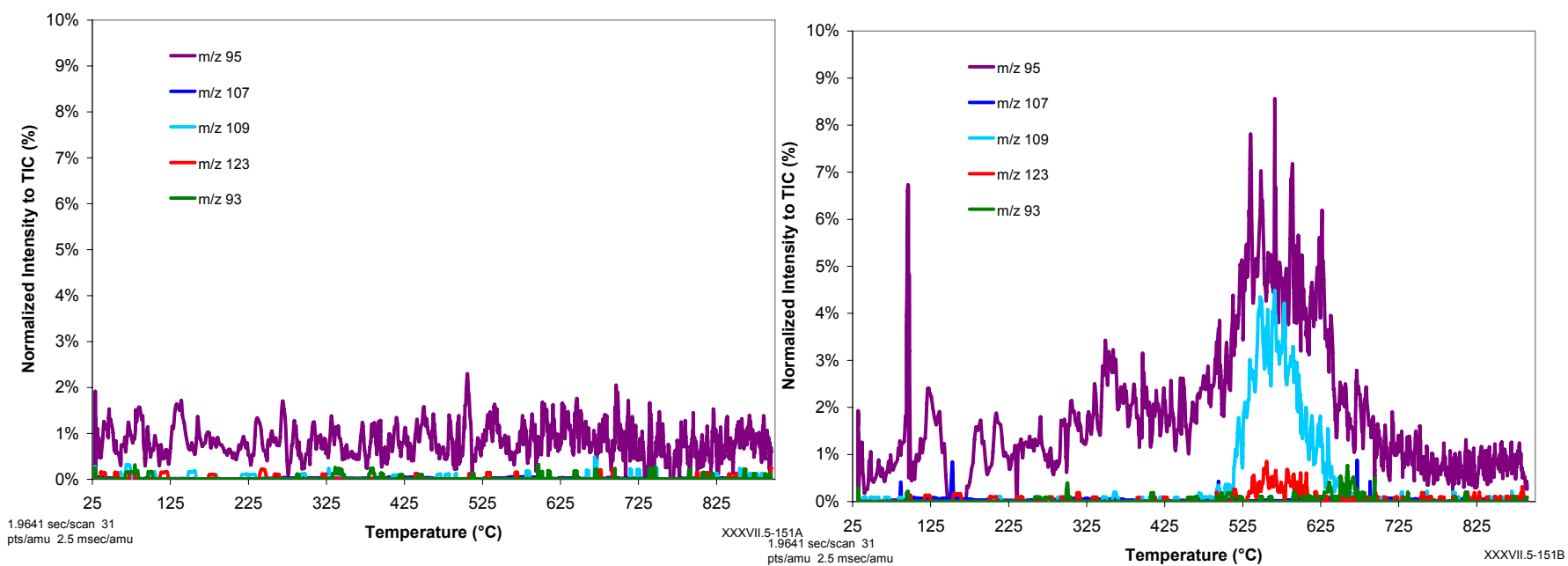


Figure 7.9 The detection of VOCs from a 5 mg sample of phenolic resin (right) and a blank (left). The VOCs detected from our analysis which correlates with Bouajula and coworkers are phenol (m/z 95), methylated phenol (m/z 109), dimethylated phenol (m/z 123), xylenes (m/z 107), and toluene (m/z 93).

7.5 CONCLUSIONS

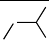

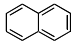

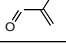
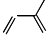
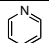
The flowing afterglow has been used to detect the VOCs eluting from graphitic board coated with a phenolic resin when it was heated from RT to 900°C. The VOCs observed agrees with what was reported in the literature. Using protonated hexamethyldisiloxane and the hydronium ion both for this analysis allowed confirmation that ammonia was being produced by the decomposition of the phenolic resin. Other VOCs were detected that were not discussed in the literature. The power of the CRMS to quantify and identify VOCs was shown here since both identification and quantification occurred in a single experiment.

7.6 REFERENCES

1. Bouajila, J.; Raffin, G.; Alamercury, S.; Waton, H.; Sanglar, C.; Grenier-Loustalot, M. F. *Polymers & Polymer Composites* **2003**, *11*, 345-357.
2. Iwakami, Y.; Takazono, M. *Bull Chem Soc Japan* **1968**, *41*, 813-817.

APPENDIX A

DATA USED TO CALCULATE k_{coll}

Neutral	μ_D (Debye) ^a	α (10^{-24} cm ³) ^a	d (g/cm ³) ^a	Index of Refraction ^a	α (10^{-24} cm ³ from GA) ^b	α (10^{-24} cm ³ from LL) ^c
	0.13		.6201	1.3537	9.98	9.99
H ₂ O	1.8546	1.45				
D ₂ O						
C ₆ H ₆		10.0				
	0.20	9.15				
MeSH	1.52		.8665	1.5491 ^d	4.71	6.99
MeCOH	2.750	4.6				
EtOH	1.69	5.41				
MeCN	3.92519	4.40				
MeCO ₂ H	1.70	5.1				
		16.5				
	0.66		.9514	1.4214	7.58	7.19
	2.68		.837	1.4144	8.06	8.29
MeCOMe	2.88	6.33			6.46	6.4
	0.25	9.99				
EtOEt	1.15	10.2				
Me ₂ S	1.554		.8483	1.4438	6.54	7.69
MeCO ₂ CH ₂ Me	1.78	9.7				
NH ₃	1.4718	2.81				
(MeO) ₃ PO	[3.18]		1.2144	1.3967	12.5	11
HCONMe ₂	3.82	7.81				
	2.22	9.5				
(Et) ₂ NH	0.92	10.2				
Et ₃ N	0.66	13.1				
Me ₃ SiOH	2.01		.8141 ^d	1.3980 ^d		10.6
(Me ₃ Si) ₂ O	0.73 ^d		.7638	1.3774		19.4

a—Unless otherwise noted, obtained from CRC Handbook 2000 1st Elec Ed

b—Polarizability of neutral estimated using the method from Miller, K.J.; Savchik, J.A. *J Amer Chem Soc* **1979**, 101, 7206-7213.

c—Lorenz, L. *Ann Phys* **1880**, 11, 70-103.

d—Beilstein Crossfire Database. Search performed on 4/25/06.

APPENDIX B

DERIVED AND RAW THERMOCHEMICAL DATA FROM THE LITERATURE

Reactant Neutral:	Reactant Neutral PA: (kcal/mol)	ΔH_{Rxn} : (kcal/mol)
Water	165	37.30
D ₂ O	167	35.30
Benzene	179.3	23.00
Cyclopentene	183.2	19.10
MeSH	184.8	17.50
Ethanol	185.6	16.70
Acetonitrile	186.2	16.10
Acetic Acid	190.5	11.80
Naphthalene	191.9	10.40
Furan	192	10.30
Acetone	194	8.30
Isoprene	197.5	4.80
Diethylether	198	4.30
Dimethylsulfide	198.6	3.70
Ethyl Acetate	199.7	2.60
Ammonia	204.0	-1.70
DMF	212.1	-9.80
Trimethylphosphate	212.9	-10.60
Pyridine	222	-19.70
Dimethylamine	222.2	-19.90
Triethylamine	234.7	-32.40

Note: Items highlighted in red are heats of reaction of formation found in the literature. Items highlighted in yellow are derived heats of reaction from the reaction of protonated hexamethyldisiloxane with the neutrals listed above (PA 202.3 kcal/mol). PA obtained from Lidstrom, P.J.; Mallard, W.G., Eds. NIST Chemistry Webbook, NIST Standard Reference Database Number 69; March 2003 ed.; National Institute of Standards and Technology: Gaithersburg, MD, 20899, 2003.

Preliminary Steps

Reactant Ion :	Reactant Ion ΔHF: (kcal/mol)	Reactant Neutral:	Reactant Neutral ΔHF: (kcal/mol)	Product Ion :	Product Ion ΔHF: (kcal/mol)	Product Neutral:	Product Neutral ΔHF: (kcal/mol)	AHRxn: (kcal/mol)
$C_3H_9Si^+$	150.00	Acetone	-52.23	$C_3H_9Si(CH_3COCH_3)^+$	52.77	None	0.00	-45
$C_3H_9Si^+$	150.00	Ethanol	-56.23	$C_3H_9Si(Ethanol)^+$	51.77	None	0.00	-42
$C_3H_9Si^+$	150.00	Ethyl Acetate	-106.46	$C_3H_9Si(Ethyl Acetate)^+$	-5.16	None	0.00	-48.7
$C_3H_9Si^+$	150.00	Water	-57.7978	Protonated Trimethylsilanol	62.10	None	0.00	-30.1
$C_3H_9Si^+$	150.00	Benzene	19.820	$C_3H_9Si(Benzene)^+$	145.92	None	0.00	-23.9
$C_3H_9Si^+$	150.00	Diethylether	-60.4	$C_3H_9Si(Diethylether)^+$	45.40	None	0.00	-44.2
$C_3H_9Si^+$	150.00	Dimethylamine	-4.7	$C_3H_9Si(Dimethylamine)^+$	85.30	None	0.00	-60
$C_3H_9Si^+$	150.00	Ammonia	-10.98	$C_3H_9Si(Ammonia)^+$	92.52	None	0.00	-46.5
H^+	365.70	Hexamethyldisiloxane	-167.40	Protonated Hexamethyldisiloxane	-4.00	None	0.00	-202.3
H^+	365.70	Trimethylsilanol	-109.00	Protonated Trimethylsilanol	62.10	None	0.00	-194.6

Trimethylsilyl transfer reaction enthalpy

$Me_3SiO(H)SiMe_3$	-4.00	Acetone	-52.23	$C_3H_9Si(CH_3COCH_3)^+$	52.77	Trimethylsilanol	-109.00	0.00
$Me_3SiO(H)SiMe_3$	-7.70	Ethyl Acetate	-106.46	$C_3H_9Si(Ethyl Acetate)^+$	-5.16	Trimethylsilanol	-109.00	0.00
$Me_3SiO(H)SiMe_3$	-1.00	Ethanol	-56.23	$C_3H_9Si(Ethanol)^+$	51.77	Trimethylsilanol	-109.00	0.00
$Me_3SiO(H)SiMe_3$	-5.50	Ammonia	-10.98	$C_3H_9Si(Ammonia)^+$	92.52	Trimethylsilanol	-109.00	0.00
$Me_3SiO(H)SiMe_3$	-19.00	Dimethylamine	-4.7	$C_3H_9Si(Dimethylamine)^+$	85.30	Trimethylsilanol	-109.00	0.00
$Me_3SiO(H)SiMe_3$	17.72	Benzene	19.2	$C_3H_9Si(Benzene)^+$	145.92	Trimethylsilanol	-109.00	0.00
$Me_3SiO(H)SiMe_3$	-3.20	Diethylether	-60.4	$C_3H_9Si(Diethylether)^+$	45.40	Trimethylsilanol	-109.00	0.00

Note: Since diethylether and benzene do not transfer a trimethylsilyl group, the limit is -4.00 kcal/mol

Note: Items highlighted in red are heats of reaction or formation found in the literature. Items highlighted in yellow are derived heats of reaction or formation.

All TMSA are measured at 468 K. There is no known TMSA for acetonitrile, isoprene, methyl mercaptan, pyridine, dimethylsulfide, DMF, (MeO)₃PO, triethylamine, furan, and acetic acid.

Neutral (or Ion)	NIST ΔH_f^a	JANAF ΔH_f^b	NIST PA ^a	TMSA	Source
Water	-57.7978	-57.80	165		30.1 Stone, A.J.; Wojtyniak, A.C.M. <i>Can. J. Chem.</i> , 1986 , 64, 575
Benzene	19.82 ± 0.12	19.8 ± 0.1	179.3		23.9 Stone, A.J.; Wojtyniak, A.C.M. <i>Can. J. Chem.</i> , 1986 , 64, 575
MeSH	-5.46 ± 0.14	-5.5 ± 0.1	184.8		
Ethanol	-56.23	-56.1 ± 0.1	185.6		42.0 Stone, A.J.; Wojtyniak, A.C.M. <i>Can. J. Chem.</i> , 1986 , 64, 575
Acetonitrile	17.7	18 ± 0.2	186.2		
Acetic Acid		-103.3 ± 0.1	187.33		
Furan	-8.29	-8.3 ± 0.1	192		
Acetone	-52.23	-51.9 ± 0.1	194		45.0 Stone, A.J.; Wojtyniak, A.C.M. <i>Can. J. Chem.</i> , 1986 , 64, 575
Trimethylsilanol			194.6		
Isoprene	18.09	17.9 ± 0.2	197.5		
Diethylether	-60.4	-60.1 ± 0.1	198		44.2 Stone, A.J.; Wojtyniak, A.C.M. <i>Can. J. Chem.</i> , 1986 , 64, 575
Dimethylsulfide	-8.96 ± 0.48	-9.0 ± 0.1	198.6		
Ethyl Acetate	-106.46	-103	199.7		48.7 Stone, A.J.; Wojtyniak, A.C.M. <i>Can. J. Chem.</i> , 1986 , 64, 575
Hexamethyldisiloxane		-186 ± 1	202.3		
Ammonia	-10.98	-11	204		46.5 Li, X.; Stone, A.J. <i>Int. J. Mass Spectrom. Ion Proc.</i> , 1990 , 101, 149.
DMF		-45.8 ± 0.4	212.1		
(MeO) ₃ PO		-265	212.9		
Pyridine	33.61 ± 0.36	33 ± 0.2	222		
Dimethylamine	-4.7	-4.4 ± 0.1	222.2		60.0 Stone, A.J.; Wojtyniak, A.C.M. <i>Can. J. Chem.</i> , 1986 , 64, 575
Triethylamine		-22.1 ± 0.2	234.7		
D ₂ O	-59.560	-59.56			
H ⁺	365.7	365.7			
C ₃ H ₆ Si ⁺	150	150			Szepes, L.; Baer, T. <i>J. Am. Chem. Soc.</i> , 1984 , 106, 273

Note: An omitted data value indicates the source does not list that neutral's property.

a--NIST chemistry webbook: webbook.nist.gov

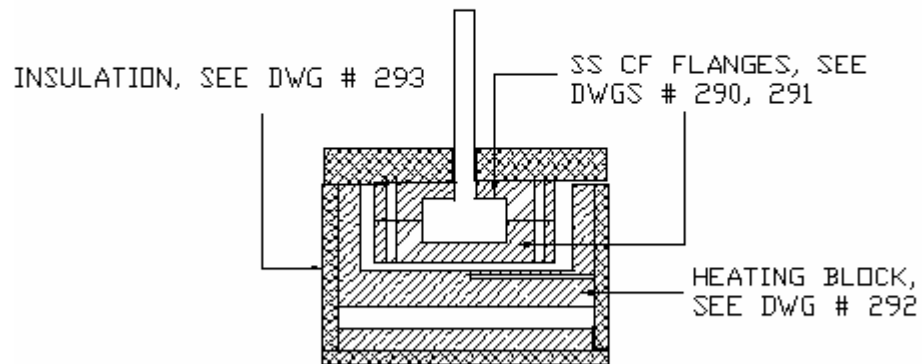
b--Gas-Phase Ion and Neutral Thermochemistry (Lias et al, *J Phy Chem Ref Data* **1988**, 17)

Reactant Ion :	Reactant Ion ΔHf: (kcal/mol)	Reactant Neutral:	Reactant Neutral ΔHf: (kcal/mol)	Product Ion :	Product Ion ΔHf: (kcal/mol)	Product Neutral:	Product Neutral ΔHf: (kcal/mol)	ΔHRxn: (kcal/mol)
C ₃ H ₉ Si ⁺	150.00	CH ₃ COCH ₃	-52.23	C ₃ H ₉ Si(CH ₃ COCH ₃) ⁺	40.00	None	-57.77	-57.77
C ₃ H ₉ Si ⁺	150.00	Ethyl Acetate	-106.46	C ₃ H ₉ Si(Ethyl Acetate) ⁺	-5.16	None	-48.7	-48.7
C ₃ H ₉ Si ⁺	150.00	Me ₂ NH	-4.7	C ₃ H ₉ Si(Me ₂ NH) ⁺	85.3	None	-60.0	-60.0
C ₃ H ₉ Si ⁺	150.00	H ₂ O	-57.7978	Me ₃ SiOH ₂ ⁺	62.10	None	-29.2	-29.2
H ⁺	365.70	Me ₃ SiOH	-108.10	Me ₃ SiOH ₂ ⁺	62.10	None	-194.6	-194.6
Me ₃ SiOH ₂ ⁺	62.10	CH ₃ COCH ₃	-52.23	C ₃ H ₉ Si(CH ₃ COCH ₃) ⁺	40.00	H ₂ O	-57.80	-27.67
Me ₃ SiOH ₂ ⁺	62.10	Ethyl Acetate	-106.46	C ₃ H ₉ Si(Ethyl Acetate) ⁺	-5.16	H ₂ O	-57.80	-18.60
Me ₃ SiOH ₂ ⁺	62.10	CH ₃ CN	18			H ₂ O	-57.80	
Me ₃ SiOH ₂ ⁺	62.10	Isoprene	18.09			H ₂ O	-57.80	
Me ₃ SiOH ₂ ⁺	62.10	Ei ₃ N	-22.2			H ₂ O	-57.80	
Me ₃ SiOH ₂ ⁺	62.10	EiOH	-56.23	C ₃ H ₉ Si(Ethanol) ⁺	51.77	H ₂ O	-57.80	-11.90
Me ₃ SiOH ₂ ⁺	62.10	CH ₃ CH ₂ COOH	-103.3			H ₂ O	-57.80	
Me ₃ SiOH ₂ ⁺	62.10	CH ₃ COOH	-90.49			H ₂ O	-57.80	
Me ₃ SiOH ₂ ⁺	62.10	Naphthalene	35.99			H ₂ O	-57.80	
Me ₃ SiOH ₂ ⁺	62.10	Furan	-8.29			H ₂ O	-57.80	
Me ₃ SiOH ₂ ⁺	62.10	Me ₂ NH	-4.7	C ₃ H ₉ Si(Me ₂ NH) ⁺	85.3	H ₂ O	-57.80	-29.90
Me ₃ SiOH ₂ ⁺	62.10	NH ₃	-10.98	NH ₃ (SiMe ₃) ⁺	92.52	H ₂ O	-57.80	-16.40

APPENDIX C

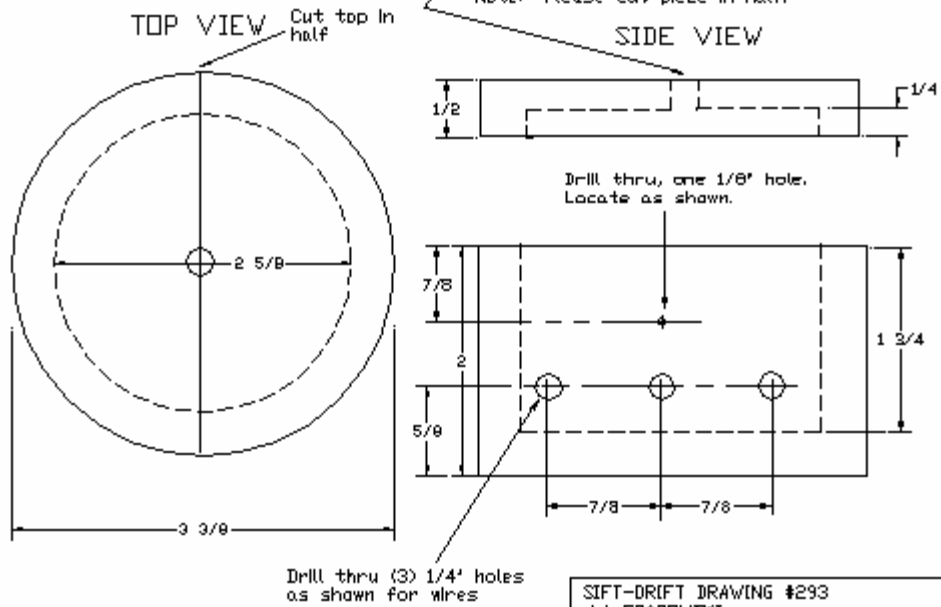
SS HEATED CELL DRAWINGS

SS HEATED CELL: OVERVIEW
NOT TO SCALE
SEE ALSO DWG # 290, 291, 292, 293
ENTIRE APPARATUS MUST WITHSTAND TEMP OF 900 DEG CELCIUS



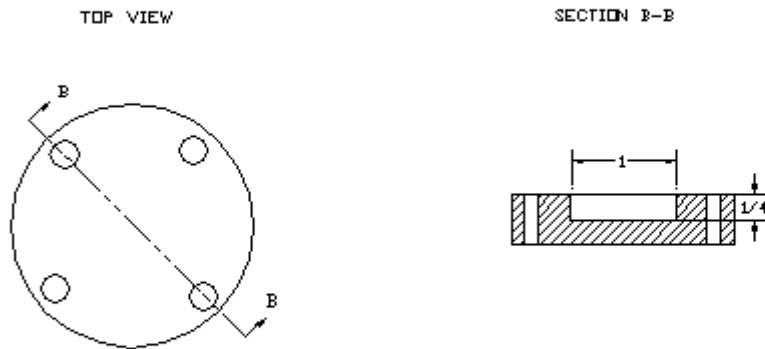
SIFT-DRIFT DRAWING #289
J.J. GRABOWSKI
DRAWN BY MARK MORRIS 16 MAY 2006

SS HEATED CELL: CALCIUM SILICATE (INSULATION)
 SCALE: FULL
 SEE ALSO DWGS # 289, 290, 291, 292
 DIMENSIONS ARE IN INCHES



SIFT-DRIFT DRAWING #293
 J.J. GRABOWSKI
 DRAWN BY: MARK MORRIS 16 MAY 2006

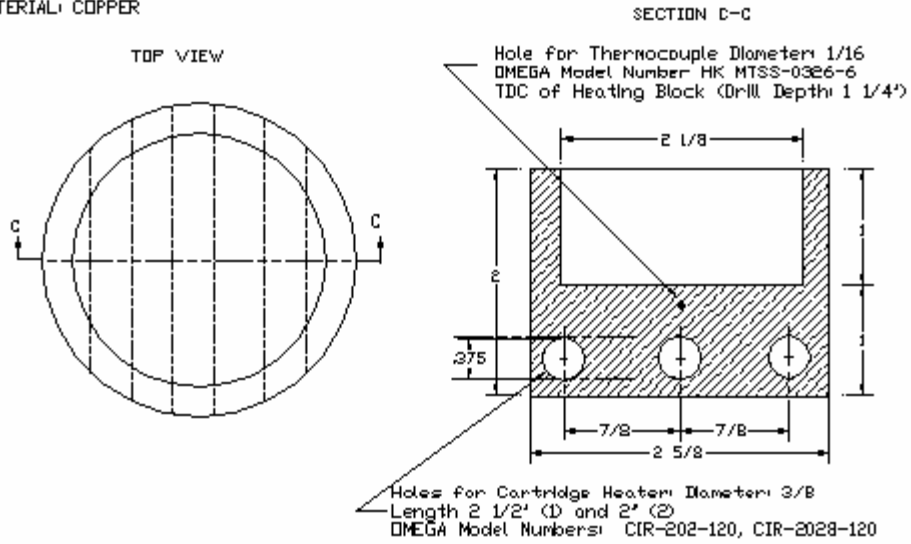
SS HEATED CELL: BOTTOM FLANGE
 SCALE: FULL
 SEE ALSO DWGS # 289, 290, 292, 293
 DIMENSIONS ARE IN INCHES
 MATERIAL: STAINLESS STEEL



MODIFICATION OF STANDARD $2 \frac{1}{8}$ ' OD CONFLAT FLANGE
 E.G. KURT LESKER PART # F0212X000N
 (FOR REF: $1 \frac{1}{8}$ ' BHC)

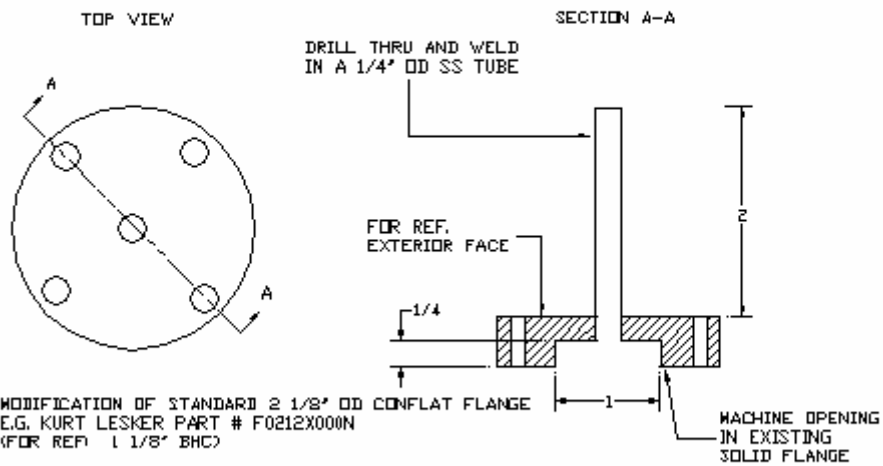
SIFT-DRIFT DRAWING #294
 J.J. GRABOWSKI
 DRAWN BY: MARK MORRIS 16 MAY 2006

SS HEATING CELL: HEATING BLOCK
 SCALE: FULL
 SEE DWGS # 289, 290, 293
 DIMENSIONS ARE IN INCHES
 MATERIAL: COPPER



SIFT-DRIFT DRAWING #292
 J.J. GRABOWSKI
 DRAWN BY: MARK NORRIS 16 MAY 2006

SS HEATED CELL: TOP FLANGE
 SCALE: FULL
 SEE ALSO DWGS # 289, 291, 292, 293
 DIMENSIONS ARE IN INCHES
 MATERIAL: STAINLESS STEEL



SIFT-DRIFT DRAWING #290
 J.J. GRABOWSKI
 DRAWN BY: MARK NORRIS 16 MAY 2006